




1994

Structural Characterization of Recombinant Polypeptides of &-Spectrin

Yirong Xu
Loyola University Chicago

Follow this and additional works at: https://ecommons.luc.edu/luc_diss

 Part of the [Chemistry Commons](#)

Recommended Citation

Xu, Yirong, "Structural Characterization of Recombinant Polypeptides of &-Spectrin" (1994). *Dissertations*. 3456.

https://ecommons.luc.edu/luc_diss/3456

This Dissertation is brought to you for free and open access by the Theses and Dissertations at Loyola eCommons. It has been accepted for inclusion in Dissertations by an authorized administrator of Loyola eCommons. For more information, please contact ecommons@luc.edu.



This work is licensed under a [Creative Commons Attribution-NonCommercial-No Derivative Works 3.0 License](#).
Copyright © 1994 Yirong Xu

LOYOLA UNIVERSITY OF CHICAGO

STRUCTURAL CHARACTERIZATION OF RECOMBINANT POLYPEPTIDES
OF α -SPECTRIN

A DISSERTATION SUBMITTED TO
THE FACULTY OF THE GRADUATE SCHOOL
IN CANDIDACY FOR THE DEGREE OF
DOCTOR OF PHILOSOPHY

DEPARTMENT OF CHEMISTRY

BY

YIRONG XU

CHICAGO, IL

MAY 1994

Copyrights by Yirong Xu, 1994

All Rights Reserved.

ACKNOWLEDGEMENTS

I wish to express my appreciation to my advisor, Dr. Leslie W.-M. Fung, for her guidance in every step of the experiments and her positive influence which encouraged me to pursue higher goals.

I would like to thank Dr. Alanah Fitch, Dr. Michael E. Johnson, Dr. Howard M. Laten and Dr. John Smarrelli for their time spent reviewing this dissertation and their valuable suggestions. Thanks are also extended to other faculties in the department, especially Dr. Mota de Freitas and Dr. Albert Herlinger, Dr. Ken Olsen and Dr. Chuck Thompson for their beneficiary discussions.

Dr. Michael E. Johnson and Dr. M. Prabhakaran at University of Illinois at Chicago and Dr. Mark Kelley at Loyola University Medical Center are acknowledged for their tremendous help in two of the collaboration projects. I learned a great deal from them.

I would like thank my fellow labmates for their help from time to time and their friendship. Especially, I would like to express my thanks to Tina Hack and Nugen Pan for their excellent assistance in my research.

All my family members and friends are deeply appreciated for their understanding, support and confidence in me which enabled me to look forward.

I owe special gratitude to my husband, Hang, with whom I shared joyful moments as well as difficult times, from whom I learned the meaning of love, care and generosity, and to whom I wish to dedicate this work.

TABLE OF CONTENTS

| | |
|---|------|
| ACKNOWLEDGMENTS | iii |
| LIST OF TABLES | vii |
| LIST OF FIGURES | viii |
| LIST OF ABBREVIATIONS | x |
| | |
| Chapter I. INTRODUCTION | |
| 1.1 Spectrin Overview | 1 |
| 1.2 Overview of Spectrin Repeats | 5 |
| | |
| Chapter II. MATERIALS AND METHODS | |
| 2.1 Chemicals | 9 |
| 2.2 Oligonucleotides and Enzymes | 9 |
| 2.3 Bacterial Stains and Plasmids | 10 |
| 2.4 DNA Manipulations | 10 |
| 2.4.1 Plasmid DNA Preparation | 10 |
| 2.4.2 DNA Digestion | 11 |
| 2.4.3 DNA Ligation | 11 |
| 2.4.4 DNA Transformation | 11 |
| 2.4.5 DNA Agarose Gel Electrophoresis | 11 |
| 2.5 Synthesis of Spectrin cDNA Fragments by PCR Amplification | 12 |
| 2.6 Construction of Expression Vectors | 13 |
| 2.7 Expression of Spectrin Fragments as Cleavable Fusion Proteins with GST | 16 |
| 2.8 Purification of Fusion Proteins | 17 |
| 2.9 Thrombin Cleavage of Fusion Proteins | 17 |
| 2.10 Purification of Sp α 41-273 and Sp α 1-446 | 18 |
| 2.11 Removal of GSH | 18 |
| 2.12 Analysis of Proteins | 18 |
| 2.12.1 Protein Concentration Assay | 18 |
| 2.12.2 Protein SDS Polyacrylamide Gel Electrophoresis | 19 |
| 2.13 Spin Labeling | 20 |
| 2.13.1 Native Samples | 20 |
| 2.13.2 Samples in Urea | 23 |
| 2.13.3 Urea-Treated Samples | 23 |
| 2.14 TNB-CN Cleavage Reaction | 24 |
| 2.15 DTNB Assay | 27 |

| | | |
|--------------|--|----|
| 2.16 | Combination of Mal6 and DTNB Reactions | 28 |
| 2.17 | EPR Measurements | 28 |
| 2.18 | EPR Data Analysis | 29 |
| 2.18.1 | SL/Sp ratio | 29 |
| 2.18.2 | Spectral Parameters | 29 |
| 2.18.3 | Spectral Addition | 30 |
| 2.18.4 | Spectral Subtraction | 30 |
| 2.19 | Stokes Radius Determination | 31 |
| 2.19.1 | Native Samples | 31 |
| 2.19.2 | Urea Treatment | 32 |
| 2.19.3 | Heat Treatment | 32 |
| | | |
| Chapter III. | RESULTS | |
| 3.1 | Spectrin Fragments Expression and Purification | 33 |
| 3.1.1 | Expression of Spectrin Fragments as Fusion Proteins with GST | 33 |
| 3.1.2 | Fusion Proteins Purification | 36 |
| 3.1.3 | Thrombin Cleavage of Fusion Proteins | 36 |
| 3.1.4 | Sp α 41-273 and Sp α 1-446 Purification | 42 |
| 3.2 | Accessibility of Sulfhydryl Groups in Sp α 41-273 and Sp α 1-446 | 42 |
| 3.2.1 | Spin Labeling | 42 |
| 3.2.1.1 | Number of Labeling Sites in Native Samples | 42 |
| 3.2.1.2 | Number of Labeling Sites in the Presence of Urea | 47 |
| 3.2.1.3 | Identification of the Labeling Sites | 50 |
| 3.2.1.3.1 | Sp α 41-273 | 50 |
| 3.2.1.3.2 | Sp α 1-446 | 56 |
| 3.2.2 | DTNB Assay | 62 |
| 3.2.3 | Combination of Mal 6 and DTNB Reactions | 62 |
| 3.3 | Studies of Spin-Labeled Sp α 41-273 and Sp α 1-446 | 67 |
| 3.3.1 | Spectral Properties at Room Temperature | 67 |
| 3.3.1.1 | Hyperfine Separation Measurements | 67 |
| 3.3.1.1.1 | A _{zz} of the Singly-Labeled Sp α 41-273 and Sp α 1-446 | 67 |
| 3.3.1.1.2 | A _{zz} of the Doubly-Labeled Sp α 1-446 | 68 |
| 3.3.1.2 | Weakly and Strongly Immobilized Components | 68 |
| 3.3.1.2.1 | Sp α 41-273 in the Native Condition | 68 |
| 3.3.1.2.2 | Sp α 41-273 in Urea | 71 |
| 3.3.1.2.3 | Spectral Subtraction | 76 |
| 3.3.1.3 | Urea-Treated Samples | 83 |
| 3.3.1.3.1 | Sp α 41-273 | 83 |
| 3.3.1.3.2 | Sp α 1-446 | 86 |
| 3.3.2 | Spectral Properties at High Temperatures | 86 |
| 3.4 | Stokes Radii of Sp α 41-273 and Sp α 1-446 | 92 |

| | | |
|----------------------|--|-----|
| Chapter IV. | DISCUSSION | |
| 4.1 | Folding of Spectrin Fragments Implied by the Thrombin Cleavage Reaction | 97 |
| 4.2 | Environment of the Cys Residues in Sp α 41-273 and Sp α 1-446 | 100 |
| 4.3 | Thermotropic Properties of Sp α 41-273 and Sp α 1-446 | 106 |
| 4.4 | The Response of Sp α 41-273 and Sp α 1-446 to Ionic Strength | 108 |
| 4.5 | The Reversibility of Conformational Changes of Sp α 41-273 and Sp α 1-446 | 110 |
| 4.6 | Conclusions | 111 |
| APPENDIX | | 113 |
| REFERENCES | | 122 |
| VITA | | 130 |

LIST OF TABLES

Table

| | | |
|----|---|----|
| 1a | Estimated and Apparent Molecular Masses of Fusion Proteins of Spectrin Fragments with GST | 37 |
| 1b | Estimated and Apparent Molecular Masses of Spectrin Fragments and of GST | 38 |
| 2 | SL/Sp Ratio of Sp α 41-273 and Sp α 1-446 Determined under Three Different Labeling Conditions | 65 |
| 3 | A_{zz} Values of the Singly-Labeled Sp α 41-273 and Sp α 1-446 | 69 |
| 4 | A_{zz} Values of the Measured and Composite EPR Spectra of the Doubly Labeled Sp α 1-446 | 70 |
| 5 | Stokes Radii of Sp α 41-273 in Low Salt and High Salt Buffers | 95 |
| 6 | Stokes Radii of Sp α 1-446 in Low Salt and High Salt Buffers | 96 |

LIST OF FIGURES

Figure

| | | |
|----|--|----|
| 1 | Construction of GST:Sp α m-n fusion protein expression vectors | 14 |
| 2 | A schematic representation of Mal6 and DTNB reactions | 21 |
| 3 | A flow chart of the TNB-CN modification and cleavage reaction | 25 |
| 4 | SDS polyacrylamide electrophoresis gels (12 % & 15 %) stained with 0.25 % Coomassie brilliant blue R | 34 |
| 5 | SDS polyacrylamide electrophoresis gels (12 % & 15 %) stained with 0.25 % Coomassie brilliant blue R | 39 |
| 6 | SDS polyacrylamide electrophoresis gels (15 %) stained with 0.25 % Coomassie brilliant blue R | 43 |
| 7 | Relationship between Mal6/Sp ratio and the SL/Sp ratio of Sp α 41-273 | 45 |
| 8 | Relationship between labeling time and the SL/Sp ratio of Sp α 41-273 | 48 |
| 9 | Schematic presentation of possible TNB-CN cleavage products of Sp α 41-273 with no or one spin label | 51 |
| 10 | SDS polyacrylamide electrophoresis gels (16 %) stained with 0.25 % Coomassie brilliant blue R | 54 |
| 11 | Schematic presentation of possible TNB-CN cleavage products of Sp α 1-446 with no or two spin labels | 57 |
| 12 | SDS polyacrylamide electrophoresis gels (16 %) stained with 0.25 % Coomassie brilliant blue R | 59 |

| | | |
|----|--|-----|
| 13 | A typical calibration curve of DTNB assay using GSH solutions of known concentration as standards | 63 |
| 14 | A typical conventional EPR spectrum of Mal6-labeled Sp α 41-273 in 5 mM sodium phosphate buffer at pH 7.4 and room temperature | 72 |
| 15 | Effects of urea on the Mal6-labeled Sp α 41-273 | 74 |
| 16 | Subtraction of the weakly immobilized component from the EPR spectrum of Mal6-labeled Sp α 41-273 | 77 |
| 17 | Effects of thrombin digestion time on the percentage of the weakly immobilized component in Sp α 41-273 | 79 |
| 18 | Effects of Mal6-labeling time on the percentage of the weakly immobilized component in Sp α 41-273 | 81 |
| 19 | Reversibility of the conformational changes of Sp α 41-273 and Sp α 1-446 induced by urea | 84 |
| 20 | Effects of temperature on the widths of the low field and high field weakly immobilized signals | 87 |
| 21 | Effect of temperature on Mal6-labeled Sp α 41-273 and Sp α 1-446 | 89 |
| 22 | Reversibility of the conformational changes induced by heat in Sp α 41-273 and Sp α 1-446 | 93 |
| 23 | Models of spectrin repeats | 104 |

LIST OF ABBREVIATIONS

| | |
|----------------------|--|
| β -ME | β -mercaptoethanol |
| ϵ_{412} | extinction coefficient of the yellow anion at 412 nm |
| ΔH_{pp} | width of the low field weakly immobilized signal |
| $\Delta H_{pp}'$ | width of the high field weakly immobilized signal |
| [GSH] | GSH concentration |
| [SH] | reactive sulfhydryl concentration |
| [Sp] | protein concentration |
| [SL] | spin label concentration |
| A_{412} | absorbance of the yellow anion at 412 nm |
| A_{protein} | absorbance of the protein at 412 nm |
| A_{rxn} | absorbance of the reaction mixture at 412 nm |
| A_{zz} | half outer hyperfine extrema |
| BSA | bovine serum albumin |
| CD | circular dichroism |
| cys | cysteine |
| DTNB | 5,5'-dithio-bis(2-nitrobenzoic acid) |
| EM | electron microscopy |
| EPR | electron paramagnetic resonance |
| E:S | enzyme to substrate molar ratio |
| EtBr | ethidium bromide |
| GSH | glutathione (reduced form) |

| | |
|---------------|--|
| GST | glutathione S-transferase |
| IPTG | isopropyl-B-D-thio-galactoside |
| K_{av} | partition coefficient |
| LB broth | 0.5% sodium chloride, 1% tryptone, 0.5% yeast extract |
| Mal6 | 4-maleimido-2,2,6,6-tetramethyl-1-piperidinyloxy |
| Mal6/Sp ratio | μl of 10^{-2} M Mal6 stock solution per mg spectrin |
| MW | molecular mass (kD) |
| NMR | nuclear magnetic resonance |
| PCR | polymerase chain reaction |
| R_s | Stokes radius |
| SDS | sodium dodecyl sulfate |
| SH/Sp ratio | number of reactive sulfhydryls per spectrin molecule |
| SL/Sp ratio | number of spin labels bound per spectrin molecule |
| TBE | 89 mM Tris, 89 mM boric acid, 2 mM EDTA |
| TNB-CN | 2-nitro-5-thiocyanobenzoic acid |
| TSS | LB medium, 10% PEG, 5% DMSO and 50 mM magnesium chloride |
| V_e | elution volume of the solute |
| V_0 | void volume |
| V_t | total bed volume |
| W | peak height of the low field weakly immobilized signal |
| W' | peak height of the high field weakly immobilized signal |

CHAPTER I

INTRODUCTION

1.1 Spectrin Overview

Spectrin is a major component of the erythroid membrane skeleton, a dense two dimensional meshwork of proteins underlying the cytoplasmic surface of the erythrocyte membrane (Marchesi and Steers, 1968; Branton *et al.*, 1981; Bennett, 1982; Gratzer, 1983; Goodman *et al.*, 1983; Gratzer, 1984; Marchesi, 1985; Bennett, 1989; 1990). The erythrocyte skeleton controls the lateral mobility of integral membrane proteins hence influencing erythrocyte surface topography (Goodman and Branton, 1978). More significantly, the erythrocyte skeleton provides support to the lipid bilayer and maintains the shape of the red cell. Therefore the skeleton is essential for the prolonged survival of the erythrocyte in the high shear environment of the vascular system (Lux, 1979; Lux and Glader, 1981; Marchesi, 1985; Elgsaeter *et al.*, 1986; Stokke *et al.*, 1986; Elgsaeter and Mikkelsen, 1991).

Spectrin was first isolated from low-ionic-strength extracts of erythrocyte membranes (Marchesi and Steers, 1968; Marchesi *et al.*, 1970). Spectrin consists of two similar but nonidentical subunits with apparent molecular masses of 260 kD (α) and 225 kD (β) on sodium dodecyl sulfate (SDS) polyacrylamide gel. The two subunits have been referred to as bands 1 and 2 (Steck, 1974) in some of the early studies. The gene for the spectrin α -subunit is located on chromosome 1 (Huebner *et al.*, 1985), while the β -subunit gene is on chromosome 14 (Prchal *et al.*, 1987; Winkelmann *et al.*, 1988). Spectrin α - and β -subunits associate side-to-side in an

antiparallel orientation (Speicher *et al.*, 1982) by an initial interaction between the α V domain at the C-terminal end of α -subunit and the β IV domain at the N-terminal end of β -subunit, the so-called nucleation site (Speicher *et al.*, 1992), and by contacts at multiple sites along the length of the dimer (Shotton *et al.*, 1979; Tyler *et al.*, 1979; Morrow *et al.*, 1980). Spectrin dimers can further associate head-to-head to form tetramers (Kam *et al.*, 1977; Ungewickell and Gratzer, 1978; Shotton *et al.*, 1979). This head-to-head assembly of tetramers involves association of the N-terminal region of the α -subunit with the C-terminal region of the β -subunit (Morris and Ralston, 1989; DeSilva *et al.*, 1992; Speicher *et al.*, 1993). Higher order oligomers form at high concentration in solution (Morrow and Marchesi, 1981), although the predominant form of spectrin on the membrane appears to be the tetramer (Byers and Branton, 1985; Liu *et al.*, 1987; Vertessy and Steck, 1989). The head-to-head binding site is suggested to play a critical role in maintaining the architecture and therefore the integrity of the red cell membrane. Many hereditary hemolytic anemias involve spectrin mutations that destabilize tetramer formation (Marchesi *et al.*, 1987; McGuire and Agre, 1988; Marchesi, 1989; Coetzer *et al.*, 1990; Garbarz *et al.*, 1990; Palek and Lambert, 1990; Delaunay and Dhermy, 1993).

Over the years, continuous efforts have been made toward understanding the physical-chemical properties, structure, and dynamics of spectrin in order to fully comprehend the function of this protein in the erythrocyte membrane skeleton. The shape and the size of isolated spectrin molecules have been determined by electron microscopy (EM) (Shotton *et al.*, 1979) as well as by a number of other techniques, including gel filtration chromatography (Ralston, 1976; Kam *et al.*, 1977, LaBrake, 1993), sedimentation velocity (Ralston and Dunbar, 1979), light scattering (Elgsaeter, 1978; Reich *et al.*, 1982), electrically induced birefringence relaxation (Mikkelsen and Elgsaeter, 1978; 1981) and viscometry (Stokke and Elgsaeter, 1981; Stokke *et al.*, 1985). These studies reveal that the spectrin heterodimer is a long, rod-shaped molecule about 100 nm in length

and 4-6 nm in diameter. The secondary structure of spectrin is largely composed of α -helix (60 - 75%) according to the circular dichroism (CD) measurements (Ralston, 1979; Calvert *et al.*, 1980) and Fourier transform infrared results (LaBrake and Fung, 1993).

The dynamic aspects of the molecule have also been extensively investigated. Nuclear magnetic resonance (NMR) of spectrin in aqueous solution displayed sharp proton resonances (Calvert *et al.*, 1980; Fung *et al.*, 1986; 1989). Spin-labeling electron paramagnetic resonance (EPR) detected multiple classes of motion in spectrin (Cassoly *et al.*, 1980; Lemaigre-Dubreuil *et al.*, 1980; Dubreuil and Cassoly, 1983; Streichman *et al.*, 1991; Jozwiak *et al.*, 1993; Hensley *et al.*, 1993), and the combination of conventional and saturation transfer EPR studies resolved these motions into time ranges of 10^{-9} s, 10^{-7} to 10^{-6} s and 10^{-3} s (Fung *et al.*, 1979; Fung and Johnson, 1983). Time-resolved phosphorescence anisotropy (Learmonth *et al.*, 1989) obtained rotational correlation times reflecting not only axial rotation but also faster motions such as intramolecular bending and torsional distortion. Light scattering studies (Budzynski *et al.*, 1992) measured fluctuational segmental motions of spectrin tetramers over a distance of 20-30 nm with relaxation times equal or less than 23 μ s. Taken together, these studies demonstrate that spectrin is a highly flexible molecule possessing considerable internal motions. Intuitively, the long flexible morphology of spectrin would seem ideally suited to its role as the major interconnecting component of the membrane skeleton.

In addition to the internal flexibility, spectrin also appears to be highly elastic. The molecule undergoes reversible extension and condensation in response to the change of the ionic strength of the buffer as indicated by measurements of viscosity (Stokke and Elgsaeter, 1981), sedimentation coefficient (Ralston and Dunbar, 1979), light scattering (Elgsaeter, 1978) and hydrodynamic properties (LaBrake, 1993). Recent studies of negatively stained spectrin in the partially expanded membrane skeleton suggest that the α - and β -subunits of spectrin twist about each other forming a two-strand helix (McGough and Josephs, 1990). Spectrin is shown to exist in a

continuum of lengths with the pitch of the two-strand helix ranging from 104 Å - 166 Å, the diameter varying from 52 Å - 36 Å and the number of turns remaining constant. It is proposed, based on this observation, that the origin of elastic properties of spectrin is the reversible deformation of a well defined quaternary structure. The ability of spectrin to adopt different shapes and to undergo reversible deformation may have physiological significance since it may be related to the deformability and elasticity of the erythrocyte.

The topology of the spectrin molecule has been probed by mild protease cleavage, monoclonal antibodies and spin labels. Limited digestion of purified spectrin with trypsin at 0 °C defines five unique proteolysis-resistant domains within the α -subunit and four domains within the β -subunit. A series of nine monoclonal antibodies recognizing a unique set of subdomain peptides have been used to demonstrate that each proteolysis-resistant domain of the α -subunit is antigenically unique (Yurchenco *et al.*, 1982). Spin-labeling EPR studies recognize hydrophobic regions that are potential membrane binding sites on the surface of the molecule (Streichman *et al.*, 1991).

Using recombinant DNA techniques, the exact locations of several functional sites of spectrin including the calmodulin binding site, the calcium binding site (Dubreuil *et al.*, 1991) and the ankyrin binding site (Kennedy *et al.*, 1991), have been identified. Recently, the SH3 domain of chicken brain spectrin has been cloned, expressed and crystallized (Musacchio *et al.*, 1992). The three dimensional structure of this 64-amino acid domain has been determined as a β -barrel made of five antiparallel β -strands.

Although significant progress has been made, detailed information regarding the structure of the majority of spectrin remains unknown. The major difficulties encountered during structural studies of spectrin are largely attributable to the high molecular weight and the elongated shape of the molecule. The two most powerful structural techniques, NMR and x-ray crystallography, can not be applied to the intact molecule due to the large size and unfavorable shape of spectrin. Unveiling the structure-function relationship of spectrin remains a challenge to the scientific

community.

1.2 Overview of Spectrin Repeats

Ever since the discovery of spectrin, some investigators have suggested that spectrin, as a large molecule, might contain repeated sequences. Current notions of molecular evolution (Doolittle, 1981; Keim *et al.*, 1981; Pink, 1981; Li, 1983) indicate that the size of a protein increases by two mechanisms, either through fusion of two dissimilar genes to produce a large hybrid product, or through duplication and fusion of a single gene to produce a large product with internal repetitive sequences. Spectrin repeat units of approximately 80 kD and 50 kD were first hypothesized based on the sizes of the peptide fragments produced by mild protease cleavage. However, peptide maps of the fragments from the mild protease cleavage of spectrin failed to detect conserved or repetitive elements. The determination of the amino acid sequence of the 80 kD α -I domain of spectrin provided the first solid evidence that spectrin contains a repetitive structure (Speicher *et al.*, 1983a; Speicher *et al.*, 1983b; Speicher and Marchesi, 1984). The availability of the cDNA sequences of both α - and β -spectrin (Curtis *et al.*, 1985; Sahr *et al.* 1990; Winkelmann *et al.*, 1990) reveals that the primary structure of spectrin is dominated by tandem, homologous motifs of about 106-amino acid residues that are referred to as repeating units. It has been well established that sequence homology reflects conformational similarity (Schulz and Schirmer, 1979; Doolittle, 1981; Keim *et al.*, 1981; Arnheim, 1983). Each homologous spectrin repeat unit thus has been suggested to represent an independent domain whose conformation is conserved among the repeats. The nearly universal presence of the 106-residue repetitive structure in the spectrin heterodimer makes this unit the most important substructural feature of the entire molecule. Essentially, the repetitive structure makes a very large, complex protein much simpler.

Although it is the general consensus in the field that each spectrin repetitive motif folds into a closely packed unit, this structure has not been experimentally proven. A structural model for the

folding of spectrin polypeptides into a series of short α -helical segments, each comprised of three helices, was first proposed by Marchesi and co-workers (Speicher and Marchesi, 1984) based on the following information: 1) spectrin contains approximately 60-75% α -helix based on measurements of circular dichroism, 2) the length of spectrin subunits of 100 nm is approximately 1/3 of the length of an extended α -helix of 2000 amino acids, 3) the amino and carboxyl termini of the subunits are located at opposite ends of the molecule in solution, 4) spectrin is more flexible in solution than rigid coiled-coil α -helical proteins such as myosin and tropomyosin. A series of triple helical units would account for the reduced length and increased flexibility of spectrin compared with other coiled-coil α -helical proteins and for the fact that ends of the polypeptide chains are located at opposite ends of the spectrin molecule.

Using various prediction methods, a number of modified models were later proposed for the 106-residue homologous sequence repeat, suggesting slightly different amounts of secondary structural elements and somewhat different arrangements of the secondary structural elements (Davison *et al.*, 1989; Xu *et al.*, 1990). Models advanced to date can be generally classified into two categories. For one type of the models (Davison *et al.*, 1989; Xu *et al.*, 1990), the phasing of the structural units coincides with the phasing of the sequence motifs according to Speicher and Marchesi's convention (Speicher and Marchesi, 1984). For the second type of the models (Speicher and Marchesi, 1984; Keonig *et al.*, 1988; Dubreuil *et al.*, 1989, Parry and Cohen, 1991; Parry *et al.*, 1992), the phasing of the structural units is somewhat staggered relative to the phasing of the sequence motifs. Because the 106-residue motif is generally repeated without interruptions, the residue that corresponds to the beginning or end of a structural unit is not self-evident. Consider, for example, the repetitive sequence of letters ABCDABCDABCDABCD. To produce a 4-letter segment of the sequence that can form a structural unit, it is essential to know whether the structure is ABCD, BCDA, CDAB, or DABC.

The first experimental evidence relating the boundaries of the folded, conformational units

to the chemical sequence of repeating motifs was provided by Winograd and co-workers (1991) for *Drosophila* α -spectrin. They have shown that the single repetitive unit and pairs of units can fold into stable conformations similar to that of native spectrin when their N-terminal ends are 26 residues downstream of the beginnings of the sequence motifs. And they also have shown that similarly sized polypeptides with other phasings do not fold into stable structures.

A recent attractive model proposed by Parry and Cohen (Parry and Cohen, 1991; Parry *et al.*, 1992) employed structural constraints imposed by both the structural features of spectrin and the α -helical coiled-coil-like packing. A specific three-helix motif is identified from each sequence repeat consisting of one long helix followed by a β -turn, followed by a short helix and another β -turn. A three-helix structural unit is then generated from this arrangement by each structural motif incorporating part of the long helix from the successive repeat. The N-terminal ends of these three-helix units are 23 residues downstream of the first residues in the conventional sequence motifs. A slightly different phasing has been proposed by another group (Speicher *et al.*, 1993). According to this model, the N-terminal ends of the conformational units reside at 31 amino acids down stream of the N-terminal ends of the sequence motifs.

For human erythrocyte spectrin, the phasing of the conformational units relative to the phasing of the sequence motifs is still not clear. The structure of the conformational units, the structural properties of repeating units in relation with each other and with those of the intact spectrin are yet to be characterized.

In this study, we have expressed seven different spectrin fragments with different lengths corresponding to the phasing of the sequence motifs or the hypothesized phasing of the structural units. Structural features of the two relatively stable fragments have been explored. The environment of the cysteine (cys) residues, the thermotropic properties, the response of the proteins to the ionic strength, and the reversibility of the conformational changes have been compared between the two fragments and compared with those of intact spectrin. The results have provided

evidence supporting the hypothesis that spectrin consists of individually folded conformational units. We have demonstrated that the general properties of one unit are not drastically affected by the addition of another unit and that small fragments of spectrin bear structural similarities to intact spectrin, although the overall folding of larger fragments appears to be more compact than that of smaller fragments.

CHAPTER II

MATERIALS AND METHODS

2.1 Chemicals

All general chemicals were reagent grade and were purchased from Fisher Scientific (Pittsburgh, PA), Sigma Chemical Company (St. Louis, MO) or Aldrich Chemical Company, Inc. (Milwaukee, WI). 5,5'-dithio-bis(2-nitrobenzoic acid) (DTNB) was obtained from CalBiochem (San Diego, CA); 4-maleimido-2,2,6,6-tetramethyl-1-piperidinyloxy (Mal6) from Aldrich Chemical Company Inc. (Milwaukee, WI); glutathione Sepharose 4B resin, ampicillin and bovine serum albumin (BSA) protein standard from Pharmacia LKB Biotechnology (Piscataway, NJ); dye reagent for protein assay from Bio-Rad (Richmond, CA); tryptone, yeast extract and Bacto-agar from Curtin Metheson Scientific, Inc. (Wooddale, IL); glycine, agarose and protein low molecular weight standards from Gibco BRL Life Technologies Inc. (Gaithersburg, MD); 2-nitro-5-thiocyanobenzoic acid (TNB-CN), protein high molecular weight standards, glutathione (reduced form, GSH) and glutathione agarose resin from Sigma Chemical Company (St. Louis, MO); isopropyl-B-D-thiogalactoside (IPTG) from Promega Company (Madison, WI).

2.2 Oligonucleotides and Enzymes

All oligonucleotide primers for the polymerase chain reaction (PCR) were synthesized by National Biosciences (Hamel, MN). *EcoRI* linker (CGGAATTCCG) was purchased from Amersham Company (Arlington Heights, IL); *XbaI* linker with nonsense codons in all three reading

frames (CTAGTCTAGACTAG) from New England BioLabs (Beverly, MA).

Restriction endonucleases were obtained from either International Biotechnology, Inc. (New Haven, CT) or Gibco BRL Life Technologies Inc. (Gaithersburg, MD); T4 DNA ligase from Bio-Rad (Richmond, CA); Klenow fragment from International Biotechnology, Inc. (New Haven, CT); thrombin and RNase A from Sigma Chemical Company (St. Louis, MO); DNA sequenase version 2.0 from United States Biochemical Company (Cleveland, OH).

2.3 Bacterial Strains and Plasmids

E. coli strains **HB101** and **NM522** were obtained from Dr. Mark Kelley of Loyola University Medical Center; **MC1022** (Cheah *et al.*, 1988; Warburton and Boseley, 1983) from Dr. N. Warburton of Searle Research and Development (High Wycombe, UK). Plasmid pJF18EH (Furste *et al.*, 1986; Persico *et al.*, 1989) was a generous gift from Dr. Michael Bagdasarian of Michigan Biotechnology Institute (Lansing, MI); pWR 590 series, pBluescript and pBR322 from Dr. Mark Kelley; pKCC 100 (Cheah *et al.*, 1988 ; Warburton and Boseley, 1983) from Dr. N. Warburton; pTTQ181 (Stark, 1987) from Dr. Michael Stark of University of Leicester (Leicester, UK); pTTQ18 (Stark, 1987) from Amersham Company (Arlington Heights, IL); pET-3a (Studier *et al.*, 1990; Rosenberg *et al.*, 1987) from Novogen (Madison, WI); pGEX-3x (Smith and Johnson, 1988) from Pharmacia LKB Biotechnology (Piscataway, NJ). Competent *E. coli* **HB101** cells were either purchased from Gibco BRL Life Technologies Inc. (Gaithersburg, MD) or home made according to Chung *et al.* (1989). *E. coli* strains **MC1022** and **NM522** were used in the preliminary studies.

2.4 DNA Manipulations

2.4.1 Plasmid DNA Preparation

Plasmid DNAs were prepared by the mini-plasmid alkaline lysis procedure either as

described in Current Protocols in Molecular Biology (Ausubel *et al.*, 1990) or as described in the instruction menu of mini plasmid preparation kit from Qiagen (Studio City, CA).

2.4.2 DNA Digestion

Digestion reactions of DNA with restriction endonucleases were carried out in buffers provided by the manufacturer of each enzyme and under reaction conditions recommended. Reaction mixtures were run on 0.7% agarose gels, as described in section 2.4.5 below, from which purified DNA fragments were extracted.

2.4.3 DNA Ligation

One unit of T4 DNA ligase was added to each ligation mixture. The ligation buffer provided by Gibco BRL Life Technologies Inc. was used. Ligation reactions were allowed to proceed at 15 °C overnight. T4 DNA ligase was heat inactivated at 70 °C before transformation.

2.4.4 DNA Transformation

For transformation, a 100 μ l aliquot of competent cells was measured into a cold micro centrifuge tube containing DNA. The cell/DNA suspension was mixed gently and incubated at 4 °C for 5 - 60 min. A 200 μ l aliquot of TSS (0.5% sodium chloride, 1% tryptone, 0.5% yeast extract (LB broth), 10% PEG, 5% DMSO and 50 mM magnesium chloride) was added. The suspension was incubated for 1 h at 37 °C with shaking (225 rpm) to allow expression of the antibiotic-resistant gene before it was plated onto a LB plate containing ampicillin (100 mg/l). Transformants were selected by standard methods described in Molecular Cloning (Sambrook *et al.*, 1989)

2.4.5 DNA Agarose Gel Electrophoresis

DNA fragments were separated on 0.7% (w/v) agarose gels. 0.35 g of agarose was dissolved in 50 ml of TBE buffer (89 mM Tris, 89 mM boric acid, 2 mM EDTA) by boiling. The agarose solution was cooled to approximately 60 °C by gentle stirring at room temperature before ethidium bromide (EtBr) was added to a final concentration of 1 µg/ml. The mixture was stirred gently for another minute before it was poured into a horizontal gel casting tray. The gel was allowed to solidify at room temperature for 15 - 20 min prior to being transferred to an electrophoresis chamber filled with TBE buffer. DNA samples containing tracing dye (orange G in 2.5% ficoll) were loaded into the sample wells of the gel and the electrophoresis was run under constant voltage of 40 V until the dye front migrated to the bottom of the gel. Lambda DNA cleaved with *HindIII/EcoRI* endonucleases was run simultaneously to serve as the molecular weight standard. DNA bands were viewed on an IBI (International Biotechnologies, Inc., New Haven, CT) ultra violet light table.

2.5 Synthesis of Spectrin cDNA Fragments by PCR Amplification.

Primers a and b were two sense oligonucleotides (synthesized by National Biosciences, Hamel, MN). Their sequences were as follows:

Primer a: (5'- CGGGAATTCACTGGTTCCGCGTATGGAGCAATTTCCCAAGGAAACCGTT -3'),

Primer b: (5'- CGGGAATTCACTGGTTCCGCGTCGGGTTGCTGAGAGGGGTCAGAAGCTT -3').

They contained an *EcoRI* restriction endonuclease site (underlined), a 12-base sequence corresponding to the thrombin recognition/cleavage site with an amino acid sequence of LVPR (double underlined), and the sequences corresponding to amino acid residues 1 through 9 and 41 through 49 of the N-terminus of α -spectrin (amino acids 1 - 9 and 41 - 49), in a sense orientation (bold).

Six anti-sense oligonucleotides, Primers A, B, C, D, E and F as follows, were also synthesized:

Primer A: 5'- TAGTCTAGAGGGATCCCTATTCTTCGTGGGCAGAATGACCCAT -3',

Primer B: 5'- TAGTCTAGAGGGATCCCTAACACTCCTGTACATACTGCTGGAA -3',

Primer C: 5'- TAGTCTAGAGGGATCCCTACACATCCCTTTTGAATCGTTGTAA -3',

Primer D: 5'- TAGTCTAGAGGGATCCCTATAAGGGTAGGTCAGGATGGTTTTTC -3',

Primer E: 5'- TAGTCTAGAGGGATCCCTACTGAGGTGCATCTGAAGGATGGGA -3',

Primer F: 5'- TAGTCTAGAGGGATCCCTATTCATCAGAGGCTTCATGATTGGC -3'.

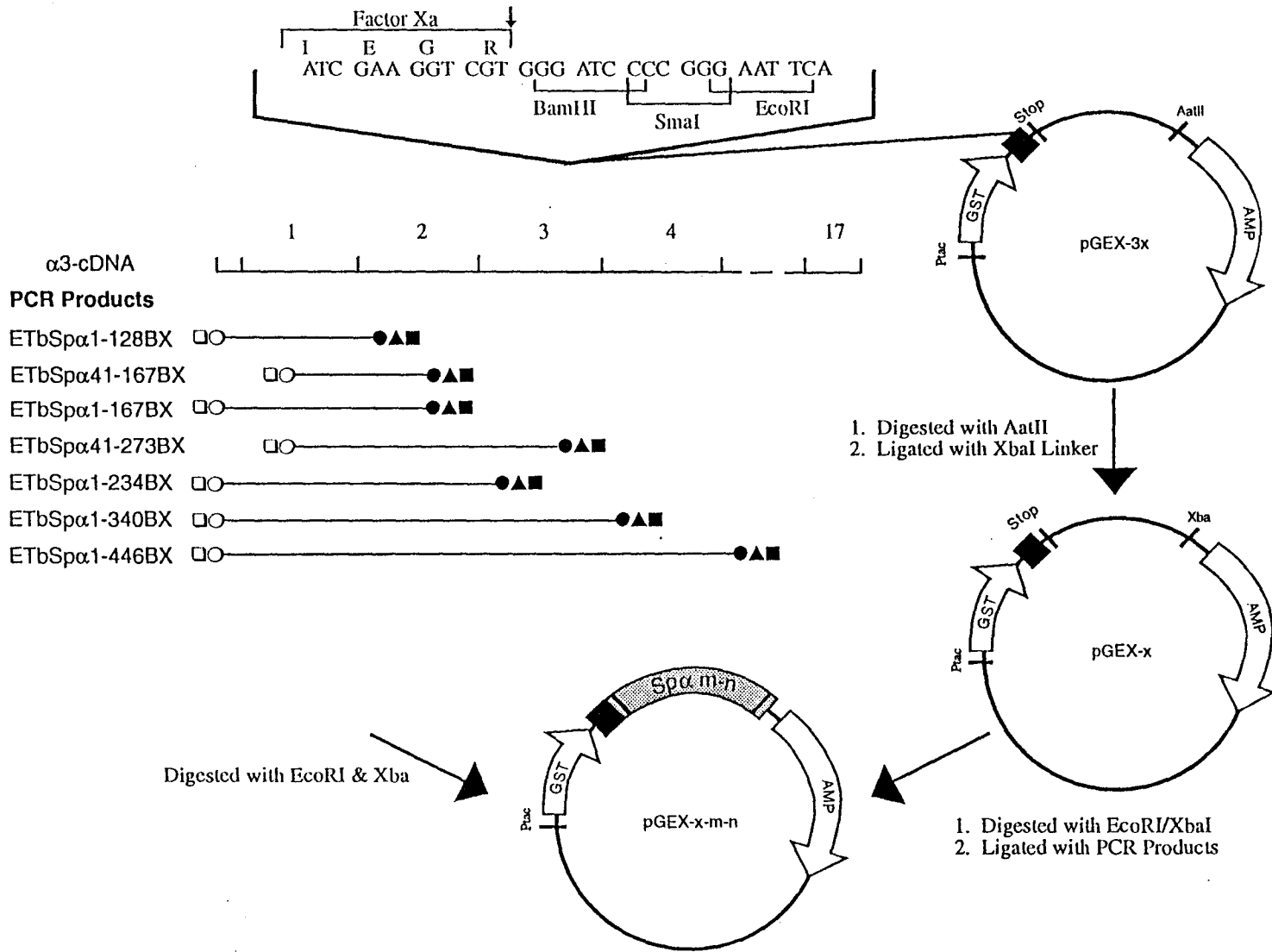
Primers A, B, C, D, E and F contained the sequences corresponding to amino acids 121 - 128, 160 - 167, 266 - 273, 227 - 234, 333 - 340 and 439 - 446 of α spectrin, respectively (bold). The primers also included a stop codon (italic), a *Bam*HI site (double underlined) and an *Xba*I site (underlined) at the 5' end.

The cDNA clone of spectrin, $\alpha 3$ (Sahr *et al.*, 1990), a generous gift from Dr. B. Forget of Yale University (New Haven, CT), was linearized by *Sac*II and used as the template. A reaction mixture (150 μ l) was prepared containing 15 μ l of the concentrated reaction buffer supplied by Gibco BRL Life Technologies Inc., 1.5 μ l of 10 mM dNTP, 1.5 μ l of either primer a (20 pmol/ μ l) paired with Primer A, B, C, D, E or F (20 pmol/ μ l) or Primer b (20 pmol/ μ l) paired with primer B or C (20 pmol/ μ l), 1 ng of template, 128 μ l of H₂O and 1 μ l of *Taq* polymerase (2 U/ μ l). This mixture was overlaid with 100 μ l of mineral oil and subjected to 30 rounds of temperature cycling: 95 °C, 30 s (denaturation); 55 °C, 2 min (annealing); 72 °C, 2 min (elongation) and a final incubation for 7 min at 72 °C in a thermal cycler (Eppendorf Microcycler) to give ETbSp α 1-128BX, ETbSp α 1-167BX, ETbSp α 1-234BX, ETbSp α 1-340BX, ETbSp α 1-446BX, ETbSp α 41-167BX or ETbSp α 41-273BX. The molecular masses (MWs) of the synthesized DNA fragments were found to match the calculated sizes.

2.6 Construction of Expression Vectors

Spectrin fusion protein expression vectors were constructed as shown in Fig. 1. The initial expression vector was pGEX-3x (Pharmacia, Piscataway, NJ) (Smith and Johnson, 1988), a

Figure 1 **Construction of GST:Sp α m-n fusion protein expression vectors.** Details are provided in text. The top line on the left represents the α 3 cDNA clone of spectrin. Each numbered section corresponds to a conventional 106 amino-acid homologous sequence motif. PCR products, ETbSp α 1-128BX, ETbSp α 41-167BX, ETbSp α 1-167BX, ETbSp α 41-273BX, ETbSp α 1-234BX, ETbSp α 1-340BX and ETbSp α 1-446BX, are depicted below the α 3 cDNA clone. Specific sites included in the primers are indicated by symbols: \square = *EcoRI*; \circ = thrombin cleavage site; \bullet = TAG stop codon; \blacktriangle = *BamHI*; \blacksquare = *XbaI*. The gene coding for glutathione-S-transferase fragment in the expression vector is indicated by GST. The amino acid sequence of the factor Xa cleavage site is displayed as single letters. The initial expression vector pGEX-3x was modified to give pGEX-x. Spectrin cDNA fragments were cloned into pGEX-x to give pGEX-x-m-n, where m and n were 1 and 128, 41 and 167, 1 and 167, 41 and 273, 1 and 234, 1 and 340, and 1 and 446, respectively.



glutathione S-transferase (GST) expression vector, which contained the coding sequence of the Factor Xa cleavage site followed by multiple cloning sites of *Bam*HI, *Sma*I and *Eco*RI. This expression vector was linearized by *Aar*II and blunt ended with dNTP and Klenow fragment. A non-phosphorylated *Xba*I linker (New England Biolabs, Beverly, MA) with stop codons (TAG) in all three reading frames was ligated into it to give the modified expression vector, pGEX-x. pGEX-x was digested with *Eco*RI and *Xba*I and dephosphorylated, then a PCR amplified spectrin cDNA fragment (ETbSp α 1-128BX, ETbSp α 41-167BX, ETbSp α 1-167BX, ETbSp α 41-273BX, ETbSp α 1-234BX, ETbSp α 1-340BX or ETbSp α 1-446BX) previously digested with *Eco*RI and *Xba*I was ligated to it, resulting in the pGEX-x-m-n spectrin fusion protein expression vector, where m and n were 1 and 128, 41 and 167, 1 and 167, 41 and 273, 1 and 234, 1 and 340 or 1 and 446, respectively.

All the synthesized DNA fragments contained an *Eco*RI site followed by the sequence coding for the thrombin cleavage site at the 5' end, a stop codon, a *Bam*HI site, and an *Xba*I site at 3' end to allow the amplified spectrin fragments to be cloned into several different vectors that we were working on. By including the thrombin recognition/cleavage site, digestion of fusion proteins with thrombin would occur exactly before the first amino acid residue of spectrin.

2.7 Expression of Spectrin Fragments as Cleavable Fusion Proteins with GST

An overnight culture of *E. coli* HB101 transformed with one of the fusion protein expression vectors was diluted twenty fold in fresh LB broth with an ampicillin concentration of 100 mg/l and was allowed to grow for about 2 h at 37 °C. When the mid-log phase ($OD_{600} = 0.6 - 1$) was reached, expression of the corresponding spectrin fusion protein was induced by adding IPTG to a final concentration of 0.1 mM. Induced cells were allowed to grow at 37 °C for another 4 - 6 h before being harvested by centrifugation at 5000 x g in a Sorvall RB-5C refrigerated centrifuge (Du Pont Company, Wilmington, DE). The supernatant was aspirated and, if necessary, the cell pellet was stored at -20 °C. The amount of fusion proteins was estimated, by densitometer scanning, to

comprise approximately 15 % of the total *E. coli* soluble proteins. The pGEX-x expression vector contained the *lacI^q* gene which allowed fusion proteins to be expressed at high levels upon IPTG induction regardless of the host strain used. Similar methods have been used to prepare other spectrin fragments (Dubreuil *et al.*, 1991; Kennedy *et al.*, 1991).

The apparent molecular masses of the fusion proteins were estimated from their band positions on a SDS electrophoresis gel, using molecular mass standards as references (described in section 2.12.2). The estimated MWs of the spectrin fragments were calculated from their amino acid sequences.

2.8 Purification of Fusion Proteins

Packed cells from one volume of culture were resuspended in 1/50 volume of 5 mM sodium phosphate, 150 mM sodium chloride, 1% Triton X-100, pH 7.4 and lysed by mild sonication on ice prior to centrifugation at 10,000 x g for 5 min at 4 °C. The supernatant was filtered through a 0.45 μ m filter and loaded onto a glutathione affinity column (GSH-Sepharose 4B from Pharmacia LKB Biotechnology, Piscataway, NJ or S-linker agarose from Sigma Chemical Company, St. Louis, MO), pre-equilibrated with 5 mM sodium phosphate, 150 mM sodium chloride, pH 7.4. The column with one of the fusion proteins bound was washed with 10 volumes of the same buffer, followed by elution of the fusion protein with 50 mM Tris, 5 mM glutathione at pH 8.

2.9 Thrombin Cleavage of Fusion Proteins

The protein concentration of purified fusion proteins was adjusted to about 1 mg/ml. The salt concentration of the protein samples was adjusted to 200 mM by 2 M sodium chloride stock solution. Thrombin (Sigma Chemical Company, St. Louis, MO) was added at an enzyme to substrate (E:S) molar ratio of either 1:500 or 1:1000. Cleavage reactions were carried out at room temperature for a set amount of time and cleavage results were evaluated by SDS gel

electrophoresis.

2.10 Purification of Sp α 41-273 and Sp α 1-446

The 8 h thrombin cleavage reaction mixture of Sp α 41-273 or Sp α 1-446 was loaded onto a glutathione affinity column pre-equilibrated with 5 mM sodium phosphate, 150 mM sodium chloride, pH 7.4. The protein was eluted at a flow rate of 40 ml/h. GST and the uncleaved fusion protein were absorbed by the column and the cleaved Sp α 41-273 or Sp α 1-446 was eluted. Protein fractions were pooled.

2.11 Removal of GSH

GSH in purified Sp α 41-273 and Sp α 1-446 was either free in solution or bound to sulfhydryl groups of spectrin fragments. Two different procedures were followed to remove the free and bound GSH. To remove the free GSH, a purified spectrin fragment was loaded directly onto a Sephadex G-25 (Pharmacia LKB Biotechnology, Piscataway, NJ) column pre-equilibrated with either 5 mM sodium phosphate, pH 7.4 (low salt buffer) or 5 mM sodium phosphate, 150 mM sodium phosphate, pH 7.4 (high salt buffer). Elution of the protein was carried out at a flow rate of 40 ml/h with the same buffer and protein fractions were pooled. To remove the bound GSH, β -mercaptoethanol (β -ME) at a final concentration of 45 mM was added to a purified spectrin fragment to reduce the bound GSH. The reaction was allowed to incubate on ice for 30 min prior to loading onto a Sephadex G-25 column pre-equilibrated with either the low salt or high salt buffer. The protein was eluted with the same buffer and fractions of the reduced protein were pooled.

2.12 Analysis of Proteins

2.12.1 Protein Concentration Assay

Protein concentrations were determined by a dye binding assay (Bradford, 1976) using the

assay kit provided by Bio-Rad (Richmond, CA). One volume of the dye reagent was diluted by four volumes of deionized H₂O and filtered through a Whatman filter paper prior to use. A series of BSA solutions with concentration of 0.2, 0.4, 0.6, 0.8 and 1 mg/ml were prepared as protein concentration standards. 5 ml of diluted reagent was added to a 100 μ l aliquot of each of the above BSA standards and protein samples for which concentrations were to be determined. Assay reaction mixtures were incubated at room temperature for 5 min and absorbances were measured at 595 nm using the diluted reagent as the blank. A₅₉₅ measurements of protein standards were plotted against their concentrations. The least squares linear fit of the data points was obtained as the calibration curve from which concentrations of unknown samples were obtained.

2.12.2 Protein SDS Polyacrylamide Gel Electrophoresis

The SDS polyacrylamide gel electrophoresis was carried out according to method of Laemmli with modifications (Laemmli, 1970). The electrophoresis sample was prepared by mixing equal volumes of protein solution with SDS sample loading buffer containing 100 mM tris acid, pH 6.8, 2% β -mercaptoethanol, 4% SDS, 0.2% bromophenol blue, 20% glycerol. The separating gel was made of 12-16% (w/v) acrylamide, 0.35-0.43% (w/v) N,N'-methylene bisacrylamide, 375 mM Tris (pH 8.8), 0.1% (w/v) SDS, 0.03% (w/v) ammonium persulfate, 0.07% (v/v) TEMED. The stacking gel was made of 3.8% (w/v) acrylamide, 0.1% (w/v) bisacrylamide, 125 mM Tris (pH 6.6), 0.05% (w/v) ammonium persulfate, 0.5% (v/v) TEMED. The electrophoresis was run in a Bio-Rad (Richmond, CA) mini-protein II electrophoresis cell under a constant voltage of 150 V. The gel was stained with a solution containing 0.25% (w/v) Coomassie Blue R-250, 40% (v/v) methanol, 7% (v/v) acetic acid, and subsequently destained with a solution containing 40% methanol and 10% acetic acid. The destained gels were shaken in 5% acetic acid for 30 min before being dried in a Bio-Rad model 543 gel dryer. Selected bands were scanned on an Isco model 1312 gel scanner and analyzed by a commercially available software (Chemresearch Chromatographic Data

Management Software from Isco, Lincoln, Nebraska).

Apparent MWs of proteins were estimated from the band positions on SDS polyacrylamide gels based on the relationship:

$$d = a + b \log MW$$

where d was the distance from the gel top to the middle of a protein band, a and b were constants obtained from the standard curve as discussed below, and MW was the apparent molecular weight of the protein. d values of protein standards were plotted against their $\log MW$ values and the linear fit of the data was used as a standard curve to give a and b values.

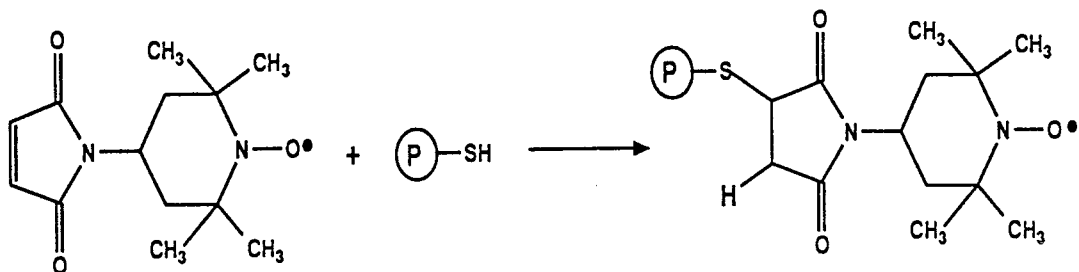
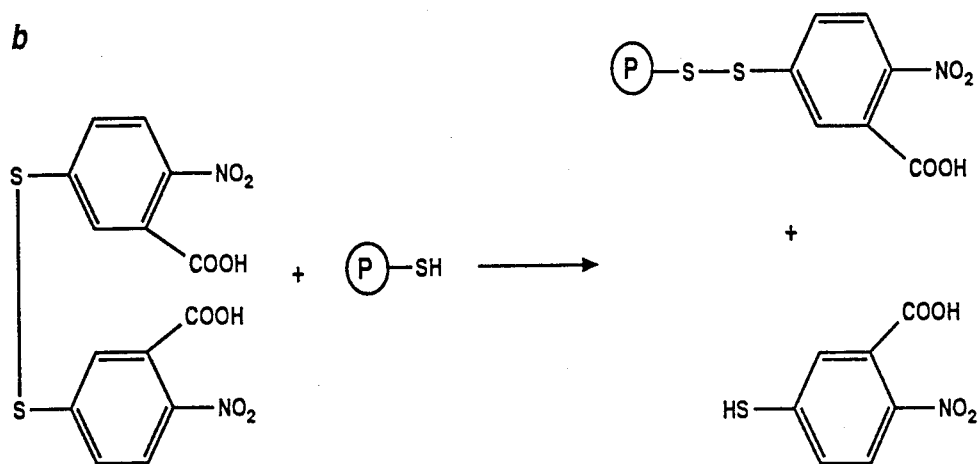
2.13 Spin Labeling

2.13.1 Native Samples

The nitroxide spin label Mal6 is a widely used sulfhydryl-specific spin label (Sandberg *et al.*, 1969; Schneider and Smith, 1970; Yu *et al.*, 1977; Fung and Simpson, 1979; Fung, 1981; Lai *et al.*, 1984; Kemple *et al.*, 1984). It can be attached selectively to free cysteine residues of a protein through covalent bonding to "report" detailed information on the local molecular environments of the labeling sites (Fig. 2a).

Mal6 was purchased from Aldrich Chemical Company, Inc. (Milwaukee, WI) and used without further purification. A 10^{-2} M Mal6 stock solution was prepared by dissolving 12.5 mg of Mal6 in 5 ml of acetonitrile. An aliquot of the Mal6 stock solution was measured into a vial and a very gentle stream of N_2 gas was applied to dry the spin labels as a thin film onto the wall of the vial in the dark. N_2 was continuously blown for another 20 min after the spin labels were dried. 1.5 mg of protein was then added to the vial. The labeling reaction was allowed to proceed at 4 °C for a desired amount of time with gentle stirring. Upon completion of the reaction, excess spin labels were removed with a Sephadex G-25 column equilibrated with either 5 mM sodium phosphate (pH 7.4) or 5 mM sodium phosphate, 150 mM sodium chloride (pH 7.4). The spin-labeled protein

Figure 2 **A schematic representation of Mal6 and DTNB reactions.** a, reaction of Mal6 (Sandberg *et al.*, 1969; Schneider and Smith, 1970; Yu *et al.*, 1977; Fung and Simpson, 1979; Fung, 1981; Lai *et al.*, 1984; Kemple *et al.*, 1984) with spectrin fragments (p-SH). b, reaction of DTNB with spectrin fragments (Ellman, 1959).

a**b**

sample of about 5 ml was then concentrated in a centricon-30 micro concentrator (Amicon, Lexington, Mass) to a final concentration of approximately 10 mg/ml by centrifugation (Sorvall SS34 rotor, 5000 rpm). Typically, an aliquot of 20 μ l of spin-labeled sample was taken for EPR measurements, another aliquot of 5 μ l sample was diluted 40 fold by 5 mM phosphate buffer (pH 7.4) for protein concentration assay and gel electrophoresis, and the remaining sample was frozen at -20 °C for future use.

To achieve selective labeling of specific cys residues to a specific extent, several conditions involving different Mal6/Sp ratios (μ l of 10^{-2} M Mal6 stock solution per mg of spectrin) and different lengths of labeling time were used in this study. The three most frequently used conditions were as follows: Mal6/Sp ratio of 40 μ l/mg for 1 h (the low spin label concentration and short time labeling condition); Mal6/Sp ratio of 40 μ l/mg for 16 h (the low spin label concentration and overnight labeling condition); Mal6/Sp ratio of 200 μ l/mg for 16 h (the high spin label concentration and overnight labeling condition).

2.13.2 Samples in Urea

Urea was added to Mal6-labeled protein samples in 5 mM sodium phosphate at pH 7.4 until final urea concentrations of 2, 3, 4, 5, or 6 M were obtained, respectively.

2.13.3 Urea-Treated Samples

The Mal6 labeling of urea-treated samples was performed according to two different procedures with a slightly different order of reaction steps.

In Procedure 1, Mal 6 labeling was performed in the presence of urea. Urea was added to 2 mg of protein (0.5 - 2 mg/ml) in 5 mM sodium phosphate buffer, pH 7.4, to yield a final urea concentration of 8 M. The spectrin fragment in 8 M urea was labeled by Mal6 according to the procedure previously described. The reaction mixture was dialyzed twice against 1 liter of 5 mM

sodium phosphate buffer at pH 7.4 for 1 h. The dialyzed sample was then eluted through a Sephadex G-25 column pre-equilibrated with the same buffer to ensure the complete removal of urea and excess spin labels. Pooled protein fractions were then concentrated to approximately 10 mg/ml, for which EPR measurements were taken.

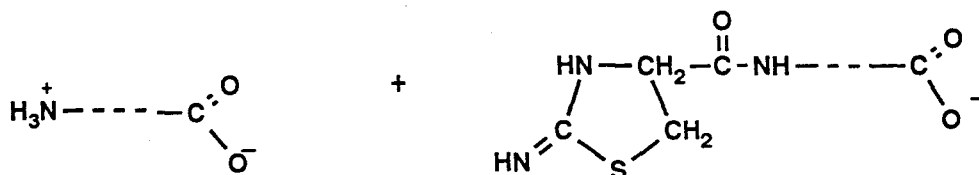
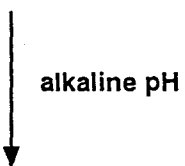
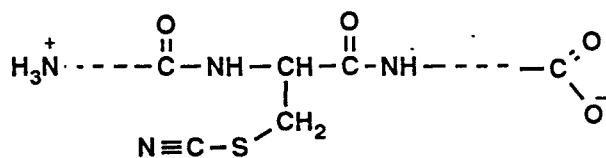
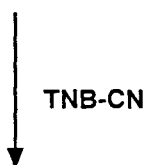
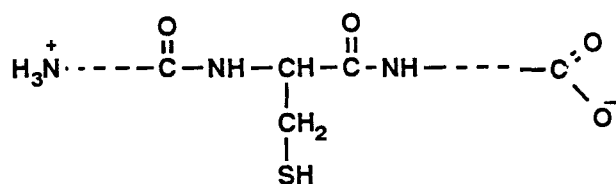
In Procedure 2, Mal6 labeling was performed after the removal of urea. Urea was added to 2 mg of protein (0.5 - 2 mg/ml) to yield a final urea concentration of 8 M and incubated overnight. The urea was then removed by two runs of 1 h dialysis against 1 liter of 5 mM sodium phosphate buffer at pH 7.4 and subsequent elution of the dialyzed sample through a Sephadex G-25 column pre-equilibrated with the same buffer. Protein fractions were then pooled and labeled by Mal6 according to the procedure described above.

2.14 TNB-CN Cleavage Reaction

TNB-CN is a sulfhydryl specific reagent (Catsimpoolas and Wood, 1966; Degani *et al.*, 1970; Jacobson *et al.*, 1973). It is capable of converting free cys residues in proteins to S-cyanocysteines. Cleavage of the amino peptide bond of the S-cyanocysteine residue is obtained upon its exposure to a basic pH at 37°C. The steps that are involved in modification and cleavage reactions are summarized in Fig. 3. Free and bound cys residues can be differentiated in a TNB-CN reaction based on the fact that the peptide bond next to a free cys residue can be cleaved in a TNB-CN reaction whereas the peptide bond next to a bound cys residue cannot be cleaved (Jacobson *et al.*, 1973).

The published procedure (Jacobson *et al.*, 1973) was followed to perform the TNB-CN cleavage reaction. Spectrin was either lyophilized or concentrated extensively to approximately 10 mg/ml. A portion of the either lyophilized or concentrated sample was dissolved in a solution of 8 M urea, 0.2 M tris acetate, 4×10^{-4} M β -ME at pH 8.5 to give a final protein concentration of 1.5 mg/ml and incubated at room temperature for 30 min. An aliquot of this mixture was set aside

Figure 3 **A flow chart of the TNB-CN modification and cleavage reaction (Jacobson et al., 1973).**



as a control sample. To the remainder, a 0.233 M (50 mg/ml) TNB-CN stock solution was added to yield a final TNB-CN concentration of 5.8 mM. Since the volume of the TNB-CN stock solution added was relatively small, the protein concentration in the reaction mixture was assumed to remain unchanged. The pH was re-adjusted to 8.5 using 1 M sodium hydroxide. All samples were incubated at room temperature for 15 min. The pH of the reaction mixture as well as that of the control sample were readjusted to 7.5 by addition of acetic acid. The cleavage reaction was carried out at 37°C for 48 h. At the end of the reaction an equal volume of SDS sample loading buffer containing 2% SDS and 1% β -ME was added to the TNB-CN reaction mixture. β -ME was used to quench the reaction. The samples were boiled and analyzed by SDS polyacrylamide gel electrophoresis.

2.15 DTNB Assay

The published procedure of the DTNB reaction (Ellman, 1959) (Fig. 2b) was followed. A 2 mM stock solution of GSH was freshly made by dissolving 15.4 mg of GSH in 25 ml H₂O immediately before the assay. Dilutions were made with 5 mM sodium phosphate (pH 7.4) to give 10, 20, 40, 60, 80, 120 and 160 μ M GSH standard solutions. A 2 mM DTNB stock solution was prepared by dissolving 0.198 g of DTNB in 250 ml of 5 mM phosphate buffer, pH 7.4. Equal volumes of a GSH standard solution and 2 mM DTNB stock solution were mixed and then incubated at room temperature for 2 min. Absorbances of reaction mixtures at 412 nm were measured using the mixture of 2 mM DTNB stock solution and buffer as the blank and plotted against GSH concentrations ([GSH]). The linear least squares fit of the data points was obtained as a calibration curve and the molar extinction coefficient of the yellow anion at 412 nm (ϵ_{412}) was read from the slope.

To determine the reactive sulfhydryl content in Sp α 41-273 and Sp α 1-446, nine volumes of a protein (0.5-1 mg/ml) were mixed with one volume of DTNB stock solution. The mixture was

incubated at room temperature for 1 h and its absorbance at 412 nm (A_{rxn}) was taken using a mixture of nine volumes of buffer and one volume of DTNB as the blank. To subtract away the contribution of the absorbance of the protein at 412 nm from the total absorption at 412 nm, A_{protein} was also obtained. A_{protein} was the absorbance of a mixture of nine volumes of protein with one volume of buffer at 412 nm. The absorbance of the reaction mixture at 412 nm contributed by the yellow anion resulted from the reaction (A_{412}) was calculated as:

$$A_{412} = A_{\text{rxn}} - A_{\text{protein}}$$

The concentration of the sulfhydryl in protein that was reactive to DTNB ([SH]) was calculated according to the formula:

$$[\text{SH}] = A_{412}/\epsilon_{412}$$

The number of reactive sulfhydryls per protein fragment (SH/Sp ratio) was calculated from the concentration of the reactive sulfhydryl ([SH]) and the concentration of the protein ([Sp]) as:

$$\text{SH/Sp} = [\text{SH}]/[\text{Sp}]$$

2.16 Combination of Mal6 and DTNB Reactions

The 2 mM DTNB stock solution was added to a spectrin sample (0.5-1 mg/ml) to give a final DTNB concentration of 0.2 mM. The reaction was allowed to proceed at 4 °C for 4 h. The reaction mixture was eluted through a Sephadex G-25 column pre-equilibrated with 5 mM sodium phosphate buffer and pH 7.4 at a flow rate of 40 ml/h. Protein fractions were pooled and the protein concentration was determined. 1.5 mg of this DTNB-reacted protein (0.2-0.75 mg/ml) was then spin labeled by Mal6 according to the procedure described in section 2.13.1.

2.17 EPR Measurements

EPR measurements were taken on a Varian E-109 EPR spectrometer. A scientific program, ASYST (MacMillan Software), modified for EPR operation was used for data acquisition and data

analysis on a Zenith personal computer. The usual EPR instrumental parameters were: incident microwave power, 1 mW; center of the field, 3250 gauss; scan range, 100 gauss; modulation amplitude, 1 gauss; time constant, 0.128; receiver gain, 10×10^3 ; scan time, 60 sec.

All the EPR measurements were taken either at room temperature (about 21 °C) or at specified temperatures. The cavity temperature was controlled by an IBM variable temperature control unit. The actual temperature of the cavity was monitored by a digital thermometer with a thermocouple immersed into the silicon fluid of the quartz tube within the cavity. Simultaneously, a water bath was pre-warmed to 2 °C below the cavity temperature upon heating or 2 °C above the cavity temperature upon cooling. The spin-labeled sample was incubated in the water bath while the temperature of the cavity was being adjusted. Once the cavity reached the set temperature, the spin-labeled sample was placed into the quartz tube. 1 min of incubation was allowed for the temperature of the sample to reach an equilibrium with the temperature of the cavity before an EPR spectrum was recorded.

Approximately 20 μ l of EPR sample contained in a glass capillary tube was placed into the cavity with a standard quartz tube half filled with silicon fluid.

2.18 EPR Data Analysis

2.18.1 SL/Sp ratio

Spin label concentrations ([SL]) were determined from double integration of the EPR spectra of spin-labeled samples. Protein concentrations ([Sp]) were determined as described previously.

Number of spin labels bound per spectrin molecule (SL/Sp ratio) was calculated as:

$$SL/Sp = [SL]/[Sp].$$

2.18.2 Spectral Parameters

An EPR spectrum (see Fig. 14, section 3.3.1.2.1) was analyzed by measuring the outer

hyperfine extrema ($2A_{zz}$), sensitive to the motion and environment of the labeling sites, and the peak height of the high field weakly immobilized signal (W'), sensitive to the percentage of the weakly immobilized component in the system. Widths of the low field and high field weakly immobilized signals, ΔH_{pp} and $\Delta H_{pp}'$ were also measured for spin-labeled Sp α 41-273 at different temperatures to determine the rotational motions of the weakly immobilized component as a function of temperature. Spin label concentrations of spin-labeled samples were obtained from double integration of the first derivative EPR spectra.

2.18.3 Spectral Addition

EPR spectra of singly-labeled Sp α 1-446 (labeled at site 1) and DTNB-treated Sp α 1-446 (labeled at site 2) were added digitally using the modified ASYST software to construct a composite EPR spectrum. An example of spectral addition is given as follows. A was an EPR spectrum of Sp α 1-446 in 5 mM sodium phosphate, pH 7.4, with a SL/Sp ratio of 0.82. B was an EPR spectrum of DTNB-treated Sp α 1-446 in 5 mM sodium phosphate, pH 7.4, with an SL/Sp ratio of 0.88. C was an EPR spectrum of Sp α 1-446 labeled at both site 1 and site 2 with an SL/Sp ratio of 1.3. To construct C', the composite EPR spectrum of Sp α 1-446 with an SL/Sp ratio of 1.3, A and B were both normalized to the amplitude of C by the central peak. Assuming that one label of the total 1.3 labels on each Sp α 1-446 was associated with site 1 and the remaining 0.3 label was associated site 2, A was multiplied by a factor of $1/1.3 = 0.77$ and B was multiplied by a factor of $0.3/1.3 = 0.23$ before the two spectra were added.

2.18.4 Spectral Subtraction

Spectral subtraction was performed for EPR samples of Sp α 41-273 according to Fung and Johnson (1983) using the modified ASYST program.

An EPR spectrum of Sp α 41-273 in 5 mM sodium phosphate at pH 7.4 treated with 5 M

urea was used to remove the weakly immobilized component in an EPR spectrum of Sp α 41-273 in 5 mM sodium phosphate, pH 7.4. The EPR spectrum of Sp α 41-273 in 5 M urea was normalized to the amplitude of the EPR spectrum Sp α 41-273 in 5 mM sodium phosphate at pH 7.4 by the central peak. The normalized EPR spectrum of Sp α 41-273 in 5 M urea was multiplied by a scaling factor such that, after the subtraction, the weakly immobilized component of the EPR spectrum of Sp α 41-273 in 5 mM sodium phosphate at pH 7.4 was subtracted completely.

The spin label concentration was calculated from the double integration of the EPR spectrum. If the spin label concentration obtained from an EPR spectrum of Sp α 41-273 in 5 mM sodium phosphate (pH 7.4) was a and the spin label concentration of the resulting EPR spectrum of the strongly immobilized component is b , the percentage of the strongly immobilized component was calculated as b/a . The percentage of the weakly immobilized component was calculated as $1 - b/a$.

2.19 Stokes Radius Determination

2.19.1 Native Samples

The Stokes radii (R_s) of native Sp α 41-273 and Sp α 1-446 in low salt buffer (5 mM sodium phosphate, pH 7.4) and high salt buffer (5 mM sodium phosphate, 150 mM sodium chloride, pH 7.4) were estimated using a 1.5 cm x 80 cm Sepharose 4B column. The column was equilibrated with high salt buffer and calibrated by thyroglobulin (669 kD, 85.0 Å), ferritin (440 kD, 61.0 Å), catalase (232 kD, 52.2 Å), BSA (67 kD, 35.5 Å) and hemoglobin (64 kD, 31.0 Å) (LaBrake, 1993). The partition coefficient (K_{av}) of each protein was calculated as $K_{av} = (V_e - V_o)/(V_t - V_o)$, where V_e = the elution volume of the solute, V_o = the void volume and V_t = the total bed volume (Ackers, 1964; Laurent and Killander, 1964). V_o was determined by elution of blue Dextran (average MW 2,000,000) through the column. Partition coefficients of the protein standards were plotted against their $\log(R_s)$ values. The regression line, $\log(R_s) = 2.56 - 1.29 K_{av}$, was used as the calibration

curve to calculate the Stokes radii of spectrin fragments under different conditions. Normally, 1 ml of 1 mg/ml protein in low salt or high salt buffer was loaded onto the Sepharose 4B column pre-equilibrated with the same buffer. The protein was eluted at a speed of 23 ml/h.

2.19.2 Urea Treatment

Urea was added to protein samples in 5 mM sodium phosphate buffer, pH 7.4, to give a final urea concentration of 8 M and incubated at 4 °C overnight. Urea was then removed by three runs of 8 h dialysis (molecular porous membrane tubing 2, Spectrum, Los Angeles, CA) against 1 liter of the same buffer (urea-treated samples). The Stokes radii of the urea-treated samples in low salt buffer were estimated under similar setting as described in section 2.19.1.

2.19.3 Heat Treatment

Boiled protein samples in 5 mM sodium phosphate buffer, pH 7.4, were heated in a 100 °C water bath for 5 - 10 min. Temperature-cycled samples were heated gradually to approximately 80 °C at 2 - 10 °C temperature intervals (2 - 5 min) followed by gradual cooling to room temperature at similar intervals. The Stokes radii of the boiled and heat-treated samples in low salt buffer were estimated under similar setting as described in section 2.19.1.

CHAPTER III

RESULTS

3.1 Spectrin Fragments Expression and Purification

3.1.1 Expression of Spectrin Fragments as Fusion Proteins with GST

The seven cDNA fragments, ETbSp α 1-128BX, ETbSp α 41-167BX, ETbSp α 1-167BX, ETbSp α 41-273BX, ETbSp α 1-234BX, ETbSp α 1-340BX, and ETbSp α 1-446BX (Fig. 1), corresponding to spectrin α -subunit amino acid residues 1 to 128, 41 to 167, 1 to 167, 41 to 273, 1 to 234, 1 to 340, and 1 to 446, respectively, were synthesized by PCR. These seven cDNA fragments were successfully cloned into the GST fusion protein expression vector pGEX-x.

Fusion proteins, GST:Sp α 1-128, GST:Sp α 41-167, GST:Sp α 1-167, GST:Sp α 41-273, GST:Sp α 1-234, GST:Sp α 1-340 and GST:Sp α 1-446, were expressed and SDS electrophoresis data are shown in Fig. 4. Lanes 1 of Fig. 4a (12% gel) and 4b (15% gel) are high molecular weight and low molecular weight protein standards, respectively. The whole cell extract of *E. coli* **HB101** transformed with the expression vector pGEX-x is as shown in lanes 2 of Fig. 4a and 2b. Major bands (indicated by *) with apparent MWs of 25 and 26 kD were observed, suggesting that these were GST bands since the estimated MW of GST is 26 kD (Smith and Johnson, 1986). The whole cell extracts of *E. coli* **HB101** transformed with spectrin fusion expression vectors pGEX-x-1-128, pGEX-x-1-234, pGEX-x-1-340, pGEX-x-1-446, pGEX-x-1-167, pGEX-x-41-167 and pGEX-x-41-273 are shown in lanes 3 - 6 of Fig. 4a and lanes 3 - 5 of Fig. 4b, respectively. Major bands (indicated by \rightarrow) with apparent MWs of 40, 52, 64, 77, 43, 39 and 49 kD were observed in the

Figure 4 **SDS polyacrylamide electrophoresis gels (12 % for a and 15 % for b) stained with 0.25 % Coomassie brilliant blue R.** These gels (0.5 mm thick) were run for about 40 min under a constant voltage of 150 V. a, lane 1: high molecular weight protein standards (kD); lanes 2, 3, 4, 5 and 6: total cell extracts of *E. coli* **HB101** harbored with pGEX-x, pGEX-x-1-128, pGEX-x-1-234, pGEX-x-1-340 and pGEX-x-1-446, respectively; lanes 7, 8, 9 and 10: purified fusion proteins GST:Sp α 1-128, GST:Sp α 1-234, GST:Sp α 1-340 and GST:Sp α 1-446, respectively. b, lane 1: low molecular weight protein standards (kD); lanes 2, 3, 4 and 5: total cell extracts of *E. coli* **HB101** harbored with pGEX-x, pGEX-x-1-167, pGEX-x-41-167 and pGEX-x-41-273, respectively; lanes 6, 7 and 8: purified fusion proteins GST:Sp α 1-167, GST:Sp α 41-167 and GST:Sp α 41-273, respectively. The positions of the GST bands are indicated by * and those of fusion protein bands by \rightarrow .

corresponding lanes. The estimated MWs of GST:Sp α 1-128, GST:S α 1-234, GST:S α 1-340, GST:S α 1-446, GST:S α 1-167, GST:S α 41-167 and GST:S α 41-273 are 41.1, 53.5, 65.4, 74.6, 45.9, 41.1 and 53.3 kD, respectively. Apparent MWs of the fusion proteins were shown to match their estimated values to within 5 kD, suggesting that the desired fusion proteins were obtained. A summary of the apparent and estimated MWs of the fusion proteins is shown in Tables 1a and 1b.

3.1.2 Fusion Protein Purification

Using the procedure described in section 2.8, approximately 3 -25 mg of fusion protein was purified from each liter of *E.coli* cell culture as shown in Table 1a. Lanes 7 - 10 of Fig. 4a and lanes 6 - 8 of Fig. 4b contained purified fusion proteins GST:Sp α 1-128, GST:Sp α 1-234, GST:Sp α 1-340, GST:Sp α 1-446, GST:Sp α 1-167, GST:Sp α 41-167 and GST:Sp α 41-273, respectively. Major bands (indicated by \rightarrow) were considered as those of the fusion proteins. Their estimated MWs were determined to be 40, 52, 64, 77, 43, 39 and 49 kD, respectively. Relatively pure fusion proteins were obtained for GST:Sp α 1-167 (lane 6, Fig. 4b), GST:Sp α 1-234 (lane 8, Fig. 4a), GST:Sp α 1-340 (lane 9, Fig. 4a) and GST:Sp α 1-446 (lane 10, Fig. 4a). Several other bands, mostly light bands with MWs lower than those of the fusion proteins, were observed in addition to the major fusion protein bands for GST:Sp α 1-128 (lane 7, Fig. 4a), GST:Sp α 41-167 (lane 7, Fig. 4b) and GST:Sp α 41-273 (lane 8, Fig. 4b), to a lesser degree, GST:Sp α 1-167 (lane 6, Fig. 4b), GST:Sp α 1-234 (lane 8, Fig. 4a) and GST:Sp α 1-340 (lane 9, Fig. 4a). Those light bands were presumably degradation products of the fusion proteins generated during the process of purification. The yield of a fusion protein appeared to correlate with its size (Table 1a).

3.1.3 Thrombin Cleavage of Fusion Proteins

SDS electrophoresis results of thrombin cleavage of fusion proteins are shown in Fig. 5.

Table 1a

Estimated and Apparent Molecular Masses of Fusion Proteins of Spectrin fragments with GST

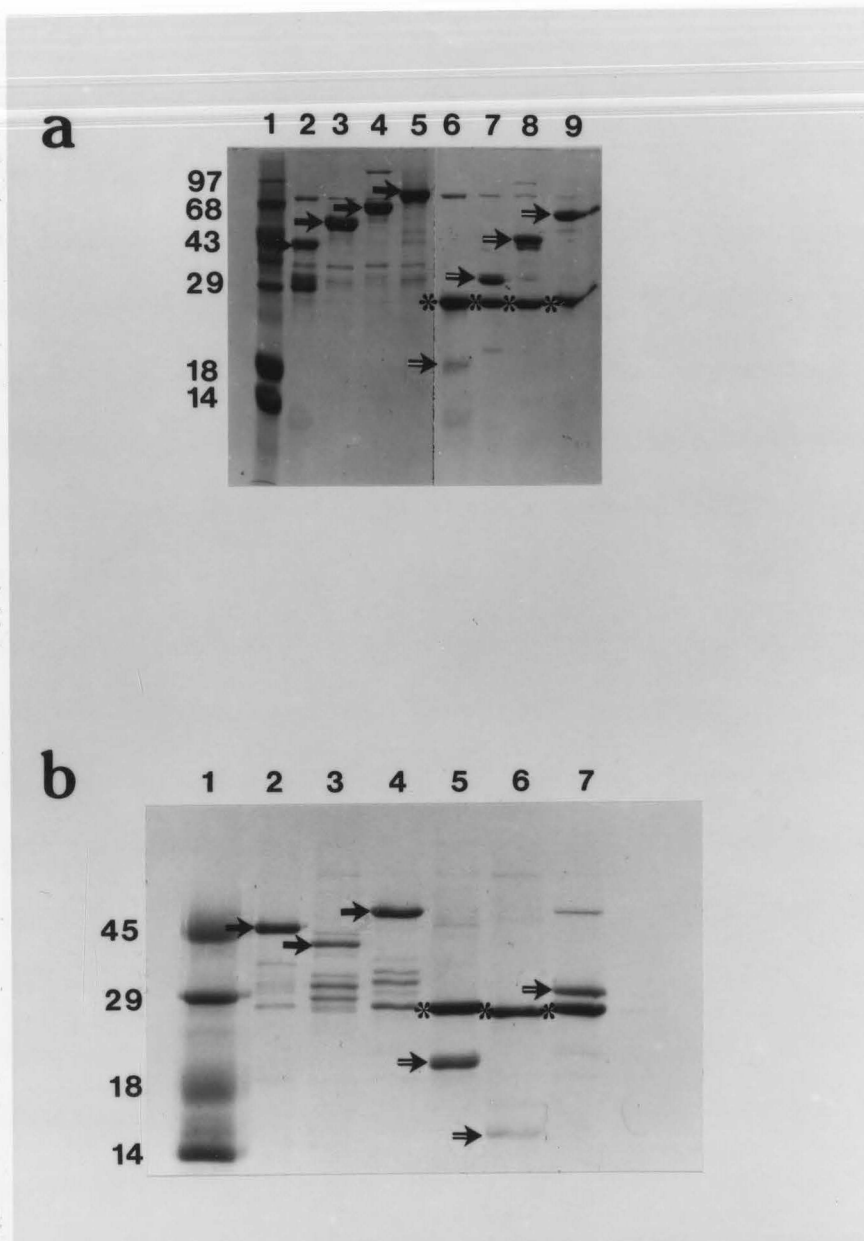
| Protein | Estimated MW (kD) | Apparent MW (kD) | | | | Yield (mg Protein/l of Cell) |
|------------------------|-------------------|------------------|---------|---------|---------|---------------------------------|
| | | Fig. 4a | Fig. 4b | Fig. 5a | Fig. 5b | |
| GST:Sp α 1-128 | 41.1 | 40 | - | 40 | - | 3 \pm 0 (n=2) |
| GST:Sp α 41-167 | 41.1 | - | 39 | - | 40 | 5 \pm 0 (n=2) |
| GST:Sp α 1-167 | 45.9 | - | 43 | - | 44 | 13 \pm 3 (n=2) |
| GST:Sp α 41-273 | 53.3 | - | 49 | - | 50 | 24 \pm 3 (n=5) |
| GST:Sp α 1-234 | 53.5 | 52 | - | 50 | - | 10 \pm 1 (n=2) |
| GST:Sp α 1-340 | 65.4 | 64 | - | 68 | - | 10 \pm 4 (n=2) |
| GST:Sp α 1-446 | 74.6 | 77 | - | 76 | - | 21 \pm 6 (n=2) |
| GST | | 25 | 26 | 25 | 27 | |

Table 1b

Estimated and Apparent Molecular Masses of Spectrin fragments and GST

| Protein | Estimated MW (kD) | Apparent MW (kD) | | |
|--------------------|-------------------|------------------|---------|--------|
| | | Fig. 5a | Fig. 5b | Fig. 6 |
| Sp α 1-128 | 15.1 | 17 | - | - |
| Sp α 41-167 | 15.1 | - | 16 | - |
| Sp α 1-167 | 19.9 | - | 21 | - |
| Sp α 41-273 | 27.3 | - | 31 | 30 |
| Sp α 1-234 | 27.5 | 31 | - | - |
| Sp α 1-340 | 39.4 | 40 | - | - |
| Sp α 1-446 | 51.6 | 50 | - | 52 |
| GST | 26 | 25 | 27 | - |

Figure 5 SDS polyacrylamide electrophoresis gels (12% for a and 15 % for b) stained with 0.25 % Coomassie brilliant blue R. These gels (0.5 mm thick) were run for about 40 min under a constant voltage of 150 V. Lanes 1 in a and b are low molecular weight standards (kD). GST:Sp α 1-128, GST:Sp α 1-234, GST:Sp α 1-340, GST:Sp α 1-446, GST:Sp α 1-167, GST:Sp α 41-167 and GST:Sp α 41-273 incubated for 24 h in the reaction buffer are shown in a, lanes 2, 3, 4 and 5 & b, lanes 2, 3 and 4, respectively. Their 24-hour thrombin reaction mixtures with an enzyme to substrate molar ratio of 1:500 are shown in a, lanes 6, 7 and 8 and 9 & b, lanes 5, 6 and 7, respectively. The positions of the fusion protein bands are indicated by \rightarrow , those of GST bands by * and those of the cleaved spectrin bands by \Rightarrow .



lanes 6 - 8 of Fig. 5a, respectively, were presumably the non-specific degradation products of Spa1-128, Spa1-234 and Spa1-340. The apparent and estimated MWs of sporein fragments are summarized in Table 1b.

Lanes 1 of Fig. 5a (12% gel) and 5b (15% gel) are high molecular weight and low molecular weight protein standards, respectively. Fusion proteins, GST:Sp α 1-128, GST:Sp α 1-234, GST:Sp α 1-340, GST:Sp α 1-446, GST:Sp α 1-167, GST:Sp α 41-167 and GST:Sp α 41-273, incubated in the thrombin reaction buffer without thrombin for 24 h are shown in lanes 2 - 5 of Fig. 5a and lanes 2 - 4 of Fig. 5b, respectively. Major bands with MWs of 40, 50, 68, 76, 44, 40 and 50 were observed and assigned to be fusion proteins, suggesting that, after 24 h of incubation in the reaction buffer without thrombin, fusion proteins stayed mostly intact. The 24-hour thrombin cleavage reaction mixtures of fusion proteins, GST:Sp α 1-128, GST:Sp α 1-234, GST:Sp α 1-340, GST:Sp α 1-446, GST:Sp α 1-167, GST:Sp α 41-167 and GST:Sp α 41-273, are shown in lanes 6 - 9 of Fig. 5a and lanes 5 - 7 of Fig. 5b, respectively, exhibiting the cleavage of fusion proteins by thrombin released spectrin fragments from the GST carrier. A relatively clean thrombin cleavage of GST:Sp α 1-167 (lane 5, Fig. 5b), GST:Sp α 41-167 (lane 6, Fig. 5b), GST:Sp α 41-273 (lane 7, Fig. 5b) and GST:Sp α 1-446 was obtained (lane 9, Fig. 5a), resulting in two bands in each lane. Bands with apparent MWs of 25 kD (indicated by *) were assigned to be GST and bands with an apparent MWs of 21, 16, 31 and 50 kD (indicated by \Rightarrow) were assigned to be spectrin fragments. The estimated MWs of Sp α 1-167, Sp α 41-167, Sp α 41-273 and Sp α 1-446 are 19.9, 15.1, 27.3 and 51.6 kD, respectively.

However, the cleavage of GST:Sp α 1-128 (lane 6, Fig. 5a), GST:Sp α 1-234 (lane 7, Fig. 5a) and GST:Sp α 1-340 (lane 8, Fig. 5a) by thrombin under the same condition resulted in single-band GST (indicated by *) and multiple-band cleavage products (lanes 6 - 8, Fig. 5a, respectively). Apparent MWs of the top cleavage bands (indicated by \Rightarrow) in the above lanes were 17, 31 and 40 kD, respectively, matching the estimated MWs of Sp α 1-128 (15.1 kD), Sp α 1-234 (27.5 kD) and Sp α 1-340 (39.4 kD) quite well. Those bands with apparent MWs lower than 17, 31 and 40 kD in lanes 6 - 8 of Fig. 5a, respectively, were presumably the non-specific degradation products of Sp α 1-128, Sp α 1-234 and Sp α 1-340. The apparent and estimated MWs of spectrin fragments are summarized in Table 1b.

3.1.4 Sp α 41-273 and Sp α 1-446 Purification

Fig. 6 shows a typical SDS polyacrylamide electrophoresis gel (15%) of the purified Sp α 41-273 (lane 2) and Sp α 1-446 (lane 3) with molecular weight standards (lane 1). Apparent MWs of purified Sp α 41-273 and Sp α 1-446 were 30 and 52 kD, respectively (Table 1b). While a single band was observed for Sp α 41-273 (lane 2, Fig. 6), two additional minor bands with apparent MWs of 49 kD and 47 kD were observed for Sp α 1-446 (lane 3, Fig. 6). Densitometer tracing of gels of two typical Sp α 1-446 preparations showed an average intensity of $93.4\% \pm 3.2\%$ ($n = 2$) for the 52 kD band. The two minor bands were assumed to be partial degradation products of Sp α 1-446.

3.2 Accessibility of Sulfhydryl Groups in Sp α 41-273 and Sp α 1-446

3.2.1 Spin Labeling

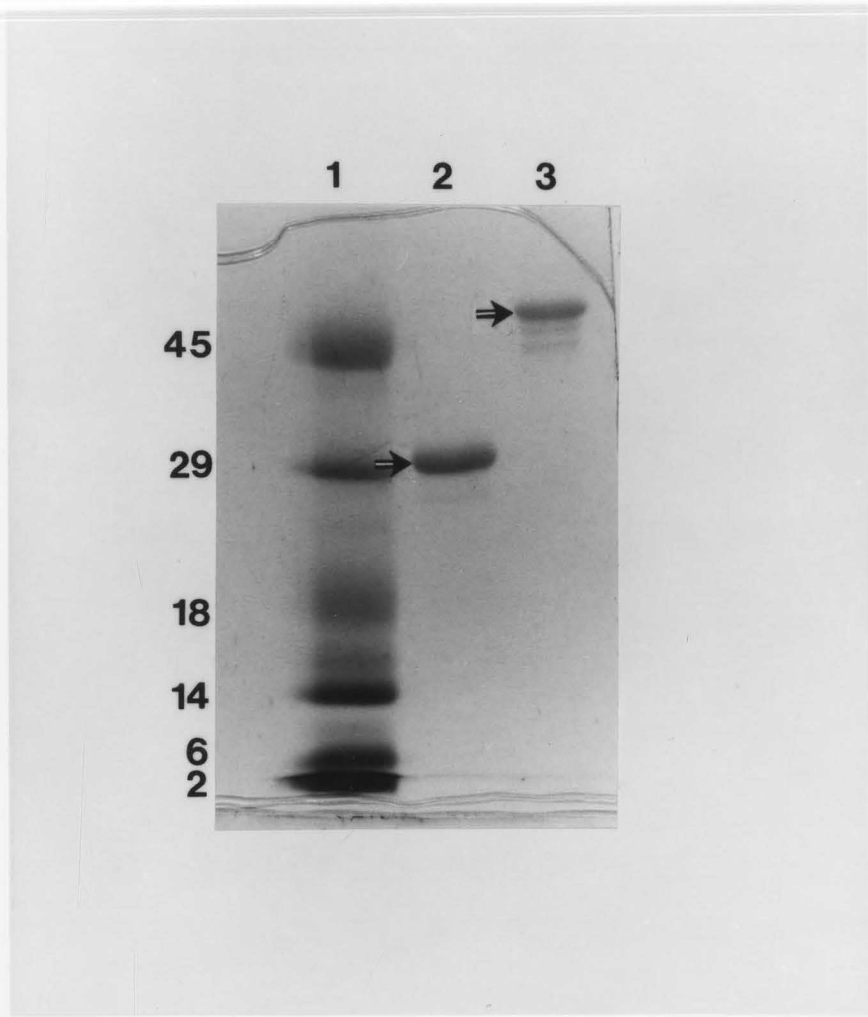
3.2.1.1 Number of Labeling Sites in Native Samples

The amino acid sequence of α -spectrin reveals that cysteines are at positions 167, 224 and 324. Thus there are two cys residues in Sp α 41-273 sequence and there are three cys residues in Sp α 1-446 sequence. The accessibility of these cys residues was probed by Mal6 (Sandberg *et al.*, 1969; Schneider and Smith, 1970; Yu *et al.*, 1977; Fung and Simpson, 1979; Fung, 1981; Lai *et al.*, 1984; Kemple *et al.*, 1984) (Fig. 2a).

Maximal SL/Sp ratios of 0.94 ± 0.04 ($n = 4$) for Sp α 41-273 and 2.04 ± 0.10 ($n = 4$) for Sp α 1-446 were obtained when 1 mg of spectrin was allowed to react with 200 μ l of 10^{-2} M Mal6 (corresponding to a Mal6 to spectrin molar ratio of 54:1) at 4 °C for longer than 12 h in 5 mM sodium phosphate (pH 7.4).

Before the maximal SL/Sp ratio was reached, the SL/Sp ratio of Sp α 41-273 was shown to increase with both the Mal6/Sp ratio and labeling time. Fig. 7 shows the relationship between the

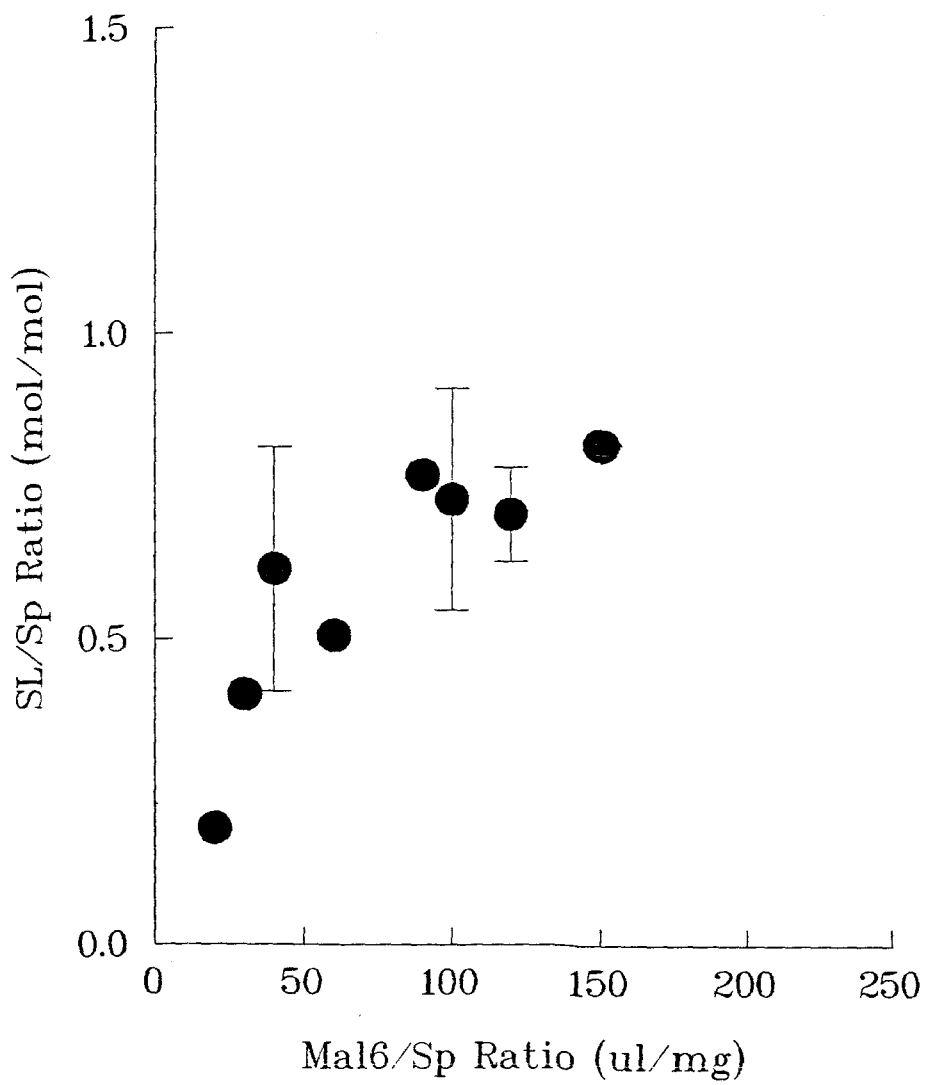
Figure 6 **SDS polyacrylamide electrophoresis gels (15 %) stained with 0.25 % Coomassie brilliant blue R.** The gel (0.5 mm thick) was run for about 40 min under a constant voltage of 150 V. lane 1: low molecular weight protein standards (kD); lane 2: purified Sp α 41-273; lane 3: purified Sp α 1-446. The positions of the spectrin bands are indicated by \Rightarrow .



Fig

Spa41-373

Figure 7 **Relationship between Mal6/Sp ratio and the SL/Sp ratio of Sp α 41-273.**
Samples were labeled at varying Mal6/Sp ratios for about 16 h.



Mal6/Sp ratio and the SL/Sp ratio of Sp α 41-273. Samples were labeled at varying Mal6/Sp ratios for about 16 h. The average SL/Sp ratio was shown to initially increase with the Mal6/Sp ratio and then level off when a Mal6/Sp ratio of greater than 90 μ l/mg (corresponding to a Mal6 to spectrin molar ratio of 25:1) was used. Fig. 8 shows the relationship between labeling time and the SL/Sp ratio of Sp α 41-273. Samples were labeled for varying amounts of time at a Mal6/Sp ratio of 120 - 150 μ l/mg (corresponding to a Mal6 to spectrin molar ratio of 33 - 41). The average SL/Sp ratio was shown to initially increase with labeling time and then level off when longer than 36 h labeling was applied. Increase in both the Mal6/Sp ratio and the labeling time were not able to bring the SL/Sp ratio of Sp α 41-273 to higher than 1. A similar saturation behavior was observed for Sp α 1-446 at a SL/Sp ratio of around 2.

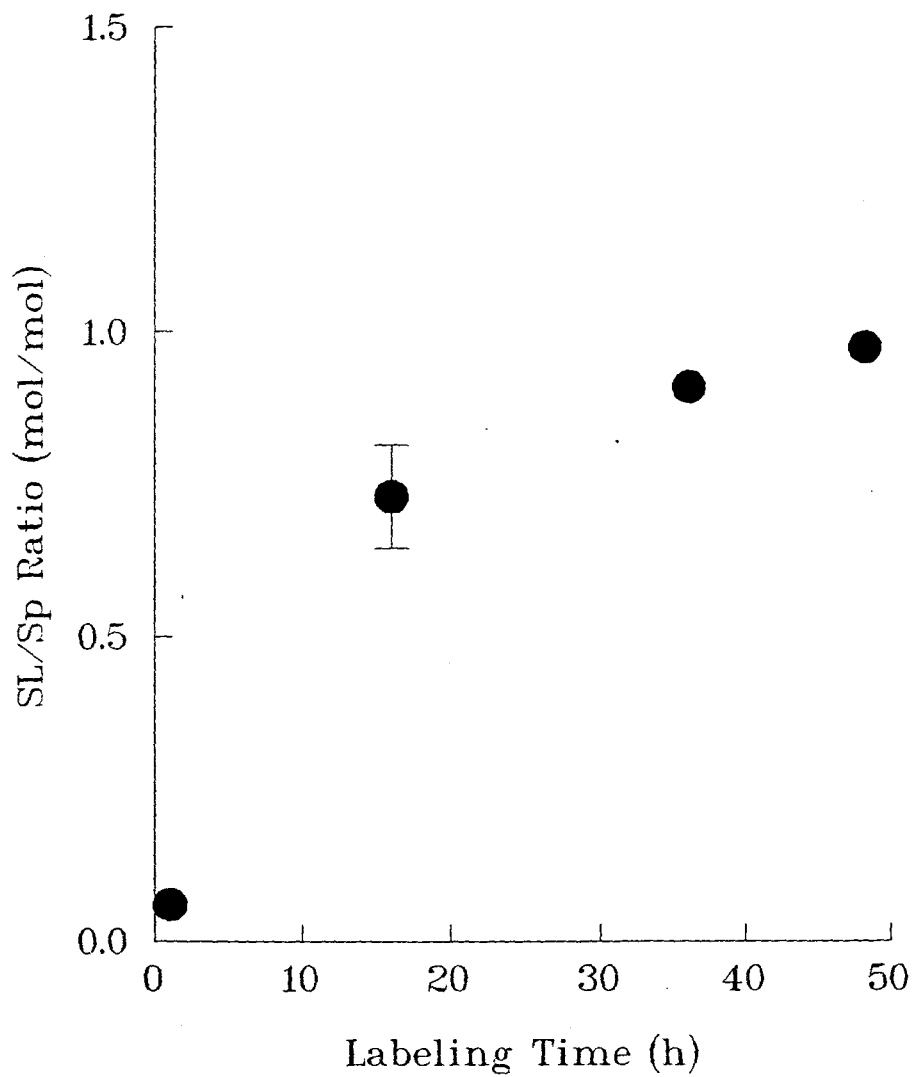
The above results suggested that there was one cys residue in Sp α 41-273 accessible to Mal6 and that there were two cys residues in Sp α 1-446 accessible to Mal6 under the same labeling condition.

3.2.1.2 Number of Labeling Sites in the Presence of Urea

In order to verify that there were indeed two cys residues in the Sp α 41-273 and three cys residues in the Sp α 1-446, we carried out the spin-labeling studies of Sp α 41-273 and Sp α 1-446 in the presence of urea. The rationale is that, if not all the cys residues are available for labeling owing to the folding and if urea unfolds proteins, as a protein denaturant, all the cys residues of Sp α 41-273 and Sp α 1-446 should be readily accessible when they are labeled in the presence of urea.

Mal6-labeling was performed in 8 molar urea according to Procedure 1 in section 2.13.3. An average SL/Sp ratio of 1.8 ± 0.1 ($n = 4$) was obtained for Sp α 41-273 in the presence of 8 M urea when varying Mal6/Sp ratios of 40 - 120 μ l/mg (corresponding to Mal6 to spectrin molar ratios of 8 - 33) were used. An increase of the Mal6/Sp ratio from 40 to 120 μ l/mg did not appear to bring about further increase of the SL/Sp ratio. The results suggested that there were, at maximum,

Figure 8 **Relationship between labeling time and the SL/Sp ratio of Sp α 41-273.** Samples were labeled for varying amounts of time at a Mal6/Sp ratio of 120 - 150 μ l/mg (corresponding to a Mal6 to spectrin molar ratio of 33 - 41).



two cys residues in Sp α 41-273 available for labeling, which was coherent with what was learned from the sequence information.

Meantime, an average SL/Sp ratio of 2.0 ± 0.2 ($n = 3$) was obtained for Sp α 1-446 in the presence of 8 M urea when a Mal6/Sp ratio of 40 ul/mg (corresponding to a Mal6 to spectrin molar ratio of 21) was used. There could be several possible explanations for the fact that the average SL/Sp ratio obtained for Sp α 1-446, under the specified experimental condition, was less than 3. First, the reaction condition was not optimized so that a maximal SL/Sp ratio was not obtained. Second, urea was not able to unfold Sp α 1-446 completely so that certain cys residues were still not accessible to Mal6. Third, there could be only two cys residues in Sp α 1-446 due to possible mutations occurred during the process of PCR synthesis or protein expression.

3.2.1.3 Identification of the Labeling Sites

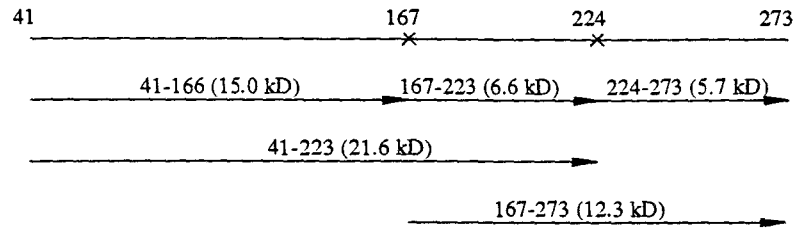
The SL/Sp ratio obtained from spin-labeling of Sp α 41-273 and Sp α 1-446 in 5 mM sodium phosphate at pH 7.4 suggests that there is one cys residue in Sp α 41-273 accessible to Mal6 and there are two cys residues in Sp α 1-446 accessible to Mal6 under the same labeling condition. In order to assign the Mal6 accessibility of the two spectrin fragments to specific cys residues, the TNB-CN cleavage reaction (Jacobson *et al.*, 1973) (Fig. 3) was performed on Sp α 41-273 and Sp α 1-446.

3.2.1.3.1 Sp α 41-273

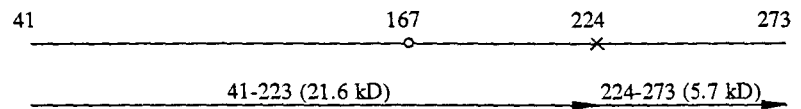
Assuming TNB-CN cleaves the peptide bond next to free cys residues (Jacobson *et al.*, 1973), potential TNB-CN cleavage products of Sp α 41-273 (27.3 kD) are shown in Fig. 9a. The five possible cleaved fragments of Sp α 41-273 are Sp α 41-223 (21.6 kD), Sp α 41-166 (15.0 kD), Sp α 167-273 (12.3 kD), Sp α 167-223 (6.6 kD) and Sp α 224-273 (5.7 kD). Assuming that TNB-

Figure 9 **Schematic presentation of possible TNB-CN cleavage products of Sp α 41-273 with no or one spin label.** a, TNB-CN cleavage products of Sp α 41-273 without spin label. b, TNB-CN cleavage of Sp α 41-273 spin labeled at cys167 or cys224. Positions of the free cys groups are indicated by x and positions of the Mal6-labeled cys residues are indicated by \bigcirc .

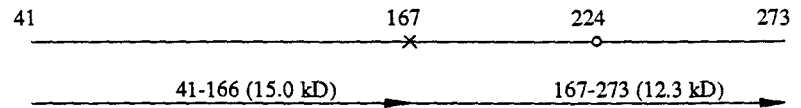
a. No spin label



b. Spin labeled at cys167



Spin labeled at cys224



CN does not cleave spin-labeled cys, a complete cleavage of Sp α 41-273 labeled at cys167 will result in two fragments, Sp α 41-223 (21.6 kD) and Sp α 224-273 (5.7 kD) (Fig. 9b). When cys224 is labeled, complete cleavage of Sp α 41-273 will result in two different fragments, Sp α 41-166 (15.0 kD) and Sp α 167-273 (12.3 kD) (Fig. 9b).

A typical SDS polyacrylamide electrophoresis gel (16%) of the TNB-CN cleavage reactions of Sp α 41-273 is shown in Fig. 10. Sp α 41-273 (27.3 kD) incubated for 48 h in the reaction buffer with no TNB-CN added is shown as a control sample in lane 2 of Fig. 10. A major band corresponding to an apparent MW of 31 kD was observed, indicating that no cleavage occurred. The 48-hour TNB-CN reaction mixture of Sp α 41-273 without spin labels (lane 3, Fig. 10) showed four bands with apparent MWs of 31, 25, 15 and 5 kD. The percentage areas of 31, 25, and 15 kD bands were 64%, 8%, and 28%, respectively. The intensity of the 5 kD band was relatively low to allow an accurate estimation of its percentage area, however this band was consistently present on gels of similar samples. The probable assignment of the bands is as follows: the 31 kD band was the uncleaved Sp α 41-273 (27.3 kD); the 25 kD band was Sp α 41-223 (21.6 kD); the 15 kD band contained Sp α 41-166 (15.0 kD) and Sp α 167-273 (12.3 kD), whose apparent MWs were too close to be resolved; the 5 kD band was the mixture of Sp α 167-223 (6.6 kD) and Sp α 224-273 (5.7 kD).

SDS polyacrylamide electrophoresis of the 48-hour TNB-CN reaction of the spin-labeled Sp α 41-273 sample with a SL/Sp ratio of 0.98 (lane 4, Fig. 10) showed that the 25 and 5 kD bands essentially disappeared from the gel while the intensities of the 31 and 15 kD bands remained high. The percentage areas of the bands occurring around the 31 and 15 kD were 73% and 27%, respectively. According to the above assignment, the 31 kD band was the uncleaved Sp α 41-273 and the 15 kD band was the combination of fragments Sp α 41-166 (15.0 kD) and Sp α 167-273 (12.3 kD). Fig. 9b showed that when cys224 was labeled, cleavage of Sp α 41-273 would result in Sp α 41-166 (15.0 kD) and Sp α 167-273 (12.3 kD). The TNB-CN cleavage reaction thus suggested that cys224

Figure 10 **SDS polyacrylamide electrophoresis gels (16 %) stained with 0.25 % Coomassie brilliant blue R.** The gel (0.5 mm thick) was run for about 40 min under a constant voltage of 150 V. Lane 1: low molecular weight protein standards (kD); lane 2: 48-hour control sample (Sp α 41-273 in the reaction buffer with no TNB-CN added); lane 3: 48-hour TNB-CN reaction of Sp α 41-273 without spin labels; lane 4: 48-hour TNB-CN reaction of Sp α 41-273 with a SL/Sp ratio of 0.98.

was the cys residue in Spo41-273 labeled by MalE and that cys167 was not accessible under the

3.2.

1973

poss

kD).

Spo

Spo

of g

depl

the j

and

446

Spo

mix

no

to a

clea

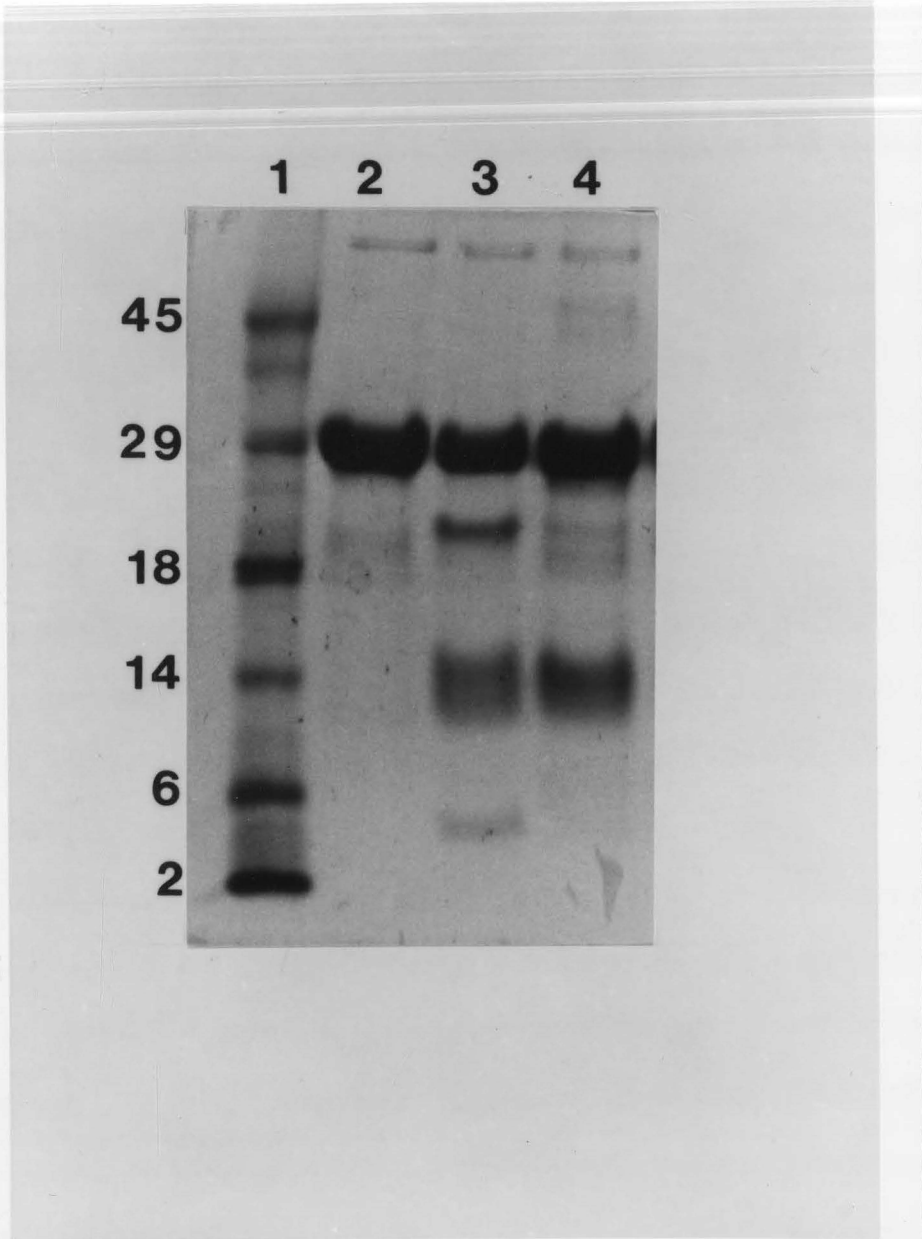
446

446

446

42,

were



son *et al.*,

11a. Nine

1-223 (26.3

5 (14.1 kD),

4 reaction if

eled, instead

inations are

cleavage of

When cys167

and Spo224-

ve fragments

age reaction

a buffer with

corresponding

ating that no

arified Spo1-

ure of Spo1-

446

446

446

42,

were

were

was the cys residue in Sp α 41-273 labeled by Mal6 and that cys167 was not accessible under the same condition.

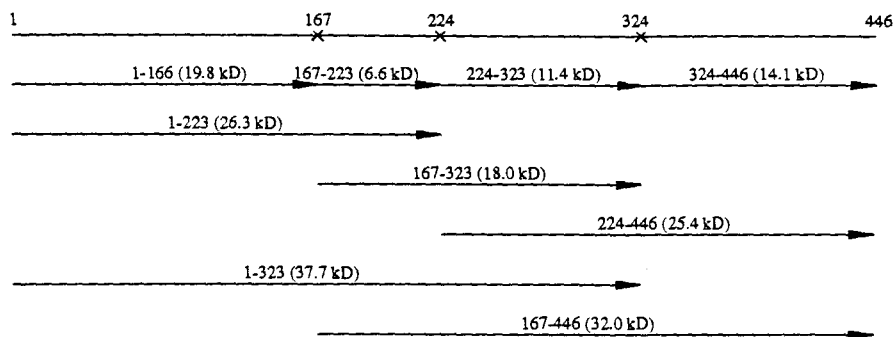
3.2.1.3.2 Sp α 1-446

Assuming TNB-CN cleaves the peptide bond next to free cys residues (Jacobson *et al.*, 1973), potential TNB-CN cleavage products of Sp α 1-446 (51.6 kD) are shown in Fig. 11a. Nine possible cleaved fragments including Sp α 1-323 (37.7 kD), Sp α 167-446 (32.0 kD), Sp α 1-223 (26.3 kD), Sp α 224-446 (25.4 kD), Sp α 1-166 (19.8 kD), Sp α 167-323 (18.0 kD), Sp α 324-446 (14.1 kD), Sp α 224-323 (11.4 kD), and Sp α 167-223 (6.6 kD) can be generated from the TNB-CN reaction if Sp α 1-446 is free of spin label as shown in Fig. 11a. When any two cys residues are labeled, instead of giving nine fragments, cleavage will give rise to only two fragments. Probable combinations are depicted in Fig. 11b. When cys167 and cys224 of Sp α 1-446 are labeled, the TNB-CN cleavage of the protein will result in fragments Sp α 1-323 (37.7 kD) and Sp α 324-446 (14.1 kD). When cys167 and cys324 are labeled, cleavage of Sp α 1-446 will yield fragments Sp α 1-223 (26.3 kD) and Sp α 224-446 (25.4 kD). When cys224 and cys324 are labeled, cleavage of Sp α 1-446 will give fragments Sp α 167-446 (32.0 kD) and Sp α 1-166 (19.8 kD).

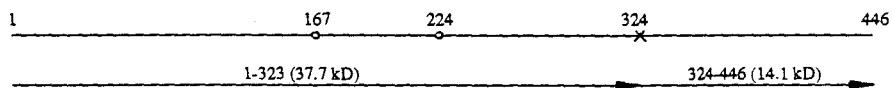
A typical SDS polyacrylamide electrophoresis gel (16%) of the TNB-CN cleavage reaction mixtures is shown in Fig. 12. Sp α 1-446 (51.6 kD) incubated for 48 h in the reaction buffer with no TNB-CN added is shown as a control sample in lane 2 of Fig. 12. A major band corresponding to an apparent MW of 51 kD was observed with several light bands underneath, indicating that no cleavage occurred in the control sample since the minor bands were typically seen in purified Sp α 1-446 sample (for example, see lane 3 of Fig. 6). The 48-hour TNB-CN reaction mixture of Sp α 1-446 without spin labels (lane 3, Fig. 12) showed eight bands corresponding to apparent MWs of 51, 42, 39, 31, 22, 19, 14 and 4 kD. The percentage areas of the 51, 42, 39, 31, and 22 kD bands were 35%, 16%, 9%, 15% and 25%, respectively. The intensities of the 19, 14, 4 kD bands were

Figure 11 **Schematic presentation of possible TNB-CN cleavage products of Sp α 1-446 with no or two spin labels.** a, TNB-CN cleavage products of Sp α 1-446 without spin label. b, TNB-CN cleavage of Sp α 1-446 spin labeled at cys167 and cys224, cys167 and cys324 or cys224 and cys324. Positions of the free cys residues are indicated by x and positions of the Mal6-labeled cys residues are indicated by \bigcirc .

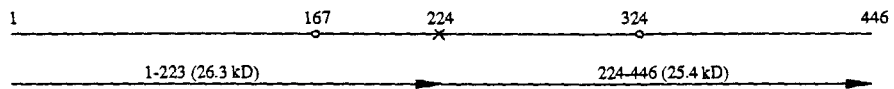
a. No spin label



b. Spin labeled at cys167, cys224



Spin labeled at cys167, cys324



Spin labeled at cys224, cys324

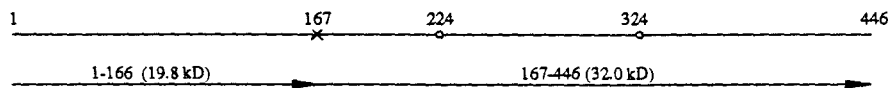


Figure 12 **SDS polyacrylamide electrophoresis gels (16 %) stained with 0.25 % Coomassie brilliant blue R.** The gel (0.5 mm thick) was run for about 40 min under a constant voltage of 150 V. Lane 1: low molecular weight protein standards (kD); lane 2: 48-hour control sample (Sp α 1-446 in the reaction buffer with no TNB-CN added); lane 3: 48-hour TNB-CN reaction of Sp α 1-446 without spin labels; lane 4: 48-hour TNB-CN reaction of Sp α 1-446 with a SL/Sp ratio of 2.03.

relatively low to allow an accurate estimation of their percentage areas. However these bands were consistently present on both of the two blots.

und

25

den

the

kD

(26)

corn

band

Spol

was

Spol

was

of th

were

the u

band

were

Spol

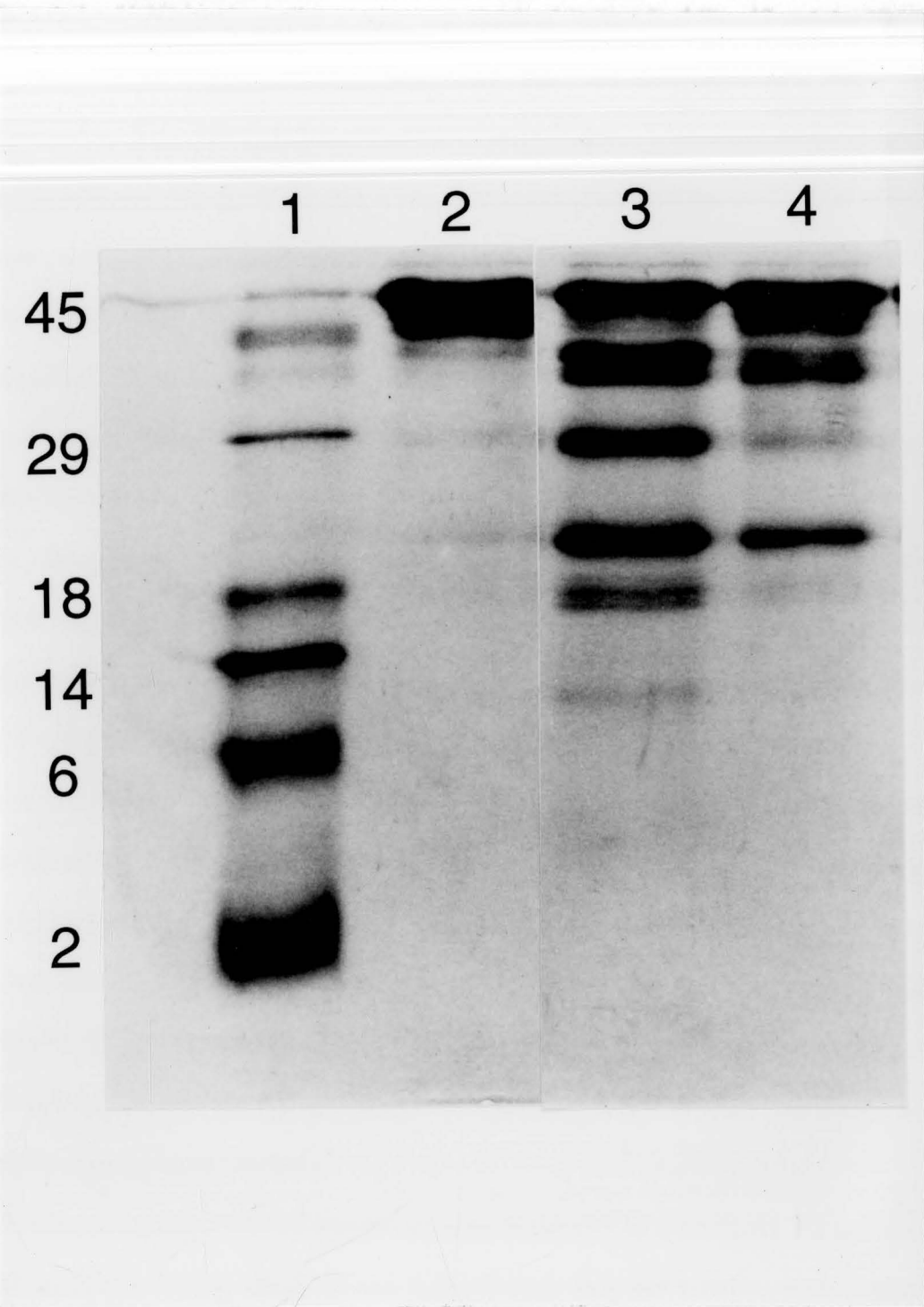
cys2

acce

low

were

cys324 in Spol-446 was also accessible to Mat6. The accessibility of cys307 and cys324 to Mat6



relatively low to allow an accurate estimation of their percentage areas, however these bands were consistently present on gels of similar samples. It was noted that there were several light bands underneath the 51 kD bands similar to what was observed in lane 2 of Fig. 12 and the 19 kD band appeared to consist of three closely-spaced bands that were recognized as a single band by densitometer tracing. The probable assignment of these bands is as follows: the 51 kD band was the uncleaved Sp α 1-446 (51.6 kD); the 42 kD band corresponded to Sp α 1-323 (37.7 kD); the 39 kD band corresponded to Sp α 167-446 (32.0 kD); the 31 kD band contained the mixture of Sp α 1-223 (26.3 kD) and Sp α 224-446 (25.4 kD), whose MWs were too close to be resolved; the 22 kD band corresponded to Sp α 1-166 (19.8 kD); the 19 kD corresponded to Sp α 167-323 (18.0 kD); the 14 kD band contained Sp α 224-323 (11.4 kD) and Sp α 324-446 (14.1 kD); the 4 kD band corresponded to Sp α 167-223 (6.6 kD).

SDS polyacrylamide electrophoresis of the 48-hour TNB-CN reaction of a fully-labeled Sp α 1-446 sample with SL/Sp = 2.03 (lane 4, Fig. 12) showed that the intensity of the 42 kD band was greatly reduced and the 31, 19, 14 and 4 kD bands essentially disappeared while the intensities of the 51, 39 and 22 kD bands remained high. The percentage areas of the 51, 39, and 22 kD bands were 65%, 19%, and 16%, respectively. According to the above assignment, the 51 kD band was the uncleaved Sp α 1-446, the 39 kD band corresponded to Sp α 167-446 (32.0 kD) and the 22 kD band corresponded to Sp α 1-166 (19.8 kD). Fig. 11b showed that only when cys224 and cys324 were both labeled, TNB-CN cleavage of Sp α 1-446 would result in the combination of fragments Sp α 167-446 (32.0 kD) and Sp α 1-166 (19.8 kD). The TNB-CN cleavage reaction suggested that cys224 and cys324 were the two cys residues in Sp α 1-446 labeled by Mal6 and cys167 was not accessible under the same condition.

In summary, the TNB-CN reaction revealed that cys167 of both Sp α 41-273 and Sp α 1-446 were not accessible to Mal6, cys224 of both Sp α 41-273 and Sp α 1-446 were accessible to Mal6, and cys324 in Sp α 1-446 was also accessible to Mal6. The accessibility of cys167 and cys224 to Mal6

remained unchanged from Sp α 41-273 to Sp α 1-446.

3.2.2 DTNB Assay

The accessibility of cys groups in Sp α 41-273 and Sp α 1-446 was also evaluated by the DTNB reaction (Ellman, 1959) (Fig. 2b). An average molar extinction coefficient (ϵ_{412}) of $13000 \pm 400 \text{ M}^{-1} \text{ cm}^{-1}$ ($n = 4$) was obtained for the yellow anion using a series of GSH solutions with the concentrations ranging from 5 to 80 μM as standards (Fig. 13). This value is in good agreement with the published value of 13600 (Ellman, 1959). Using this extinction coefficient, average SH/Sp ratios of Sp α 41-273 and Sp α 1-446 in 5 mM sodium phosphate buffer (pH 7.4) at room temperature were found to be 0.01 ± 0.01 ($n = 3$) and 0.95 ± 0.08 ($n = 5$), respectively. Prolonged incubation of Sp α 41-273 and Sp α 1-446 with DTNB did not result in higher SH/Sp ratios (data not shown). The results suggested that, under the above condition, there was no cys in Sp α 41-273 and there was one cys in Sp α 1-446 accessible to DTNB. Since cys324 is present in Sp α 1-446 but not in Sp α 41-273, it is likely that cys324 was the one that reacted with DTNB in Sp α 1-446. Both cys167 and cys224 seemed to be inaccessible to DTNB in Sp α 41-273 and Sp α 1-446. Thus the accessibility of cys167 and cys224 to DTNB remained unchanged from Sp α 41-273 to Sp α 1-446.

3.2.3 Combination of Mal6 and DTNB Reactions

Based on the above observations, Mal6 and DTNB were used in combination to further characterize the reactivity of individual sulfhydryl groups in Sp α 41-273 and Sp α 1-446.

When Sp α 41-273 and Sp α 1-446 were labeled for 1 h at a Mal6/Sp ratio of 40 $\mu\text{l}/\text{mg}$ (corresponding to a Mal6 to spectrin molar ratio of 11:1) (low spin label concentration and short time labeling condition), a SL/Sp ratio of 0.06 ($n = 1$) for Sp α 41-273 and an average SL/Sp ratio of 0.83 ± 0.04 ($n = 3$) for Sp α 1-446 was obtained (Table 2). It was found, however, for Sp α 1-446 samples previously reacted with DTNB, the SL/Sp ratio decreased from an average value of

Figure 13 **A typical calibration curve of the DTNB assay using GSH solutions of known concentration as standards.** A series of GSH standard solutions with concentrations of 10, 20, 40, 60, 80, 120 and 160 μM were prepared. One volume of each GSH standard solution was added to one volume of the 2 mM DTNB stock solution and then incubated at room temperature for 2 min. The absorbance at 412 nm was measured and plotted against the concentration of the GSH standard solution. The linear regression line of the data points was used as a calibration curve. The molar extinction coefficient at 412 nm was read from the slope of the calibration curve.

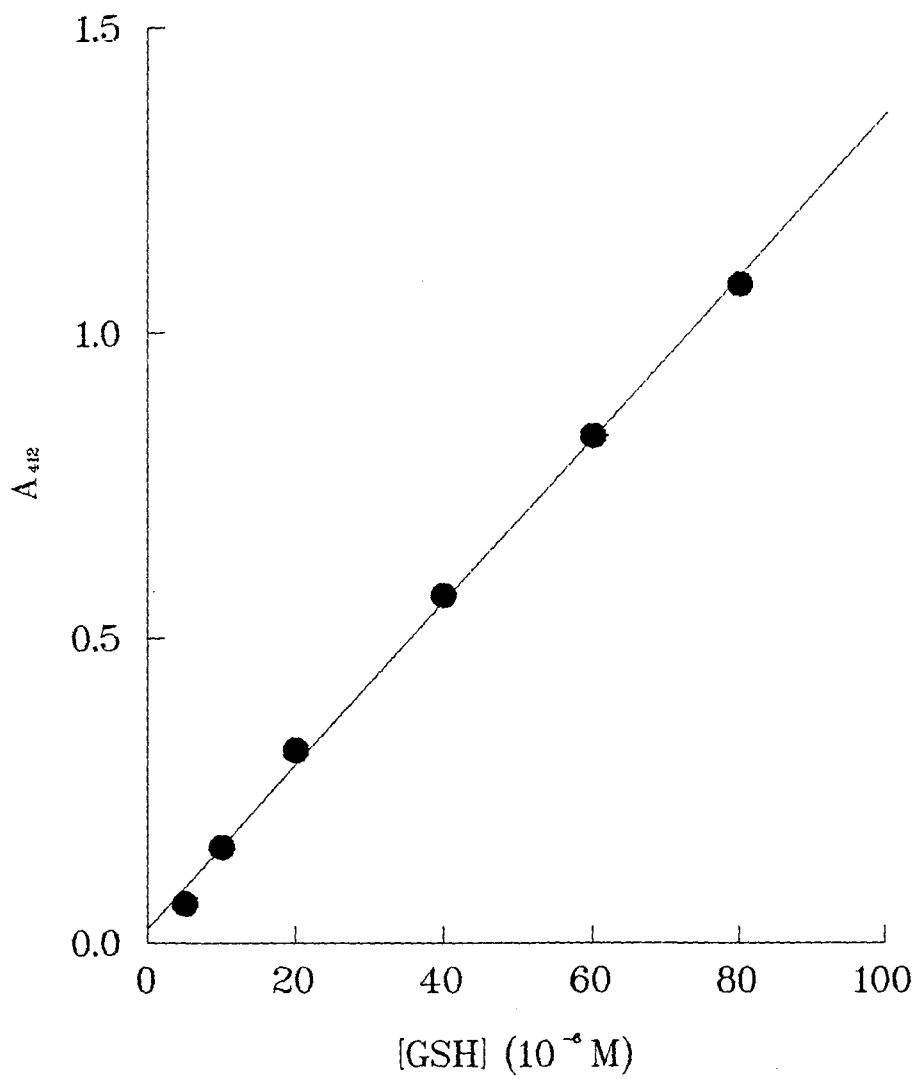


Table 2 SL/Sp Ratios of Sp α 41-273 and Sp α 1-446 Determined under Three Different Labeling Conditions

| Labeling Condition | SL/Sp Ratio | | |
|-----------------------|---|--|--|
| | Sp α 1-446 without DTNB treatment | Sp α 1-446 with DTNB treatment | Sp α 41-273 without DTNB Treatment |
| 1 | 0.83 \pm 0.04 (n=3) | 0.08 (n=1) | 0.06 (n=1) |
| 2 | 1.25 \pm 0.27 (n=5) | 0.45 \pm 0.32 (n=5) | 0.46 \pm 0.01 (n=2) |
| 3 | 2.06 \pm 0.04 (n=2) | 0.95 \pm 0.10 (n=2) | 0.95 \pm 0.04 (n=3) |

Condition 1: low spin label concentration and short time labeling condition.

Condition 2: low spin label concentration and overnight labeling condition.

Condition 3: high spin label concentration and overnight labeling condition.

0.83 (n=3) to 0.08 (n = 1) under labeling condition 1. These results suggested that the cys in Sp α 1-446 fully labeled by Mal6 under low spin label concentration and short time labeling condition was also the cys that reacted to DTNB.

When Sp α 1-446 was labeled for a long time (about 16 h) at a Mal6/Sp ratio of 40 μ l/mg (low spin label concentration and overnight labeling condition), an average SL/Sp ratio of 1.25 ± 0.27 (n = 5) was obtained. The results suggested that there were more than one cys residues in Sp α 1-446 accessible to Mal6 under low spin label concentration and overnight labeling condition. Under the same condition, DTNB-treated Sp α 1-446 exhibited an average SL/Sp ratio of 0.45 ± 0.32 (n = 5). The SL/Sp ratio for Sp α 41-273 without previous DTNB treatment was 0.46 ± 0.01 (n = 5) (Table 2).

When Sp α 1-446 was labeled for about 16 h at a high Mal6/Sp ratio (200 μ l/mg, corresponding to a Mal6 to spectrin molar ratio of 54:1) (high spin label concentration and overnight labeling condition), an average SL/Sp ratio of 2.06 ± 0.04 (n = 2) was obtained. These results suggested that the reactivity of the two sites toward Mal6 in Sp α 1-446 could be very different, although both were accessible. Site 1 in Sp α 1-446 was able to be fully labeled in 1 h at a Mal6/Sp ratio of 40 μ l/mg while site 2 was not able to be completely labeled unless a Mal6/Sp ratio of 200 μ l/mg and 16 h labeling were applied. When Sp α 1-446 was treated with DTNB, the SL/Sp ratio obtained for Sp α 1-446 was 0.95 ± 0.10 (n = 2). The SL/Sp ratio of Sp α 41-273 labeled under the same condition without DTNB treatment was 0.95 ± 0.04 (n = 3) (Table 2). The similar labeling behavior of the DTNB-treated Sp α 1-446 and Sp α 41-273 without DTNB treatment suggested that the reactivity of the labeling site in Sp α 41-273 was similar to that of site 2 in Sp α 1-446.

DTNB reaction suggested that cys324 was the only cys residues reactive to DTNB in Sp α 1-446. TNB-CN reaction indicated that cys224 and cys324 of Sp α 1-446 and cys224 of Sp α 41-273 were accessible to Mal6. The assignment can be made, based on the combination of spin labeling and DTNB reactions results, that site 1 was cys324, the highly reactive cys, and site 2 was the

cys224, the less reactive cys in Sp α 1-446. Furthermore, the reactivity of cys224 appeared to remain unchanged from Sp α 1-273 to Sp α 1-446, since the labeling behavior of Sp α 1-446 became similar to that of Sp α 1-273 once cys324 of Sp α 1-446 was blocked by DTNB.

3.3 Studies of Spin-Labeled Sp α 1-273 and Sp α 1-446

3.3.1 Spectral Properties at Room Temperature

3.3.1.1 Hyperfine Separation Measurements

3.3.1.1.1 A_{zz} of the Singly-Labeled Sp α 1-273 and Sp α 1-446

EPR lineshape can be interpreted in terms of molecular dynamics to yield information on the nature of the local molecular environment (Goldman *et al.*, 1975; Fung and Johnson, 1984). One useful parameter of describing the EPR spectra is A_{zz} (Fig. 14), defined as half of the outer hyperfine extrema (Goldman *et al.*, 1975). A_{zz} is sensitive to mobility of the spin label, polarity of the labeling site and other factors such as temperature.

An average A_{zz} of 31.8 ± 0.2 G ($n = 3$) was obtained from room temperature EPR spectra of Sp α 1-273 with an average SL/Sp ratio of 0.59 ± 0.14 ($n = 3$) in 5 mM sodium phosphate, pH 7.4. A_{zz} values were shown to remain constant for DTNB-treated Sp α 1-446 with SL/Sp ratios ranging from 0.18 to 0.91 (32.2 - 32.3 G). A_{zz} values of the DTNB-treated Sp α 1-446 were similar (only about 0.5 G difference) to that of Sp α 1-273. Since cys224 was singly-labeled by Mal6 in Sp α 1-273 and DTNB-treated Sp α 1-446 according to the combination of DTNB and Mal6 reactions, the above results suggested that spin labels attached to cys224 of Sp α 1-273 and Sp α 1-446 experienced similar motions and local environments.

The average A_{zz} value of Sp α 1-446 without prior DTNB treatment, with SL/Sp of 0.85 ± 0.04 ($n = 2$) in 5 mM sodium phosphate at pH 7.4, was 29.5 ± 0.0 G ($n = 2$). Since cys324 of Sp α 1-446 was suggested to be singly-labeled by Mal6 under this condition, the 2.8 G difference in A_{zz} values of Sp α 1-446 with and without treatment with DTNB suggested that spin labels attached

to cys224 and cys324 of Sp α 1-446 experienced different motions or local environments. The larger A_{zz} value of cys224 indicated that the spin label at cys224 was either experiencing slower motion or higher polarity as compared to cys324. A summary of A_{zz} of the singly-labeled Sp α 41-273 and Sp α 1-446 is given in Table 3.

3.3.1.1.2 A_{zz} of the Doubly-Labeled Sp α 1-446

Meanwhile, the A_{zz} values of Sp α 1-446 doubly-labeled at cys224 and cys324 were measured and compared with the A_{zz} values of the composite spectra resulted from the addition of the spectra of Sp α 1-446 singly-labeled at cys224 or cys324. When the SL/Sp ratio of Sp α 1-446 samples in 5 mM sodium phosphate at pH 7.4 was 1.30, 1.52, 1.65, 1.90, 2.03, 2.09 or 2.13, A_{zz} value was 29.8, 30.4, 30.7, 31.1, 31.1, 31.2, or 31.1, respectively (Table 4). The A_{zz} values increased with SL/Sp ratios when SL/Sp ratios were greater than 1. Assuming that the labeling of the second cys in Sp α 1-446 did not occur until the first cys was completely labeled by Mal6, the EPR spectrum of Sp α 1-446 with SL/Sp ratio greater than 1 would be a composite one of the singly-labeled Sp α 1-446 (labeled at site 1) and of the DTNB-treated Sp α 1-446 (labeled at site 2). The A_{zz} values of the composite EPR spectra resulted from spectral addition of EPR spectra of the singly-labeled Sp α 1-446 and of the DTNB-treated Sp α 1-446 were 30.2, 30.5, 30.6, 31.0, 31.0, 31.0 and 31.0, respectively (Table 4). These values matched A_{zz} values of the doubly-labeled Sp α 1-446 spectra. This confirmed not only that Sp α 1-446 consisted of two different labeling sites (cys224 and cys324) with cys224 being less reactive and cys324 being more reactive, but also that the A_{zz} value of Sp α 1-446 labeled at cys224 was larger than that of Sp α 1-446 labeled at cys324, since the additional spectral contribution from labels at cys224 gave rise to an increase in the A_{zz} value.

3.3.1.2 Weakly and Strongly Immobilized Components

3.3.1.2.1 Sp α 41-273 in the Native Condition

Table 3

 A_{zz} Values of the Singly-Labeled Sp α 41-273 and Sp α 1-446

| Protein | SL/Sp | A_{zz} (G) | Avg A_{zz} (G) |
|-------------------------------------|-------|--------------|----------------------|
| Sp α 41-273 | 0.75 | 31.7 | 31.8 \pm 0.2 (n=3) |
| | 0.52 | 31.7 | |
| | 0.50 | 32.0 | |
| DTNB-Treated Sp α 1-446 | 0.18 | 32.3 | 32.3 \pm 0.1 (n=5) |
| | 1.02 | 32.3 | |
| | 0.45 | 32.3 | |
| | 0.88 | 32.2 | |
| | 0.91 | 32.2 | |
| Singly-Labeled Sp α 1-446 | 0.82 | 29.5 | 29.5 \pm 0.0 (n=2) |
| | 0.88 | 29.5 | |

Table 4 A_{zz} Values of the Measured and Composite EPR Spectra of the Doubly-Labeled $\text{Sp}\alpha 1-446$

| SL/Sp | A_{zz} (G) (Measured Spectrum) | A_{zz} (G) (Composite Spectrum) |
|-------|-------------------------------------|--------------------------------------|
| 1.30 | 29.8 | 30.2 |
| 1.52 | 30.4 | 30.5 |
| 1.65 | 30.7 | 30.6 |
| 1.90 | 31.1 | 31.0 |
| 2.03 | 31.1 | 31.0 |
| 2.09 | 31.2 | 31.0 |
| 2.13 | 31.1 | 31.0 |

Fig. 14 shows a typical conventional EPR spectrum of the singly-labeled Sp α 41-273 (SL/Sp = 0.79) in 5 mM sodium phosphate buffer, pH 7.4, at room temperature. The spectrum contained two major components reflecting two different degrees of spin label immobilization, namely a strongly immobilized component (or a slow motion component with a rotational correlation time of about 10^{-7} s) and a weakly immobilized component (or a fast motion component with a rotational correlation time of about 10^{-10} s). The strongly immobilized component gave three broader signals and the weakly immobilized component gave three sharper signals. The central peaks from both components overlapped with each other. The amplitudes of the low field and high field signals of the strongly and weakly immobilized components were defined as S, S', W and W' as shown in Fig. 14. The signal intensity of each component depended on the percentage of the corresponding motion in the system.

3.3.1.2.2 Sp α 41-273 in Urea

Fig. 15 shows a series of spectra of Mal6-labeled Sp α 41-273 in 5 mM sodium phosphate, pH 7.4, with 0, 2, 3, 4, 5 and 6 M urea. It was observed that, upon increasing urea concentration, the signal amplitude of the strongly immobilized component (S, S') decreased and the signal amplitude of the weakly immobilized component (W, W') increased. The strongly immobilized component was apparently converted gradually to the weakly immobilized component. At 4 M urea concentration, the strongly immobilized signals were not detectable, and the amplitudes of the weakly immobilized signals reached their maximal values (with $W' = 4.5$ cm). An increase in urea concentration above 4 M brought no further increase in the amplitudes of the weakly immobilized signals.

Since urea is generally considered as a protein denaturant which induces unfolding of peptides (Tanford, 1968; Pace, 1975; 1986; 1990), the motional conversion observed in the EPR

Figure 14 **A typical conventional EPR spectrum of Mal6-labeled Sp α 41-273 in 5 mM sodium phosphate buffer at pH 7.4 and room temperature.** The spectrum is composed of weakly (W, W') and strongly (S, S') immobilized components. Outer hyperfine extrema are indicated by $2A_{zz}$. EPR spectral parameters: field set, 3250 gauss; scan range, 100 gauss; receiver gain, 10×10^3 ; modulation amplitude, 1 gauss; modulation frequency, 100 kHz; microwave power, 2 mW; frequency, 8.95 GHz; time constant, 1.28 sec; scan time, 1 min.

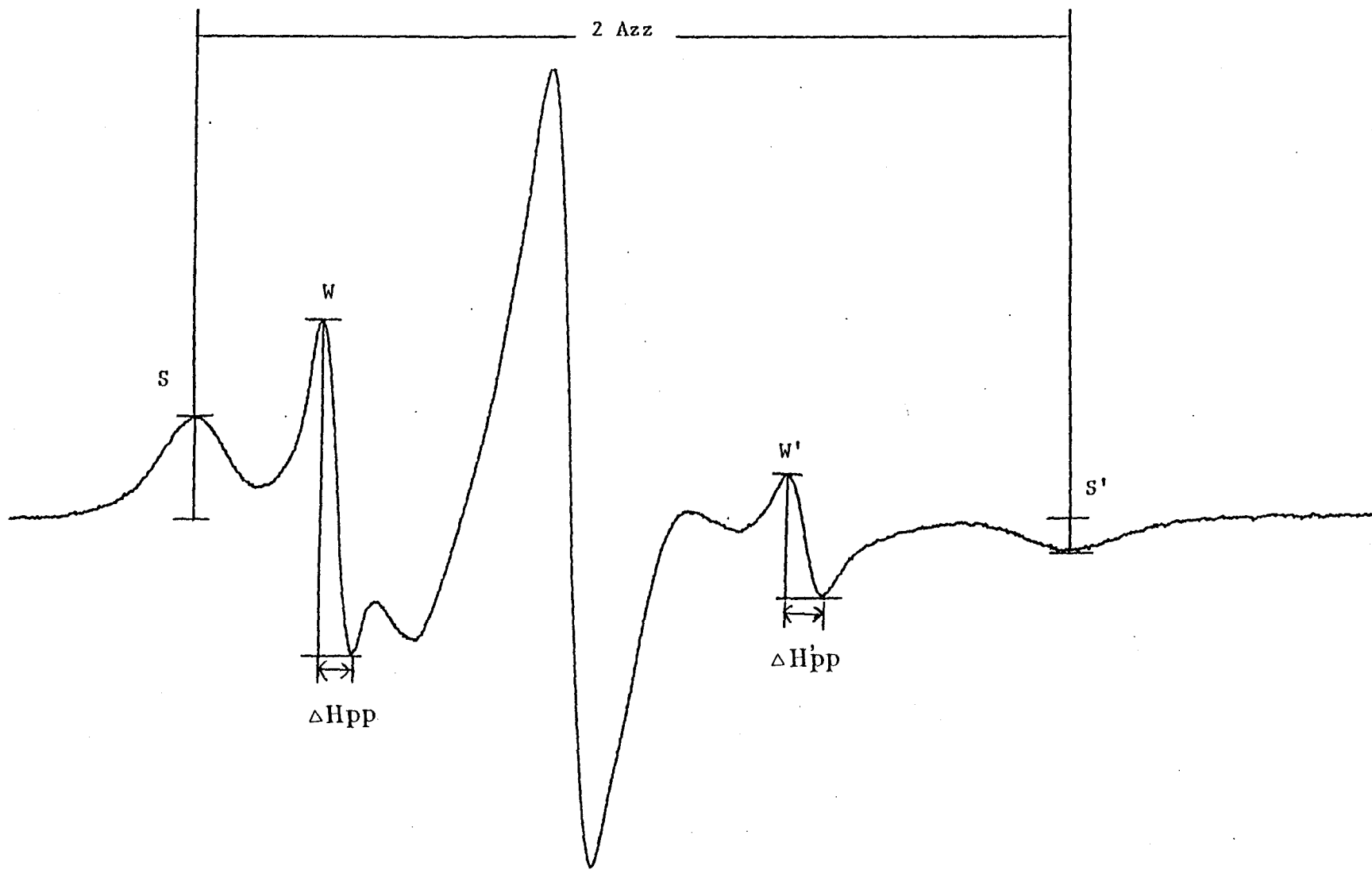
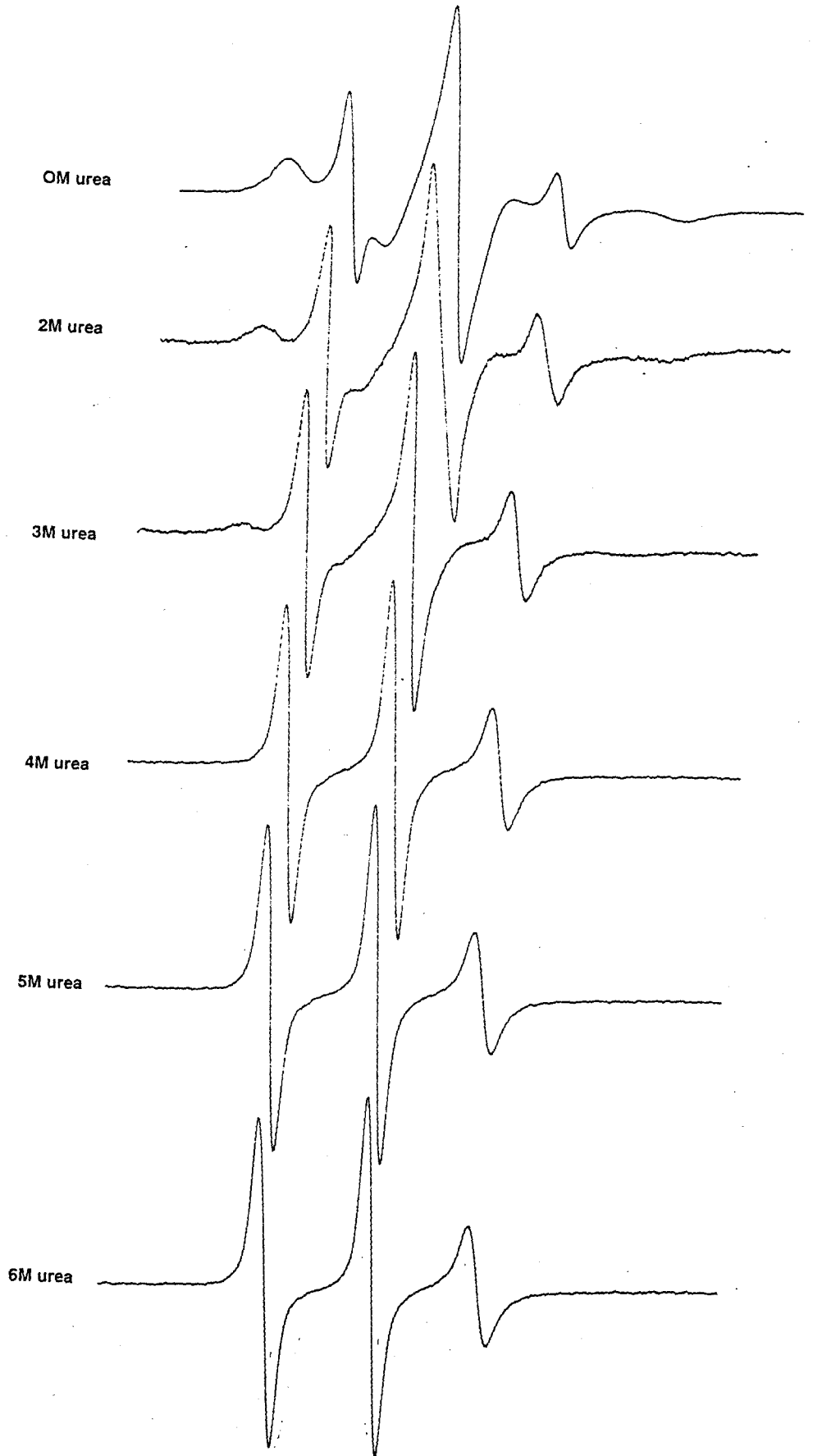


Figure 15 **Effects of urea on the Mal6-labeled Sp α 41-273.** Urea was added to Mal6-labeled Sp α 41-273 in 5 mM sodium phosphate at pH 7.4 until the final urea concentrations of 2, 3, 4, 5 and 6 M were obtained, respectively. EPR spectra were taken at room temperature. EPR settings are as described in the legend of Figure 14. Note that the sizes of the EPR spectra shown in this figure are about 46% of those of the original printouts.



spectra of Sp α 41-273 solutions containing varying urea concentrations presumably reflected the unfolding of the protein during this process. The single component of the weakly immobilized motion associated with the EPR spectra of Sp α 41-273 at urea concentrations above 4 M was considered to be a signature of Sp α 41-273 in a denatured state.

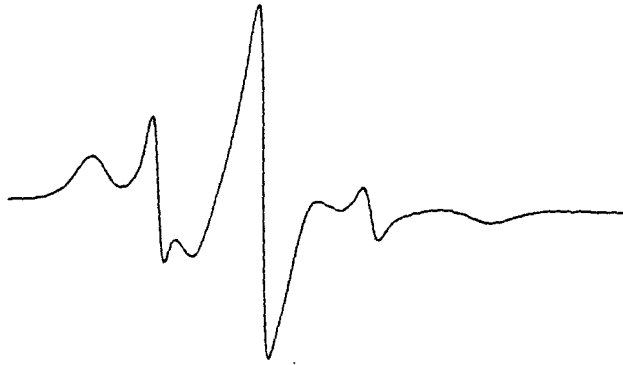
3.3.1.2.3 Spectral Subtraction

The EPR spectrum of Sp α 41-273 in 5 mM sodium phosphate buffer, pH 7.4, with 5 M urea (Fig. 16b) was used to remove the weakly immobilized component from the EPR spectrum of native Sp α 41-273 in 5 mM sodium phosphate buffer, pH 7.4 (Fig. 16a). The resulting spectrum resembled that of a single-component system with strongly immobilized motion (Fig. 16c). The strongly immobilized component of a series of Sp α 41-273 samples in 5 mM sodium phosphate, pH 7.4, with SL/Sp of 0.78 ± 0.22 ($n = 4$) was estimated to contribute an average of $84 \pm 4\%$ ($n = 4$) of the total motion in Sp α 41-273 (Fig. 17). The weakly immobilized component was estimated to contribute an average of $16 \pm 4\%$ ($n = 4$) of the total motion. The samples were digested for 8 h and labeled for 16 h subsequently. When the thrombin digestion time during the sample preparation was increased to 10, 16 or 18 h, with spin-labeling time remained at 16 h, the weakly immobilized component in the system was found to be 26% (SL/Sp = 0.70), 31% (SL/Sp = 0.69) and 33% (SL/Sp = 0.61), respectively (Fig. 17). The percentage of the weakly immobilized component in these samples increased with the thrombin digestion time.

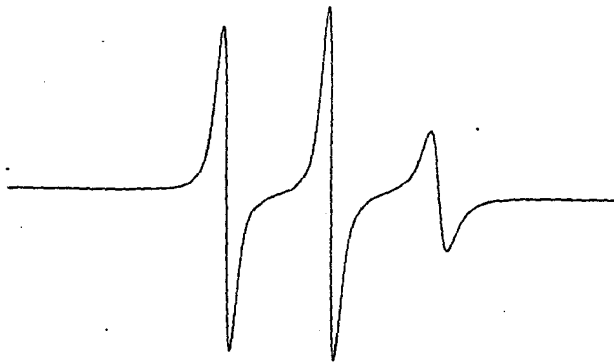
The samples discussed above were labeled for a constant amount of time (16 h). When the thrombin digestion time remained constant at 8 h and the spin labeling-time varied, the percentage of the weakly immobilized component in the system changed. For samples obtained from the same protein preparation, 14, 15, 16, 26, or 38 h of labeling time led to 3% (SL/Sp = 0.52), 6% (SL/Sp = 0.77), 8% (SL/Sp = 0.76), 10% (SL/Sp = 0.77), or 14% (SL/Sp = 0.91), respectively (Fig. 18). The percentage of the weakly immobilized component in these samples increased also with the

Figure 16 **Subtraction of the weakly immobilized component from the EPR spectrum of Mal6-labeled Sp α 41-273.** a, EPR spectrum of Mal6-labeled Sp α 41-273 in 5 mM sodium phosphate, pH 7.4. b, EPR spectrum of Mal6-labeled Sp α 41-273 in 5 mM sodium phosphate, pH 7.4, with 5 M urea. c, EPR spectrum of the single component of strongly immobilized motion resulting from spectral subtraction of b from a. Note that the sizes of the EPR spectra shown in this figure are about 38% of those of the original printouts.

a.



b.



c.

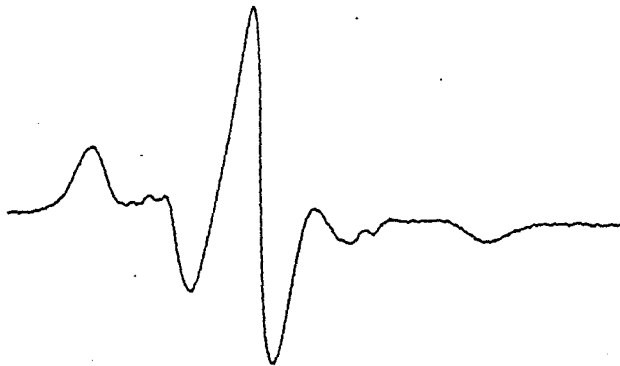
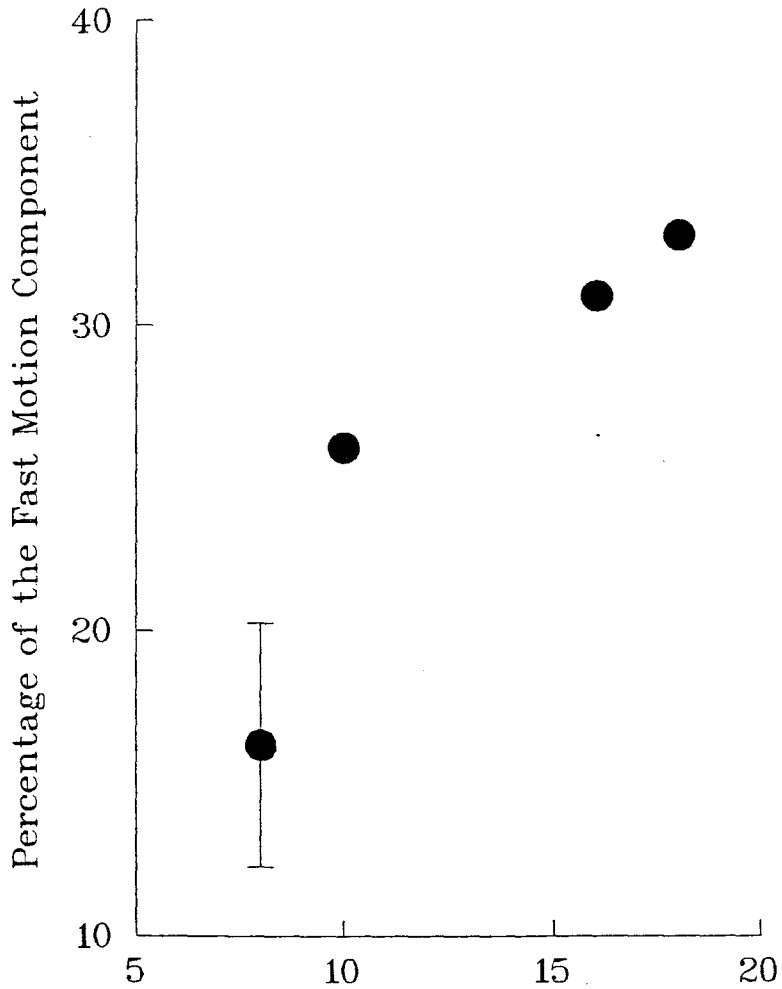
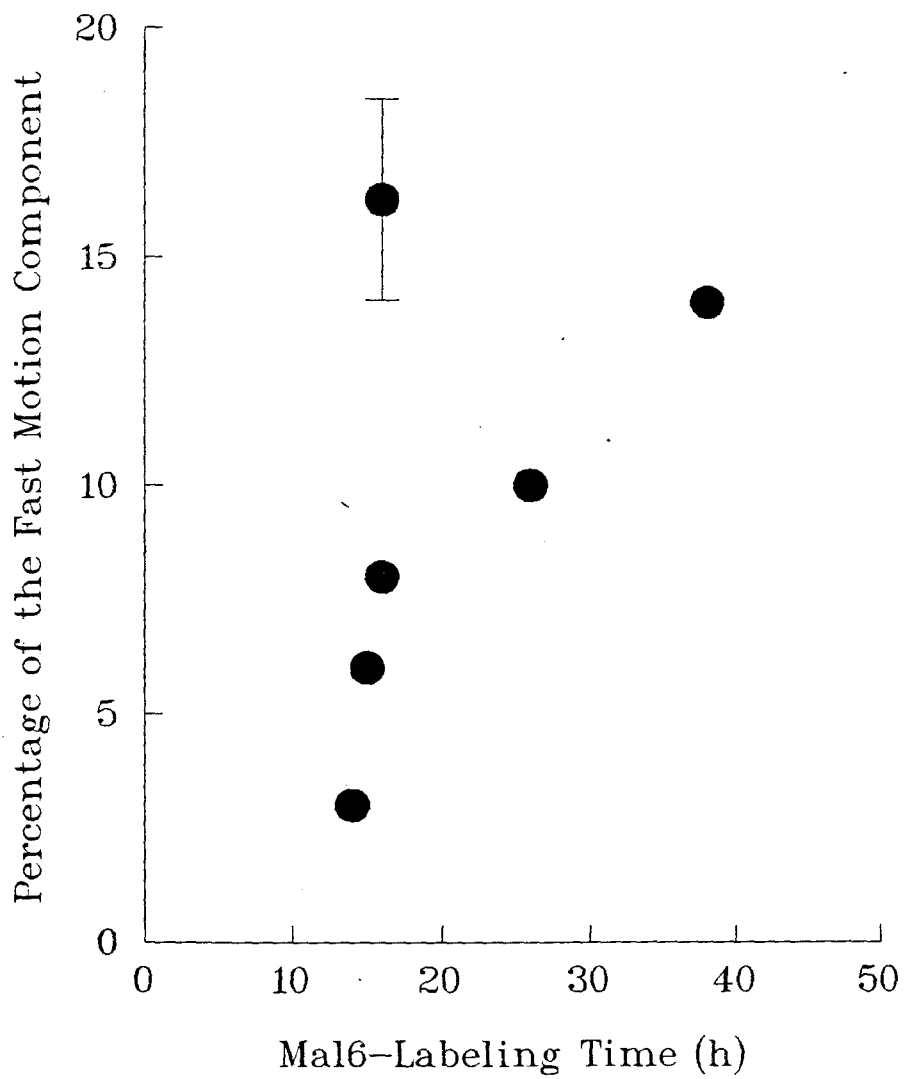


Figure 17 **Effects of thrombin digestion time on the percentage of the weakly immobilized component in Sp α 41-273.** EPR samples were labeled in 5 mM sodium phosphate buffer at pH 7.4 for 16 h and EPR spectra were taken in the same buffer at room temperature. Four samples digested by thrombin for 8 h (SL/Sp = 0.78 ± 0.22) are shown in ● with an error bar. Three other samples were digested by thrombin for 10 h (SL/Sp = 0.70), 16 h (SL/Sp = 0.69) and 18 h (SL/Sp = 0.61). The percentage of the weakly immobilized component of the samples was obtained from the spectral subtraction and the double integration of the resulting spectra.



Thrombin Digestion Time of Protein Preparation (h)

Figure 18 **Effects of Mal6-labeling time on the percentage of the weakly immobilized component in Sp α 41-273.** EPR samples were labeled in 5 mM sodium phosphate buffer at pH 7.4 and EPR spectra were taken in the same buffer at room temperature. One preparation of the Sp α 41-273 sample which was digested with thrombin for 8 h and labeled by Mal6 for 14 h (SL/Sp = 0.52), 15 h (SL/Sp = 0.77), 16 h (SL/Sp = 0.76), 26 h (SL/Sp = 0.77), and 38 h (SL/Sp = 0.91) is shown in ● without error bars. Four other preparations of Sp α 41-273, obtained three months later, were digested with thrombin for 8 h and labeled by Mal6 for 16 h are shown in ● with an error bar. The percentage of the weakly immobilized component of the samples was obtained from the spectral subtraction and double integration of the resulting spectra.



spin-labeling time. The 16-hour labeling data shown with the error bar were obtained about 3 months later. The higher percentage of the weakly immobilized component associated with the latter samples was suggested to be a result of the older age of the glutathione column from which samples were prepared (see below).

The storage time of samples at 4 °C and the age of the glutathione affinity column used for sample preparations also appeared to have some effects on the percentage of the weakly immobilized component in the system. The longer the period that the sample was stored at 4 °C, the higher the percentage of the weakly immobilized component appeared to be in the system (data not shown). Also, it was noticed the older the age of the glutathione affinity column, the higher the percentage of the weakly immobilized component of the sample prepared, with other conditions remaining the same.

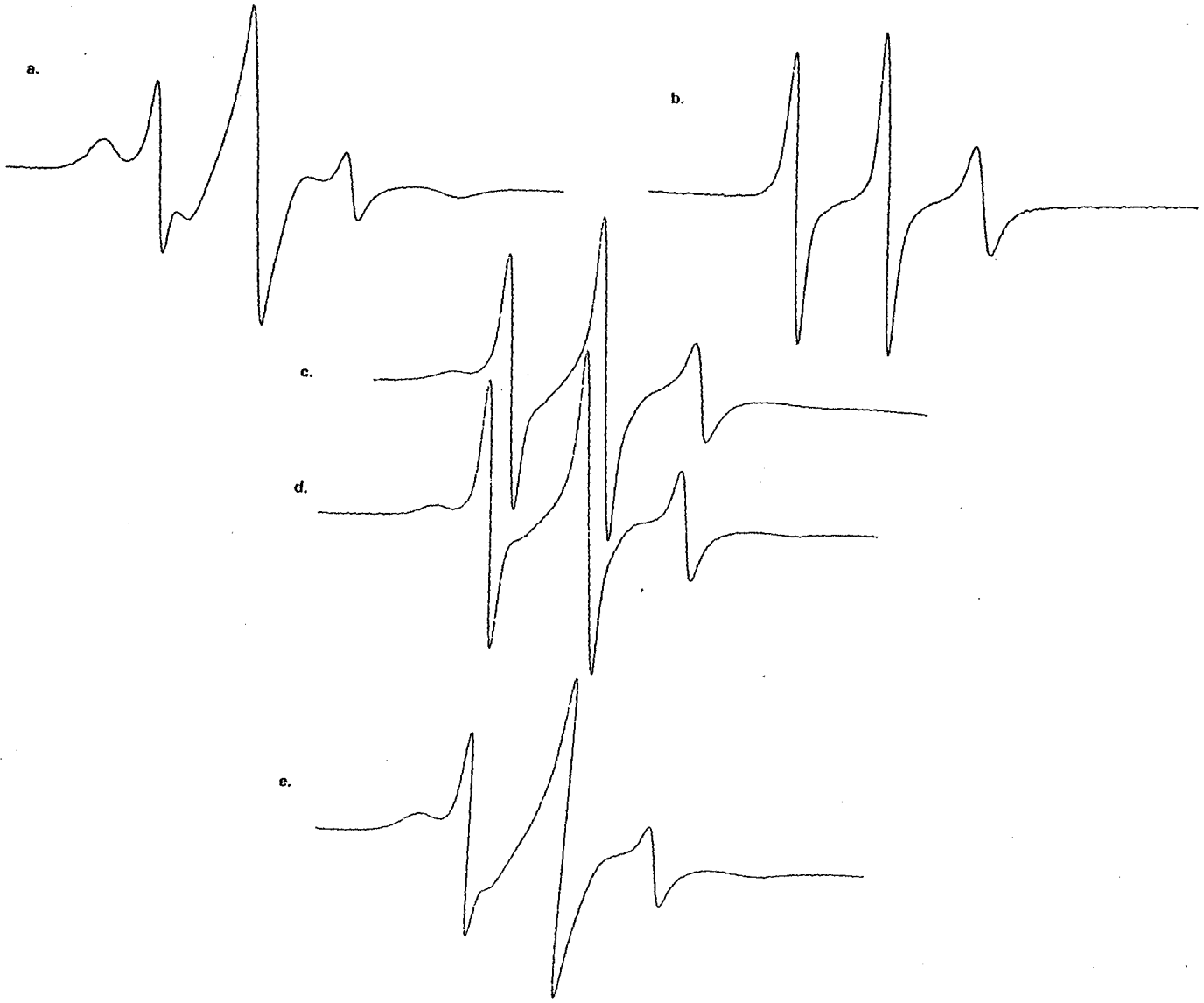
3.3.1.3 Urea-Treated Samples

3.3.1.3.1 Sp α 41-273

A typical EPR spectrum of Sp α 41-273 previously treated with urea (Procedure 1 or Procedure 2 in section 2.13.3) was obtained in 5 mM sodium phosphate (pH 7.4) (Fig. 19c or Fig. 19d, respectively). A small amount of strongly immobilized signals and a large amount of weakly immobilized signals were observed on both spectra.

To compare the motional features of samples in different conditions, W' was determined as a measure of the amount of weakly immobilized motion in the system. An average W' obtained for native Sp α 41-273 (samples derived from 8 h thrombin cleavage and 16 h labeling in 5 mM sodium phosphate at pH 7.4) with an average SL/Sp ratio of 0.77 ± 0.17 (Fig. 19a) was 2.6 ± 0.3 cm ($n = 6$). An average W' of the denatured Sp α 41-273 (sample in 5 mM sodium phosphate with urea concentration of higher than 4 M) (Fig. 19b) was 4.5 ± 0.0 cm ($n = 2$). An average value of W' of urea-treated Sp α 41-273, with Procedure 1 (labeled in the presence of urea) (Fig. 19c) or

Figure 19 **Reversibility of the conformational changes of Sp α 41-273 and Sp α 1-446 induced by urea.** a, EPR spectrum of Sp α 41-273 in 5 mM sodium phosphate, pH 7.4. b, EPR spectrum of Sp α 41-273 in 5 mM sodium phosphate, pH 7.4, with over 4 M urea. c, EPR spectrum of urea-treated Sp α 41-273 (Procedure 1). d, EPR spectrum of urea-treated Sp α 41-273 (Procedure 2). e, EPR spectrum of urea-treated Sp α 1-446 (Procedure 1). Note that the sizes of the EPR spectra shown in this figure are about 39% of those of the original printouts.



Procedure 2 (labeled after the removal of urea) (Fig. 19d), was 3.9 ± 0.3 cm ($n = 2$) or 4.2 cm ($n = 1$), respectively.

3.3.1.3.2 Sp α 1-446

A small amount of strongly immobilized signals was also observed from the room temperature EPR spectra of urea-treated Sp α 1-446 (Procedure 1, labeled in the presence of urea) in 5 mM sodium phosphate, pH 7.4. An average W' obtained for urea-treated Sp α 1-446 (Procedure 1) with an average SL/Sp ratio of 1.85 ± 0.02 (Fig. 19e) was 3.0 ± 0.5 cm ($n = 2$), whereas an average W' obtained for native Sp α 1-446 (8 h thrombin digestion and 16 h labeling in 5 mM sodium phosphate, pH 7.4) with SL/Sp ratios of 0.88 and 2.03 was of 1.1 ± 0.3 cm ($n = 2$).

3.3.2 Spectral Properties at High Temperatures

In Fig. 20, the line widths of the low field and high field weakly immobilized signals, ΔH_{pp} and $\Delta H_{pp}'$, of the spectrum of a Sp α 1-273 sample in 5 mM sodium phosphate, pH 7.4, with an SL/Sp ratio of 0.76 were plotted against temperature. A flat featureless line was observed for both ΔH_{pp} and $\Delta H_{pp}'$ throughout the temperature range of 26.4 - 50.4 °C, indicating that the line widths of the weakly immobilized signals were not a function of temperature. As a result, the percentage of the weakly immobilized component in the system should correlate directly with the amplitudes (W , W') of the weakly immobilized signals at different temperatures. W' was chosen to be measured as a convenient spectral parameter to follow the motional transition during the heat denaturation process.

Since W' varied as a function of temperature not only due to the conversion of the strongly immobilized component to the weakly immobilized component in the system at higher temperatures, but also due to the fact that the motion in the protein at higher temperatures became faster. The change of W' per unit change of temperature, dW'/dt , was calculated (Fig. 21).

Figure 20 **Effects of temperature on the widths of the low field and high field weakly immobilized signals.** EPR spectra were obtained for Mal6-labeled Sp α 41-273 in 5 mM sodium phosphate (pH 7.4) at a series of temperatures, from which the widths of the low field and high field weakly immobilized signals were measured. The width of the low field weakly immobilized signal (ΔH_{pp}) is represented by \circ and the width of the high field weakly immobilized signal ($\Delta H_{pp}'$) by \bullet .

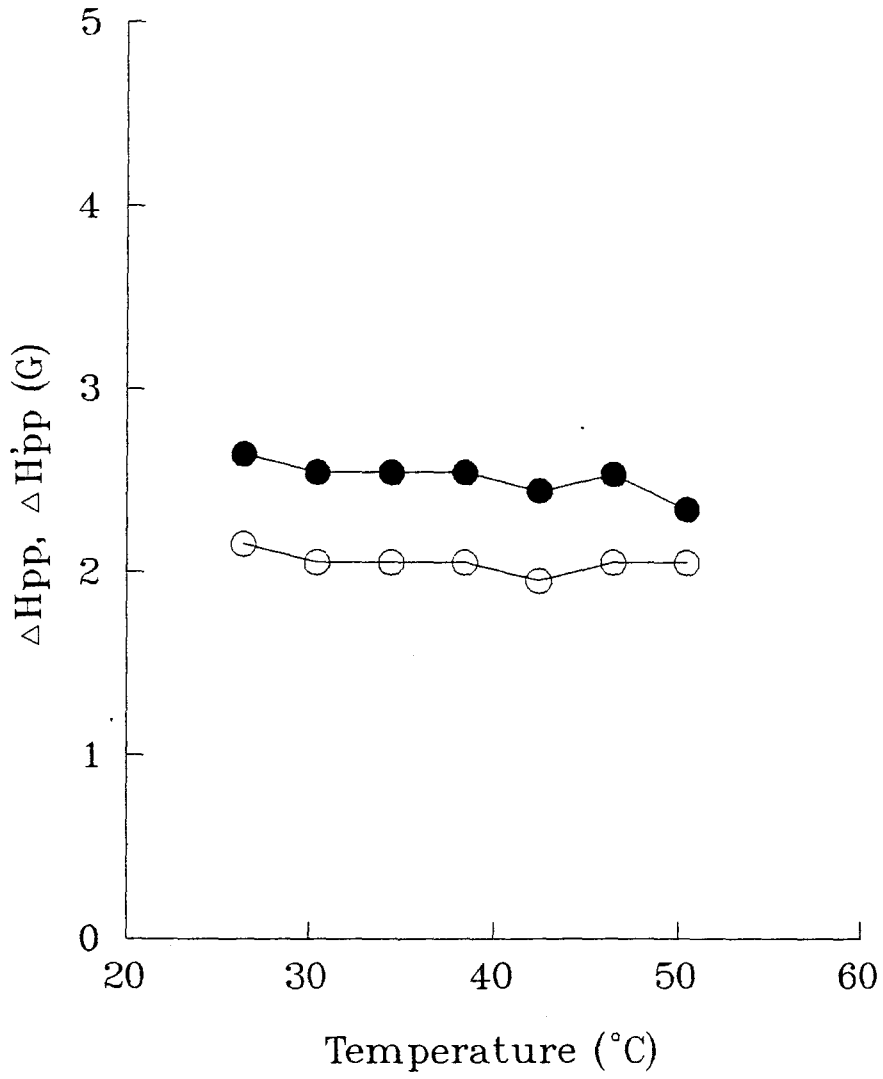
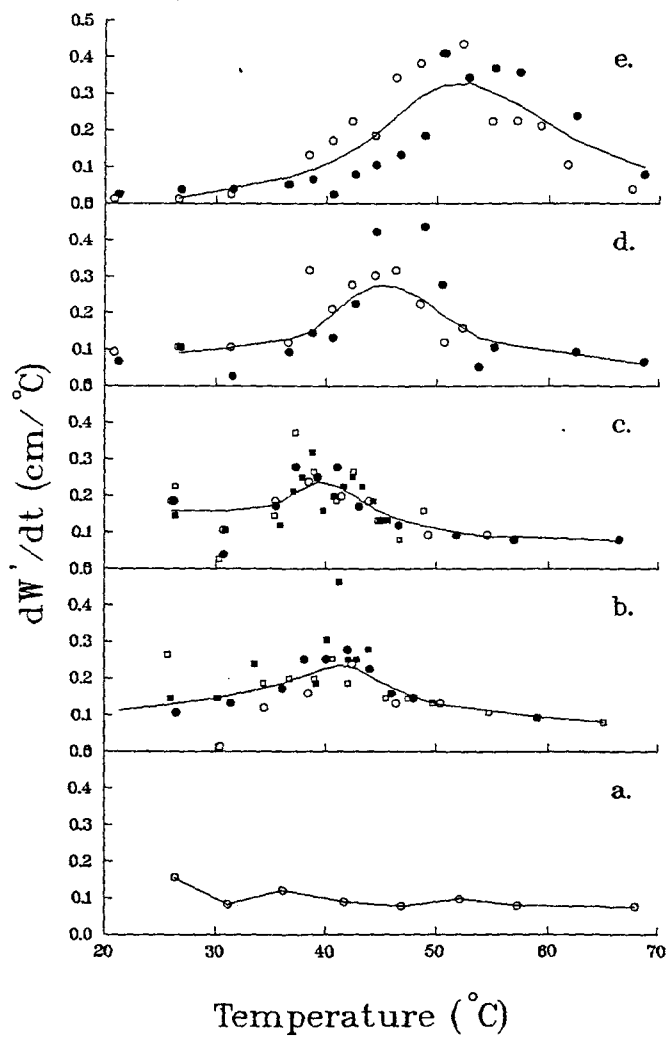


Figure 21 **Effect of temperature on Mal6-labeled Sp α 41-273 and Sp α 1-446.** a, Sp α 41-273 in 5 mM sodium phosphate at pH 7.4 with 4 M urea. b, Sp α 41-273 in 5 mM sodium phosphate at pH 7.4 (low salt buffer). c, Sp α 41-273 in 5 mM sodium phosphate, 150 mM sodium chloride at pH 7.4 (high salt buffer). d, Sp α 1-446 labeled at cys224 in 5 mM sodium phosphate, pH 7.4. e, Sp α 1-446 labeled at cys324 in 5 mM sodium phosphate, pH 7.4. Data points obtained from different samples runs were represented \circ , \bullet , \square and \blacksquare , respectively.



A flat baseline throughout the temperature range of 20 - 70 °C was observed for Sp α 41-273 in 5 mM sodium phosphate (pH 7.4) with 5 M urea (Fig. 21a), indicating that no conversion between the motional components occurred upon heating of the presumably fully denatured Sp α 41-273 in 5 M urea.

However, the dW'/dt plot of Sp α 41-273 in low salt buffer (5 mM sodium phosphate buffer, pH 7.4) varied as a function of temperature. The collective data points from four different sample runs smoothed by Lowess algorithm showed a peak centered around 41 °C (Fig. 21b). The average peak temperature determined from individual runs was 42 ± 1 °C ($n=4$). The data pooling and smoothing were employed to average out the data fluctuations from run to run and point to point, which appeared to be successful since the peak temperature obtained from the smooth plot of the collective data was within 1 °C difference from the average value of individual runs. A Student's t-test showed that, at the 95% significance limit, the smoothed peak temperature (41 °C) was statistically not different from the average peak temperature (42 °C) of individual runs. Additionally, the smoothing operation did not seem to be biased by a single outlying value, since removal of the largest dW'/dt value did not change the overall shape of the smoothed curve.

The collective dW'/dt plot of Sp α 41-273 in high salt buffer (5 mM sodium phosphate, 150 mM sodium chloride, pH 7.4) exhibited a peak centered at 39°C (Fig. 21c). A single peak at 45 °C (Fig. 21d) or 51 °C (Fig. 21e) was observed for the collective dW'/dt plot of Sp α 1-446 labeled at cys224 or cys324 in low salt buffer, respectively. The average peak temperature determined from individual runs was 40 ± 1 °C ($n=3$), 45 ± 3 °C ($n=2$), or 51 ± 1 °C ($n=2$) for Sp α 41-273 in high salt buffer, Sp α 1-446 labeled at cys224 or cys324 in low salt buffer, respectively. Student's t-tests showed that, at the 95% significance limit, the smoothed peak temperature (39, 45, or 51 °C) was statistically not different from the average peak temperature (40, 45, or 51 °C) of individual runs.

The reversibility of the motional conversion induced by heat was also followed by W'

measurements. Fig. 22a is a W' versus temperature plot of Sp α 41-273 (SL/Sp = 0.79) in 5 mM sodium phosphate (pH 7.4) upon gradual heating from room temperature (22 °C) to 75.6 °C and subsequent cooling back to room temperature. W' values on the cooling curve were always higher than those on the heating curve, showing the hysteresis behavior. A similar observation was obtained for Sp α 1-446 labeled at site 2 (SL/Sp = 0.88) in 5 mM sodium phosphate at pH 7.4 (Fig. 22b). The higher W' values of the heat-treated samples of Sp α 41-273 and Sp α 1-446 suggested that the motions of the two proteins around the labeling site at the same temperature before and after heating were not the same.

3.4 Stokes Radii of Sp α 41-273 and Sp α 1-446

The Stokes radii of native Sp α 41-273 and Sp α 1-446 were determined in both low salt (5 mM sodium phosphate, pH 7.4) and high salt (5 mM sodium phosphate, 150 mM sodium chloride, pH 7.4) buffers. The Stokes radius of Sp α 41-273 was observed to increase from 33.2 ± 2.8 Å ($n = 2$) in high salt buffer to 55.8 ± 2.7 Å ($n = 4$) in low salt buffer at 4 °C (Table 5). The Stokes radius of Sp α 1-446 increased from 35.6 ± 3.3 Å ($n = 3$) in high salt buffer to 56.0 ± 7.7 Å ($n = 3$) in low salt buffer (Table 6). The Stokes radius of urea-treated Sp α 41-273 in low salt buffer was 52.3 Å ($n = 1$) (Table 5). The average Stokes radius of Sp α 41-273 that was boiled at 100 °C for 5 min in low salt buffer was 52.3 ± 3.2 Å ($n = 2$) (Table 5). Sp α 41-273 that was heated from room temperature to 80 °C at 10 °C intervals and cooled down to room temperature similarly at 10 °C intervals in low salt buffer exhibited an average Stokes radius of 56.4 ± 5.0 Å ($n = 2$) (Table 5).

Figure 22 **Reversibility of the conformational changes induced by heat in Sp α 41-273 and Sp α 1-446.** Sp α 41-273 and Sp α 1-446 were heated gradually from room temperature to approximately 70 °C and cooled subsequently to room temperature and EPR spectra were taken at various temperature intervals during both the heating and the cooling processes. a, Sp α 41-273 in 5 mM sodium phosphate, pH 7.4. b, Sp α 1-446 in sodium phosphate, pH 7.4. W' values of Sp α 41-273 and Sp α 1-446 upon heating are represented by ○ and W' values of Sp α 41-273 upon cooling are represented by ●.

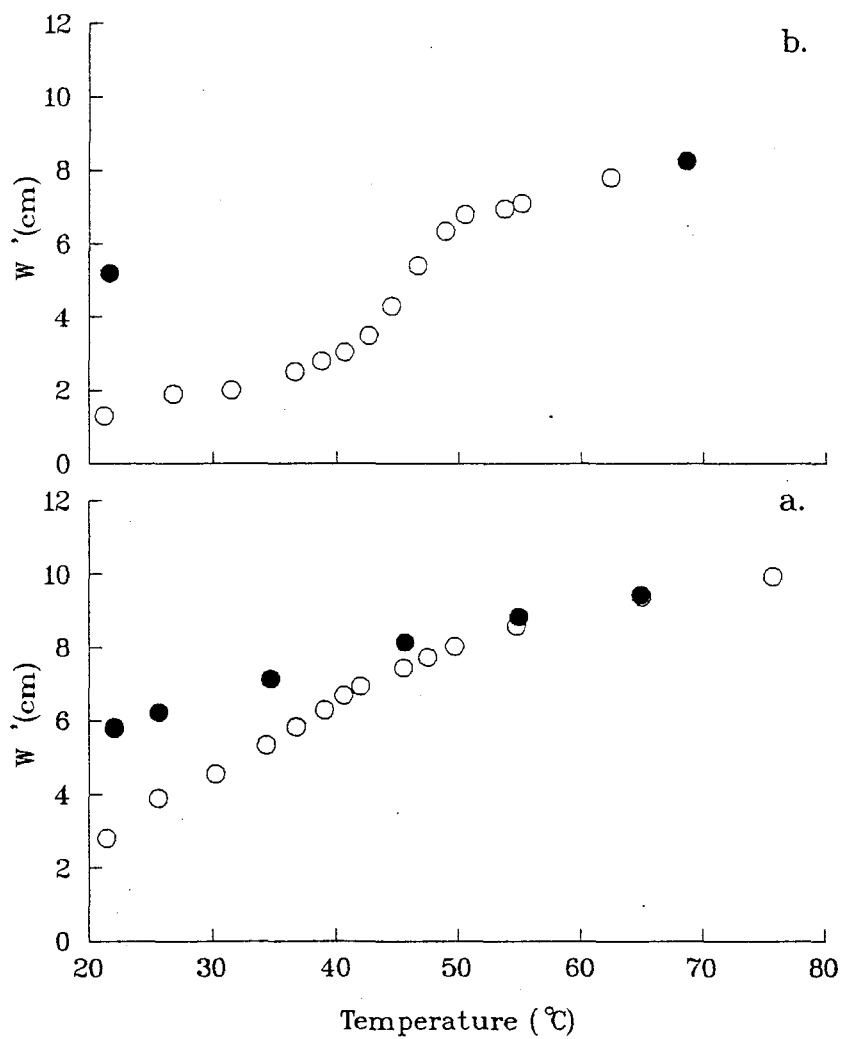


Table 5 Stokes Radii of Sp α 41-273 in Low Salt and High Salt Buffers

| Protein | Salt condition | Rs (Å) | Average Rs (Å) |
|--------------------|----------------|--------|----------------------|
| Native | Low Salt | 52.1 | 55.8 \pm 2.7 (n=4) |
| | | 58.6 | |
| | | 55.8 | |
| | | 56.7 | |
| | High Salt | 31.2 | 33.2 \pm 2.8 (n=2) |
| | | 35.2 | |
| Urea-Treated | Low Salt | 52.3 | 52.3 (n=1) |
| Boiled | Low Salt | 50.0 | 52.3 \pm 3.2 (n=2) |
| | | 54.6 | |
| Temperature-Cycled | Low Salt | 53.1 | 56.4 \pm 5.0 (n=2) |
| | | 59.6 | |

Table 6 Stokes Radii of Sp α 1-446 in Low Salt and High Salt Buffers

| Salt condition | Rs (Å) | Average Rs (Å) |
|----------------|--------|----------------------|
| Low Salt | 47.3 | |
| | 61.7 | |
| | 59.9 | 56.0 \pm 7.7 (n=3) |
| High Salt | 39.2 | |
| | 32.6 | |
| | 35.0 | 35.6 \pm 3.3 (n=3) |

CHAPTER IV

DISCUSSION

4.1 Folding of Spectrin Fragments Implied by the Thrombin Cleavage Reaction

The amino acid and cDNA sequences of α and β -subunits of spectrin reveal the universal presence of a single type of repetitive structure with a periodicity of 106 amino acid residues (Speicher *et al.*, 1983a; Speicher *et al.*, 1983b; Speicher and Marchesi, 1984; Curtis *et al.*, 1985; Sahr *et al.*, 1990; Winkelmann *et al.*, 1990). The sequence homology is suggested to reflect conformational similarity (Schulz and Schirmner, 1979; Doolittle, 1981; Keim *et al.*, 1981; Arnheim, 1983). If indeed the repetitive sequence is indicative of the repetitive structure, recombinant spectrin fragments encoded by sequences of one or more repetitive motifs should express the corresponding structure of these units and therefore should bear structural similarity to each other and to intact spectrin. According to Winograd *et al.* (1991), N-terminal ends of conformational units are 26 residues downstream of the beginnings of the sequence motifs. They have shown that a spectrin fragment containing more than one but less than three spectrin sequence repeats could fold as one complete, stably-folded unit with unstably-folded or "floppy", protease sensitive ends (Winograd *et al.*, 1991). Proteins containing "floppy" ends are susceptible to proteolysis and give rise to partially degraded products with smaller molecular weights.

In an attempt to experimentally test the hypothesis of the individual folding of erythrocyte spectrin repeats and to investigate the structure of these repeats in relationship to that of the intact spectrin, seven spectrin fragments have been expressed as GST fusion proteins. Four of the spectrin

fragments, Sp α 1-128, Sp α 1-234, Sp α 1-340 and Sp α 1-446, consist of N-terminal 23 amino-acid non-repeating region followed by the first one, two, three and four sequence motifs of α -spectrin, respectively. Three of the spectrin fragments, Sp α 1-167, Sp α 41-167, and Sp α 41-273, follow the phasing of the conformational units proposed by Winograd *et al.* (1991) instead of the sequence motifs, with several extra amino acids at both ends. Sp α 1-167, Sp α 41-167, and Sp α 41-273 consist of sequences covering the first conformational repeat of α -spectrin with the N-terminal end, without the N-terminal end, and the first two conformational units of α -spectrin without the N-terminal end, respectively.

We have shown specific cleavage of the fusion proteins, Sp α 41-167, Sp α 1-167, Sp α 41-273 and Sp α 1-446, by thrombin at the designated thrombin recognition/cleavage site under our experimental condition, resulting in single-band spectrin fragments and single-band GST carrier on SDS polyacrylamide electrophoresis gels. Similarly, specific cleavage of Sp α 1-128, Sp α 1-234 and Sp α 1-340 by thrombin was also obtained. However, in addition to the specific cleavage, nonspecific partial degradation of Sp α 1-128, Sp α 1-234 and Sp α 1-340 was also observed, as indicated by multiple-band spectrin fragments and single-band GST carrier on SDS polyacrylamide electrophoresis gels (see Fig. 5, section 3.1.3).

Sp α 41-273 and Sp α 1-446 were further purified as nonfusion proteins. Although both stayed intact after a 24-hour thrombin cleavage reaction, they displayed different stability after further purification: Sp α 41-273 remained intact as a single band and Sp α 1-446 was partially degraded as revealed by several minor bands with MWs lower than that of intact Sp α 1-446 on SDS gel (see Fig. 6, section 3.1.4). The minor degradation observed for the purified Sp α 1-446 is considered an extension of the nonspecific degradation occurring during the thrombin cleavage reaction, since a similar buffer condition and thrombin concentration were maintained in protein samples throughout the process of removing GST.

The nonspecific degradation of Sp α 1-128, Sp α 1-234, Sp α 1-340 and Sp α 1-446 is suggested

to reflect the existence of loose folding at the ends of these proteins. Amino acid sequencing of the N-terminal end of Sp α 1-234 resulted from the 24 h thrombin cleavage reaction showed that no degradation occurred at the N-terminal end of the protein. This leads to the assignment that Sp α 1-128, Sp α 1-234, Sp α 1-340 and Sp α 1-446 may contain loose folding at the C-terminal ends where the nonspecific degradation may actually take place. Since Sp α 1-128, Sp α 1-234, Sp α 1-340 and Sp α 1-446 each ends at the end of a 106-residue sequence motif of human erythrocyte spectrin according to Speicher and Marchesi's convention (1984), such a motif therefore may not correspond to a stably-folded, conformational unit. On the other hand, the lack of partial degradation of Sp α 1-167, Sp α 41-167 and Sp α 41-273 upon or after the thrombin cleavage, suggests that these three fragments contain little or no "floppy ends". Our results indicate that the phasing of the structural units proposed by Winograd *et al.* (1991) may be very close to the phasing of the real conformational repeats of human erythrocyte spectrin.

In addition to the difference in the numbers of thrombin cleavage bands observed for different spectrin fragments, the intensities of the cleaved spectrin bands were also different. The intensities of the smaller fragments (for example Sp α 1-128 and Sp α 41-167) were much lower than those of the larger fragments (for example Sp α 41-273 and Sp α 1-446), suggesting that, for proteins with similar phasing, the overall stabilities of the smaller fragments are lower than those of the larger fragments. Differences in stability of the spectrin fragments with different sizes may be due to, for example, 1) the larger fragments may contain one or more protease resistant, stable units whereas the smaller fragments may not; 2) the larger fragments may enjoy more compact folding than the smaller units, since more interactions could exist between repeats in the larger fragments than in the smaller units.

The nonspecific degradation of the spectrin fragments occurring during the thrombin cleavage reaction is probably due to either the contamination of other proteases in thrombin or to the nonspecific recognition/cleavage reaction of thrombin itself. An accurate assessment of the

thrombin cleavage specificity cannot be made until the purity of thrombin is known and a better understanding of its substrate recognition mechanism is obtained.

The selection of the proteins for spin-labeling and other structural studies were based on two criteria, the stability of the spectrin fragments and the presence of cys residues in the sequence. The stability was required by the relatively lengthy process of spin-labeling and the presence of cys was required since a cys-specific spin label was selected for this study. Among the seven spectrin fragments expressed, the four fragments containing at least one cys residue are Sp α 1-167, Sp α 41-167, Sp α 41-273, and Sp α 1-446. However, the only cys residue present in Sp α 1-167 and Sp α 41-167 is cys167, which is the last amino acid in the sequence. To avoid possible complications due to the loose folding at the ends of the fragments (Winograd *et al.*, 1991), Sp α 41-167 and Sp α 1-167 were not considered for spin-labeling and other studies. Instead, Sp α 41-273 and Sp α 1-446, which also demonstrated relatively high stability in the thrombin cleavage reaction, were chosen for further purification and structural characterization.

4.2 Environment of the Cys Residues in Sp α 41-273 and Sp α 1-446

In the absence of a crystal structure, amino acid side chains modification reactions in conjunction with spectroscopic techniques may yield valuable information on protein conformations. Cys residues are often the first target for such approaches for a number of reasons. First, the cysteine content of most proteins is relatively low (< 3 mol%), allowing easier discrimination and identification. Second, partly owing to their reactivity, cys residues are often implicated in the function of proteins. Third, there are a large variety of cys specific (or actually sulfhydryl specific) reagents available, including compounds that introduce reporter groups for spectrophotometric, EPR, NMR, fluorometric, and biochemical analysis (Grip and Daemen, 1982).

Reactions of cys residues of spectrin, isolated or in membrane, have been examined by a number of studies. Some of the early spin labeling EPR studies have attempted to address the issue

of the mobility and the chemical environments of the cys residues (Chapman *et al.*, 1969; Sandberg *et al.*, 1969; Schneider and Smith, 1970; Berger *et al.*, 1971; Adams *et al.*, 1976; Butterfield 1977; Fung *et al.*, 1979; Fung and Simpson, 1979; Fung, 1981; 1983; Fung and Johnson, 1983). Conventional EPR spectra provided information about molecular motions in the fast time range of 10^{-11} - 10^{-7} s (Chapman *et al.*, 1969; Sandberg *et al.*, 1969; Schneider and Smith, 1970; Berger *et al.*, 1971; Adams *et al.*, 1976; Fung and Simpson, 1979; Fung, 1983) while saturation transfer EPR recorded relatively slower motions in the range of 10^{-7} - 10^{-3} s (Fung *et al.*, 1979; Fung and Simpson, 1979; Fung, 1981; Fung and Johnson, 1983). The combination of these two techniques have allowed detection of a wide range of molecular events occurring in the close vicinity of the spin labeled cys residues in spectrin. However, at the time these studies were conducted, there was very limited information regarding the structure of spectrin and the membrane. It was difficult to relate the motional information to the molecular topology of spectrin, particularly to the molecular environments of the cys residues.

Another area of the spectrin research related to the chemistry of cys residues is the oxidation study. It has been used to illustrate the interactions of the different membrane elements and the role of the cys residues of spectrin in maintaining the integrity of erythrocytes. It has been shown that the oxidation induced by agents such as diamide and sodium tetrathionate was associated with the formation of disulfide bonds that cross link spectrin and other membrane proteins (Haest *et al.*, 1977). Consequently, these agents led to membrane leakiness (Deuticke *et al.*, 1983), membrane stiffness (Fischer *et al.*, 1978) and abolishment of the phospholipid asymmetry normally existing in the erythrocyte membrane. On the other hand, sole blockage of sulfhydryl groups by oxidation reagents such as N-ethylmaleimide induced thermal instability and skeletal mechanical fragility. It has been proposed that the decrease of association of spectrin dimers and increase of the dissociation of spectrin tetramers were responsible for the destabilization of erythrocyte membranes (Streichman *et al.*, 1988).

With the availability of the spectrin sequence and the capability of expressing small spectrin fragments, in this study, we have investigated the accessibility and reactivity of three individual cys residues in two spectrin fragments, Sp α 41-273 and Sp α 1-446. The TNB-CN reaction revealed that cys167 of both Sp α 41-273 and Sp α 1-446 were not accessible to Mal6, cys224 of both Sp α 41-273 and Sp α 1-446 were accessible to Mal6, and cys324 in Sp α 1-446 was also accessible to Mal6. The inaccessibility of cys167 and accessibility of cys224 to Mal6 remained unchanged from Sp α 41-273 to Sp α 1-446. DTNB reaction indicated that both cys167 and cys224 of both Sp α 41-273 and Sp α 1-446 were not accessible to DTNB, although cys324 of Sp α 1-446 was accessible. The inaccessibility of cys167 and cys224 to DTNB remained unchanged from Sp α 41-273 to Sp α 1-446. Additionally, the combination of spin-labeling and DTNB reactions showed that cys224 and cys324 of Sp α 1-446 displayed different reactivity toward Mal6 and that cys224 of Sp α 41-273 and Sp α 1-446 displayed similar reactivity toward Mal6. The reactivity of cys224 appeared to remain unchanged from Sp α 41-273 to Sp α 1-446. Furthermore, Sp α 41-273 and Sp α 1-446 labeled at cys224 showed similar A_{zz} values whereas Sp α 1-446 labeled at cys224 and cys324 showed different A_{zz} values. This suggested that spin labels attached to cys224 of Sp α 41-273 and Sp α 1-446 experienced similar motions and local environments whereas spin labels attached to cys224 and cys324 of Sp α 1-446 experienced different motions or local environments.

In summary, we have demonstrated that the chemical environments of the two common cys residues (cys167 and cys224) were kept the alike in Sp α 41-273 and Sp α 1-446. Apparently, the additional sequence introduced to Sp α 41-273 to give Sp α 1-446 did not introduce conformational changes around cys167 and cys224 that would affect their accessibility and reactivity to Mal6 and DTNB. One can infer that spectrin repeats are individually folded so that folding of one repeat is not affected by the existence of another repeat.

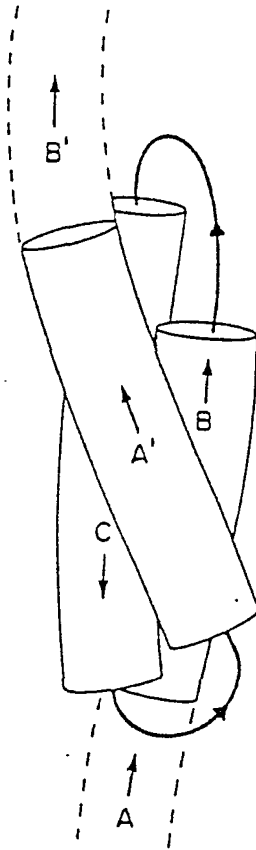
The implication of different accessibility and reactivity of the three cys residues on the local environments of these cys residues is considered. Cys167 is distinguished from the other two cys

residues. The inaccessibility of cys167 to both Mal6 and DTNB is suggested to reflect a relatively closed local environment of cys167. It is likely to be buried inside the protein, therefore, beyond the reach of Mal6 and DTNB. Cys324 differs from cys224 not only in its accessibility to DTNB, but also in its higher reactivity to Mal6. It is probable that cys324 is positioned on the surface of the protein, therefore, readily accessible to Mal6 and DTNB. The inaccessibility of cys224 to DTNB and its lower reactivity to Mal6 are suggested to indicate a negatively charged and partially buried location of cys224, since DTNB and Mal6 are both two-ring compounds and the difference between the two probes lies mainly in the difference of their charges. DTNB contains two carboxyl groups that are largely dissociated in aqueous solution giving two negative charges to the molecule, whereas Mal6 is essentially uncharged. It is likely that DTNB is prevented from reaching cys224 as a result of the charge repulsion and that Mal6 reacts slowly with cys224 due to the steric hindrance encountered.

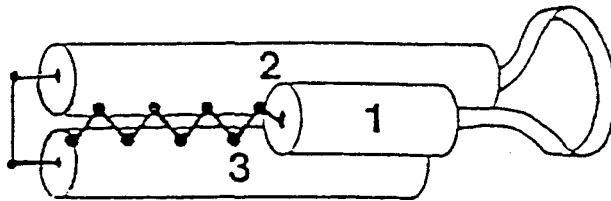
Our speculation on the environments of the three cys residues is supported by the triple-helix model of spectrin repeats (Fig. 23a) proposed by Parry and Cohen (Parry and Cohen, 1991; Parry *et al.*, 1992). In their model, cys167 is located in the middle of a helix B, cys224 is located in the middle of a random-coil loop region between a helix C and A', and cys324 is located at the end of a helix C. Analysis of the amino acid sequence of the loop region where cys224 is located reveals that, within the neighborhood of five amino acids, there are 3 negatively charged residues. Considering that the loop region is where the two triple-helix units join together, one would anticipate this area being partially buried and yet bearing a certain degree of flexibility. Thus, according to the Parry and Cohen's model cys224 is indeed positioned in a negatively charged, partially buried location. Helical projections of the six helices composing the second and third conformational units of α -spectrin showed that these six helices displayed amphipathic distribution of amino acid residues, with hydrophobic residues clustering on one side of the wheel and

Figure 23 **Models of spectrin repeats.** a, presentation of spatial arrangements of B, C, and A' helices that form the three-helix motif in the Parry and Cohen's model (Parry and Cohen, 1991; Parry *et al.*, 1992). b, schematic presentation of the first conformational unit of the Speicher *et al.*'s model (1993).

a.



b.



hydrophilic residues on the other side. Such distribution is suggested to reflect a close association of these helices with one another along the hydrophobic faces (Speicher *et al.*, 1993). Since cys167 is found on the hydrophobic face of the helix B where helix-helix interaction is suggested to take place, it is conceivable that it is buried inside of the hydrophobic core of the triple-helix cluster. On the contrary, cys324 appears to be exposed on the surface of the molecule since it is found on the hydrophilic face of the helix C where the interaction with the solvent is suggested to take place. Taken together, the locations of the cys residues in the Parry and Cohen's model fit well with the postulated environment of each residue based on our experiments. It explains the inaccessibility of cys167 to both DTNB and Mal6, the inaccessibility of cys224 to the negatively charged DTNB and the low reactivity to Mal6 as well as the high accessibility and reactivity of cys324 to both Mal6 and DTNB.

Recently, a modified triple-helix model (Fig. 23b) with slightly different phasing and secondary structure has been proposed by Speicher *et al.* (1993). In this model, cys167 is on the hydrophobic face of the helix 1 while cys224 and cys324 are both on the hydrophilic face of the helix 2 according to the helical wheel projection. This suggests that cys167 is buried inside the molecule while cys224 and cys324 are both exposed on the surface of the molecule. The similar environments of cys167 and cys224 in Sp α 41-273 and Sp α 1-446, respectively, implied by this model cannot explain the difference in accessibility and reactivity observed for the two cys residues in our experiments. Some additional interactions, for example the dimerization of spectrin repeats, are required for this model to account for the distinct chemical environments of cys224 and cys324.

4.3 Thermotropic Properties of Sp α 41-273 and Sp α 1-446

Because of the proposed role of spectrin in maintaining the shape of the erythrocyte and in providing the stability to the erythrocyte membrane, the stability of spectrin in relationship to the stability of the erythrocyte membrane is of significance. Effects of temperature on spectrin, whether

bound to the membrane or isolated, have been studied by many investigators with a variety of techniques such as CD, scanning calorimetry (Brandts *et al.*, 1977), optical rotatory dispersion (ORD) (Ralston and Dunbar, 1979), light scattering (Boe *et al.*, 1979), trypsin susceptibility (Speicher *et al.*, 1980; 1983a), fluorescence polarization (Yoshino and Marchesi, 1984), and spin-labeling EPR (Cassoley *et al.*, 1980; Minetti *et al.*, 1986).

Although most of these studies observed a clear transition around 49 °C, transitions at other temperatures were also observed depending on the buffer condition of the samples, the nature of the probes employed and methods used to determine transition temperatures. For example, Minetti *et al.* (1986) used both CD and spin-labeling EPR to study the thermotropic properties of spectrin. CD detected a structural transition around 48 °C and EPR detected a transition around 40 °C. It was hypothesized that different techniques could detect thermotropic properties of different folding domains (Minetti *et al.*, 1986). However, experimentally, this hypothesis was not tested, because the techniques then did not allow the selective probing of a specific domain.

The availability of small fragments of spectrin and our ability to selectively label a specific cys residue have provided us with a more definitive approach to study the thermotropic properties of spectrin.

Sp α 41-273 and Sp α 1-446 labeled at cys224 in 5 mM sodium phosphate, pH 7.4, displayed transitions around 41 °C and 45 °C, respectively. The higher transition temperature of Sp α 1-446 suggests that, although the local conformation of cys224 does not change from Sp α 41-273 to Sp α 1-446, the overall stability of Sp α 1-446 may be higher than that of Sp α 41-273. When cys324 instead of cys224 was labeled, the transition temperature of Sp α 1-446 increased from 45 °C to 51 °C. The difference in the transition temperatures of cys324 and cys224 can be explained by their distinct "domain" locations in the molecule. As suggested above that in the Parry and Cohen's model, cys324 is part of the helix C while cys224 is part of the random-coil loop region connecting the helix C and A'. It is conceivable that cys324 senses the unfolding of secondary structure which

takes place at higher temperature while cys224 senses the unfolding of the tertiary structure which takes place at lower temperature. Recent studies on protein folding have shown that although protein folding/unfolding is generally a highly cooperative process, a folding intermediate known as "molten globule" (Kim and Baldwin, 1982; 1990; Baum *et al.*, 1989; Hughson *et al.*, 1990; Christensen and Pain, 1991; Ewbank and Creighton, 1991) is often observed. The molten globule intermediates of different proteins appear to have some common features, primarily a native-like secondary structure and a disrupted tertiary structure (Ohgushi and Wada, 1983; Ptitsyn, 1987). It is possible that the 40 °C transition observed by EPR and the 49 °C transition observed by CD for intact spectrin may represent the unfolding of the tertiary structure and secondary structure of spectrin, respectively. These two transitions, thus, may actually correspond to the 41 - 45 °C and 51 °C transitions observed for Sp α 41-273 and Sp α 1-446 labeled at cys224 and for Sp α 1-446 labeled at cys324. In this respect, the thermotropic properties of spectrin fragments share similarity to those of intact spectrin. However, caution should be taken in comparing the thermotropic properties of the spectrin fragments with those of intact spectrin, since the thermotropic properties of intact spectrin are often collective or averaged properties contributed by several probes at several different locations while the thermotropic properties of a selectively-labeled spectrin fragment are individualized ones unique to the particular local environment.

The transition temperature of Sp α 41-273 labeled at cys224 in 5 mM sodium phosphate at pH 7.4 with 150 mM sodium chloride was around 39 °C. It differed slightly from the transition temperature of Sp α 41-273 labeled at cys224 in 5 mM sodium phosphate at pH 7.4 (41 °C). The result suggests that molecular interactions occurring around cys224 of Sp α 41-273 under the two buffer conditions may differ slightly.

4.4 The Response of Sp α 41-273 and Sp α 1-446 to Ionic Strength

The erythrocyte membrane skeleton contracts or expands in response to the increase or

decrease of ionic strength of the buffer (Shen *et al.*, 1986). Purified spectrin exhibits similar behavior (Ralston, 1976; LaBrake, 1993). The response of spectrin to ionic strength is a unique feature of this protein and is considered to be the structural basis of the elasticity of the erythrocyte membrane.

The Stokes radius of a molecule is defined as its effective hydrated radius (Cantor and Schimmel, 1980). It is a convenient parameter for measuring the dimension of a protein. The Stokes radii of spectrin in different ionic strengths have been determined (Ralston, 1976; Kam *et al.*, 1977; LaBrake, 1993). The Stokes radius of spectrin dimers is reported to increase from 124 Å in 5 mM sodium phosphate, 150 mM sodium chloride, pH 7.4 (high salt buffer) to 178 Å in 5 mM sodium phosphate, pH 7.4 (low salt buffer). The Stokes radius of spectrin tetramers is reported to increase from 250 Å in high salt buffer to 330 Å in low salt buffer (LaBrake, 1993). In order to compare the effect of ionic strength on the spectrin fragments to that on intact spectrin, the Stokes radii of Sp α 41-273 and Sp α 1-446 were determined in both low salt and high salt buffers. The Stokes radius of Sp α 41-273 was found to increase from 33.2 Å in high salt buffer to 55.8 Å in low salt buffer. The Stokes radius of Sp α 1-446 was found to increase from 35.6 Å in high salt buffer to 56.0 Å in low salt buffer. Although much smaller in size, Sp α 41-273 and Sp α 1-446 share the similar characteristic as intact spectrin and are more condensed in high salt buffer and more extended in low salt buffer. Our results support the hypothesis that spectrin is composed of individually folded units of similar conformations.

It should also be pointed out that Sp α 41-273 and Sp α 1-446 had similar Stokes radius values under the similar salt condition despite the fact that the molecular weight of Sp α 1-446 is larger than that of Sp α 41-273. It is possible that the overall folding of Sp α 1-446 may be more compact than that of Sp α 41-273. It is also possible that the small difference between the dimensions of Sp α 41-273 and Sp α 1-446 was not able to be resolved by Stokes radius measurements.

4.5 The Reversibility of Conformational Changes of Sp α 41-273 and Sp α 1-446

It is reported by Yoshino and Marchesi (Yoshino and Marchesi, 1984) that, after removal of urea, spectrin α - and β -subunits prepared in 3 M urea regain their α -helical content when analyzed by CD. Such preparation of α - and β -subunits can be reconstituted into dimers that appear essentially the same as native spectrin. However, both subunits displayed other features that distinguished themselves from native spectrin including abnormal mobility on nondenaturing polyacrylamide gel electrophoresis, intrinsic tryptophan fluorescence and anisotropy.

It is reported by Brandts and coworkers (Brandts *et al.*, 1977) as well as by Ralston and Dunbar (1979) that heating of spectrin above its transition temperature produces conformational changes that are irreversible. Studies by Yoshino and Minari (1987) come to essentially the same conclusion.

The reversibility of the conformational changes induced by heat and urea in Sp α 41-273 and Sp α 1-446 has been investigated using Stokes radius measurements and spin-labeling EPR. We showed that the Stokes radius of urea-treated, boiled or temperature-cycled Sp α 41-273 in 5 mM sodium phosphate buffer at pH 7.4 was 52.3 Å, 52.3 Å or 56.4 Å, respectively, indicating no difference from that of native Sp α 41-273 (55.8 Å) within the limit of experimental errors. Thus, conformational changes induced by urea or heat are not detectable by the Stokes radius measurements.

On the other hand, EPR spectra of urea- and heat-treated Sp α 41-273 and Sp α 1-446 displayed features distinct from those of native samples and samples in urea (section 3.3.1.3, Fig. 19). The amount of the weakly immobilized component in urea-treated samples, as measured by W' , fell between those of the native samples and samples in urea, implying that the conformational changes induced in Sp α 41-273 and Sp α 1-446 by urea are not completely reversible. In order to eliminate the possibility that the proper refolding spectrin fragments after removal of urea was impeded as a result of the steric hindrance of the incorporated spin labels, urea-treated Sp α 41-273

samples were prepared by two different procedures, Procedure 1 (labeled in the presence of urea) and Procedure 2 (labeled after the removal of urea). Similar results were obtained from the two procedures, confirming that the presence of spin labels is not the factor that perturbed the renaturation. The W' values of Sp α 41-273 and Sp α 1-446 before and after the heat treatment were also significantly different (section 3.3.2, Fig. 22), suggesting that conformational changes induced by heat are not reversible.

Therefore, depending on the sensitivity of a technique to a particular conformational change, different measures of reversibility are observed for Sp α 41-273 and Sp α 1-446. Generally speaking, similar to intact spectrin, urea- and heat-treated Sp α 41-273 and Sp α 1-446 are able to reverse their conformation to certain degree but not to completion.

4.6 Conclusions

Seven spectrin fragments with different lengths have been expressed as fusion proteins with GST. Different stabilities were observed for the different fragments following thrombin cleavage. Sp α 1-128, Sp α 1-234, Sp α 1-340 and Sp α 1-446 constructed based on the phasing of the conventional sequence motifs suffered different extents of nonspecific degradation while Sp α 41-167, Sp α 1-167 and Sp α 41-273 constructed based on the hypothesized phasing of the structural units showed little or no nonspecific degradation. The results imply that the hypothesized phasing of the structural units may be very close to the actual phasing of the conformational units.

Structural features of two of the relatively stable spectrin fragments, Sp α 41-273 and Sp α 1-446, have been studied. The chemical environments of the common cys residues (cys167 and cys224) were kept the same in Sp α 41-273 and Sp α 1-446. The dimensions of Sp α 41-273 and Sp α 1-446, as measured by Stokes radii, responded to the change of ionic strength in a similar fashion as intact spectrin, being more extended in low salt buffer and more condensed in high salt buffer. Structural transitions of Sp α 41-273 and Sp α 1-446 occurring around similar temperature ranges as

those of intact spectrin were detected by spin-labeling EPR. After urea and heat denaturation, Sp α 41-273 and Sp α 1-446 were able to partially reverse their conformation as if they were intact molecules. These results suggest that the folding of one unit is not affected by the existence of another unit and that small spectrin fragments bear structural similarity to each other and to intact spectrin.

On the other hand, the Sp α 41-273 and Sp α 1-446 exhibited essentially the same Stokes radii despite the fact that the molecular weight of Sp α 1-446 is larger. A higher transition temperature was observed for Sp α 1-446 than for Sp α 41-273 when they were labeled at the same site. For spectrin fragments with the similar phasing, the larger ones displayed higher stability in the thrombin cleavage reaction. These results appear to infer that, although the individual folding of each unit remains unaffected by the addition of a neighboring unit, the structure of the resulting fragment may not equal to the simple addition of the two smaller units. There could be additional interactions between the units giving rise to the additional compactness of the larger fragments.

The data presented in this dissertation provided evidence supporting the hypothesis that spectrin consists of individually folded conformational units.

APPENDIX

PUBLISHED WORK BY THE AUTHOR

Journal of Biomolecular Structure & Dynamics, ISSN 0739-1102
Volume 8, Issue Number 1 (1990), ²Adenine Press (1990).

Secondary Structure Prediction for the Spectrin 106-Amino Acid Segment, and a Proposed Model for Tertiary Structure

Y. Xu¹, M. Prabhakaran², M.E. Johnson² and L.W.-M. Fung^{1*}

¹Department of Chemistry
Loyola University of Chicago
6525 N. Sheridan Road
Chicago, IL 60626

²Department of Medicinal Chemistry and Pharmacognosy
University of Illinois at Chicago
P.O. Box 6998
Chicago, IL, 60680

Abstract

A collective secondary structure prediction for the human erythrocyte spectrin 106-residue repeat segment is developed, based on the sequences of nine segments that have been reported in the literature, utilizing a consensus of several secondary structure prediction methods for locating turn regions. The analysis predicts a five-fold structure, with three α -helices and two β -strand regions, and differs from previous models on the lengths of the helices and the existence of β -strand structure. We also demonstrate that this structural motif can be folded into tertiary structures that satisfy the experimental spectrin data and several general principles of protein organization.

Introduction

Spectrin is a major protein in the human erythrocyte membrane skeleton that plays an important role in determining the mechanical properties and the unique biconcave shape of the erythrocyte (1-3), and consists of α ($M_r = 240,000$) and β ($M_r = 220,000$) subunits. The two subunits associate side-to-side in an antiparallel orientation (4) to give a flexible rod approximately 1,000 Å long, as visualized by electron microscopy (EM) (5). Circular dichroism (CD) measurements indicate 65-70% α -helical content (6). Amino acid sequence and cDNA sequence analyses (7-9) reveal that about 90% of spectrin, by mass, is comprised of repetitive structural units of 106 amino acid residues. Other spectrin-like proteins, including brain spectrin (10), dystrophin (11,12), and α -actinin (13) also have similar repetitive units. From EM data (5) and the number of repeat units (7-9), the 106-residue segment must have dimensions of $\sim 55 \times 30$ Å, similar to the dimensions of other globular proteins.

*Author to whom correspondence should be addressed.

A triple helical model has been suggested for the 106-amino acid segment based on Chou-Fasman analysis (14). This model is simple and attractive, with the unit length matching the expected 55 Å linear length (5). However, the triple helical model somewhat over-predicts (~80-85%) the overall α -helix content, the helical length is unusually large (55 Å) for globular domains, the number of secondary structure elements is low for a globular domain of this size (15,16), the lack of any β structure is somewhat unusual, and the simple antiparallel packing of helices of roughly equal length is more common for transmembrane protein domains than for cytoplasmic globular protein domains. An alternative four-helix model has also recently been developed by Davison and coworkers (13), based on multiple secondary structure predictions of aligned α -actinin and spectrin sequences. However, their model includes one helix that is longer than the domain length, and there does not appear to be a good folding pattern that will permit the segment to form a repeating structural unit.

In this study, we develop a detailed secondary structure prediction for the 106-residue segment of spectrin by combining sequence information from all of the sequenced segments. A model for possible tertiary structure arrangement of the five major secondary structure regions is then developed, using data derived from EM and CD as additional constraints. A five-fold structural pattern is obtained that can be folded to give tertiary structures with features that satisfy both the experimental spectrin data, and several general principles of protein organization. This folded model can also be docked in antiparallel arrangement to provide a possible arrangement for the dimer unit.

Methods

Secondary Structure Assignments. The complete sequences for nine of the thirty-six 106-residue segments, $\alpha 1$, $\alpha 2$, $\alpha 3$, $\alpha 4$, $\alpha 5$, $\alpha 8$, $\alpha 15$, $\alpha 16$, and $\beta 18$, have been published (8,9,14). Sequence homology implies conformational conservation, and all nine 106-residue segments should have similar secondary and tertiary structures. Thus we used a collective secondary structure prediction method (17) to improve the reliability of our predicted secondary structure, since the summation will average out the differences in prediction pattern from one repeat to another. In analyzing secondary structure, we have used a unitary alignment since the 106-residue length is highly conserved (4). The "phase" of the 106-residue segment may be somewhat uncertain (4,14), but the uncertainty is probably no more than five residues, so we have used the published positioning for the segments. We evaluated the occurrence of each predicted structural pattern (α -helix, β -sheet and turn) in the nine segments to identify similarities in pattern predictions.

In our analysis we have first determined the most probable turn locations using a combination of Chou-Fasman secondary structure prediction methods (CF) (18), minima in hydrophobicity plots and the pattern recognition methods of Cohen and coworkers (15), followed by CF secondary structure prediction of the regions between turns. Minima in hydrophobicity plots have been shown to correspond to turn regions, while broad maxima correspond to interior secondary structure regions

Spectrin Secondary Structure Prediction

057

(helix and sheet), with helices often beginning at hydrophobic centers (19). Thus, the collective hydrophobicity plot was evaluated for turn and helix/sheet positioning and compared with the CF prediction. The turn patterns predicted by CF and hydrophobicity were then compared with Cohen's pattern recognition predictions (15), which have shown success rates of 90-95% for turn prediction in homologous proteins. Since the repeat segments are assumed to be structurally homologous, a secondary structure prediction was then developed specifically for the $\alpha 2$ segment as an example of the collective prediction, and as the first step toward generation of a tertiary structure model. This segment was selected, rather than $\alpha 1$ or $\beta 18$, for example, to avoid possible irregularities due to the dimer binding site(s) in the terminal ends of the spectrin monomers.

Tertiary Structure Model. The initial secondary structure elements were built using the molecular design package SYBYL. The graphics package FRODO was then used to build the monomer and dimer structures. Backbone dihedral angles were confined within allowed ϕ, ψ regions. The CHARMM molecular mechanics program was used to anneal the structures and calculate structural parameters.

Folding of secondary structures is the least developed aspect of protein folding schemes (20). There is no specific algorithm available for folding the secondary structural units of a protein to its tertiary structure. However, a number of principles for protein organization such as average helix length, the stability of helical structures in relation to their dipole arrangements, burial of β -sheets, higher stability of antiparallel β -sheet in comparison with parallel β -sheet, and the occurrence of β -sheet in a right-handed orientation have been deduced (21), and were utilized in the construction of a tertiary model for the 106-residue segment. The distance between C_{α} atoms of adjacent helices was kept greater than about 6.5 Å (22). Structural motifs for connecting secondary structure elements in model construction were obtained from α/α and α/β protein crystal structures in the Brookhaven Protein Data Bank (23). (See Richardson (21) for definitions of protein classification.) van der Waals contacts and ionic bonds between the charged residues were maximized to facilitate monomer to dimer formation.

After folding the three dimensional models, they were subjected to 1,000 steps of conjugate gradient energy minimization, followed by 2,000 steps of molecular dynamics at 1,000 K, then cooled by 1,000 steps of steepest descent minimization. Accessibility calculations utilizing a 1.4 Å radius probe were performed to measure surface exposure area, hydrophobic binding energy and the ratio of polar and non-polar surface area.

The number of van der Waals contacts, the physical contacts between monomers in the dimer form, the number of hydrogen bonds, conformational energy, accessible surface area, and polar/non-polar surface area ratios were calculated for the dimer and the two monomers, one of which is perturbed slightly in docking, to evaluate the models. The radius of gyration, R_g , and the three axial parameters (a, b, c) along the three orthogonal axes were also obtained.

058

Xu et al.

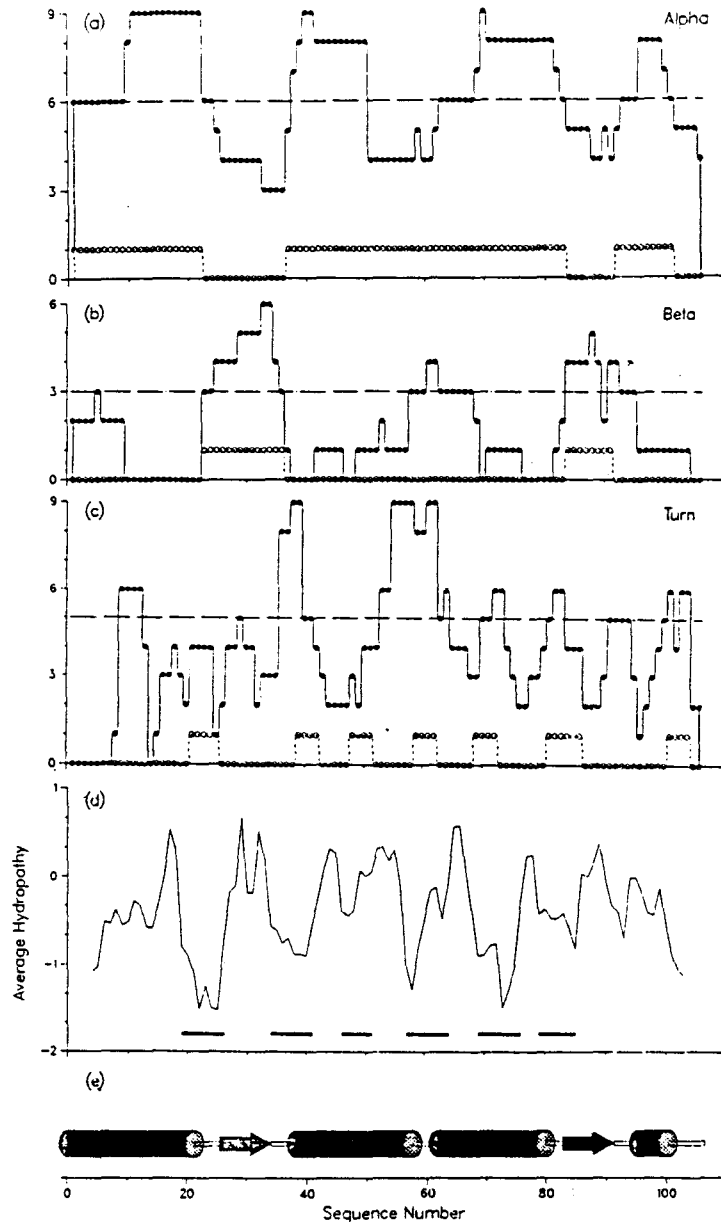


Figure 1: Collective and α_2 individual Chou-Fasman and hydropathy analyses for the nine 106-residue segments of spectrin whose sequences have been reported. The solid line histograms represent the number of amino acids predicted to be in (a) helical, (b) β -sheet, or (c) turn structures at each position in the sequence. Thresholds for each of the structure types are shown as horizontal lines for the collective predictions. Based on the CD measurement of 65-70% α -helix, 6 was used as the threshold for occurrence of α -helix; a turn threshold of 5 was used, corresponding to more than half of the residues being predicted as turn residues within the nine segments. Values greater than the threshold represent higher probability for the individual structures. The dashed line histograms represent the predictions for the α_2 sequence. The hydropathy plot (d) uses a normalized linear version (24) of the Kyte and Doolittle (25) hydropathy scale, with positive values for hydrophobic residues, negative values for hydrophilic residues, and a span setting of 7; values shown are the average for the nine segments. Regions of minima for potential turn positioning are marked at the bottom of the plot. (e) Schematic representation of the secondary structure predicted in this work.

Results and Discussion

Secondary Structure Prediction. In developing a secondary structure prediction, we have followed the basic strategy described by Cohen and coworkers (15,16) of first determining the most probable turn positions, and then assigning secondary structure between high probability turns. The CF turn prediction for both the α_2 and the collective sequence are shown in Figure 1c. CF turns were considered possible if a sequence of at least 4 residues appeared as turn residues in either the collective prediction (at or above the threshold, as indicated in the figure), or in the α_2 individual prediction. CF turn positions were then compared with regions of minima in the hydropathy plot (19) as noted in Figure 1d; turns not at minima were eliminated. The remaining possible turns were then evaluated by the pattern recognition algorithms of Cohen and coworkers (15,16) as being high probability (T) or moderate to low probability (t) turns. CF predictions for α -helix or β -sheet (Figures 1a and 1b) were then incorporated into the sequence, with the requirement that there be a span of at least 10 residues (α -helix) or 8 residues (β -sheet) from one turn to the next.

The resulting secondary structure scheme consists of three major α -helices, two β -strands, four high probability and two moderate probability turn elements, in the sequence: α_1 (residues 1-21), T_1 (22-25), β_1 (26-35), T_2 (36-39), α_2 (40-58), T_3 (59-62), α_3 (63-80), T_4 (81-84), β_2 (85-91), t_5 (92-95), α_4 (96-100) and t_6 (101-106). These 12 fragments can be arranged into a 5-fold pattern, with Region I being $\alpha_1 + T_1$, Region II being $T_1 + \beta_1 + T_2$, Region III being $T_2 + \alpha_2 + T_3$, Region IV being $T_3 + \alpha_3 + T_4$, and Region V being $T_4 + \beta_2 + t_5$. The C-terminal region is probably the most flexible part, with a possible one-turn α -helix (α_4) and two adjacent turns (t_5 and t_6) forming a connecting link between segments. The structure is shown schematically in Figure 1e, and clearly indicates the existence of a more complicated secondary structure scheme than a simple triple helical structure. At least four turns and two β -sheet regions of fairly high probability are predicted in addition to the three helix regions.

An alternative strategy of first fixing the positions of high probability α -helices (Figure 1a) and β -strands (Figure 1b), and then positioning turns at the highest probability turn positions between these secondary structure elements yields essentially equivalent results. Likewise, the use of other secondary prediction methods yield similar results for the prediction of α -helix and β -strand, with the methods of Garnier (26) predicting 80% α -helix and 10% β -strand, and those of Nagano (27) predicting 60% α -helix and 10% β -strand. Thus, there is reasonable confidence in the amount and positioning of all of the secondary structure elements.

The average lengths of the predicted α and β elements are 19.3 and 8.5 residues, respectively, which is within the range observed by Cohen and co-workers (16) for α/α and α/β proteins of similar size; the predicted helices are all shorter than 55 Å (~35 residues), the linear length of a simple triple helix (1,14). The predicted helical content of 62% is also in good agreement with the published CD measurements of 65-70% (6). Comparison of our five-fold secondary structure model of the spectrin repeat with the triple helical model (14) indicates some similarities, but also significant differences. Both models agree on the approximate position of helical regions, but differ

in helix lengths. Our model also predicts the existence of a couple short β -strand segments, not seen in the triple helix model. The correlation of this model with that of Davison and coworkers (13) is comparable; positioning of high probability helical segments is similar, and some of the turns coincide fairly closely, but no β -strand structure is predicted in their model.

Tertiary Structure Model. In developing a tertiary structure model, we concentrate on packing the five secondary structure elements within the constraints of experimental data and general principles of protein folding (21). We constructed several three dimensional models for the α_2 monomer, and a dimer consisting of two α_2 monomers docked in an antiparallel arrangement. Two different types of models were constructed, based on their inter-subunit arrangements: interdigitated models, and side-by-side models. The monomer for the interdigitated model was constructed with a fairly open inter-subunit contact surface, with the β -strands having a left-handed twist. The dimer was formed with tight packing, resulting in significant perturbation of the monomer structures after molecular dynamics annealing of the dimer structure. The model is quite stable, and would probably require denaturing conditions to separate the two monomers, but the number of physical contacts between monomers and the number of hydrogen bonds appear to be unreasonably high, suggesting that this type of model is probably not feasible.

The most probable α_2 model was developed by association of the helical segments around the β -sheets. This secondary structure arrangement has analogies in known globular proteins. The $\alpha_1 - \beta_1$ segment resembles a similar segment in flavodoxin residues 90-120 (28); the $\alpha_2 - \alpha_3$ arrangement resembles the GH helix region of deoxy hemoglobin (29), while the $\beta_1 - \alpha_2$ segment resembles flavodoxin residues 1-15 (26), the $\alpha_3 - \beta_2$ arrangement resembles residues 135-149 of subtilisin (30), and the C-terminal connecting region resembles the Ribonuclease A N-terminal (31), but in reversed order ($\beta\alpha$, rather than $\alpha\beta$). The alignment of β -sheets to form a right-handed antiparallel β -sheet surrounded by three linear helices leads to an energetically stable monomer that is consistent with the experimentally observed linear dimensions and α -helical content. The two antiparallel α helices (α_2, α_3) are then ideally positioned to form dimer contacts with the opposite pair of helical strands of a neighboring monomer unit. This approach was extended by docking two monomers to form a dimer. Stereo ribbon plots for the C_α backbone of two monomers docked to form a dimer are shown in Figure 2. In building the dimer, our primary concern was to accommodate van der Waals interactions between the monomers. No specific attempt was made to form salt bridges between monomers in our dimer model, although antiparallel α -helices with high contents of charged residues should form stable dimers by means of salt bridges.

The model dimensions are $\sim 49 \times 33 \times 29 \text{ \AA}$, in good agreement with EM data. We have measured both the hydrophilic and hydrophobic forces in the formation of dimers. There are about 60 hydrogen bonds within the α_2 monomer, and eight hydrogen bonds between the two monomers, indicating fairly specific hydrophilic bonding between the monomers. The hydrophobic energy, as calculated from solvent accessibility, shows that dimer formation produces burial of non-polar residues from solvent.



Figure 2: Stereo ribbon plot of the tertiary structure model, with two 106-residue segments docked in an antiparallel arrangement as a model for the possible dimer arrangement. The plot was generated using the INSIGHT molecular graphics program (Biosym Technologies).

The model is stabilized about equally by hydrophobic and hydrophilic forces. We have also verified that $\alpha 2$ monomers can be connected sequentially in extended repeats to form a linear molecule with appropriate linear dimensions. At the same time, it is to be emphasized that this is a single tertiary structure model that has been constructed from predicted secondary structure elements, using principles of protein architecture (21) as a guide, but no detailed analysis of folding possibilities (22) has been done. Thus, the tertiary model should be taken as a demonstration that the predicted secondary structure elements can be folded into a reasonable tertiary structure to meet the constraints of known experimental data: it is not intended to provide detailed structural information.

Summary

We have shown that the triple helical model suggested for the spectrin 106-residue segment is probably over-simplified. A combination of hydropathy analysis, the pattern recognition methods of Cohen and coworkers (15,16), and Chou-Fasman analysis predict the existence of at least four high probability turns within the sequence at positions incompatible with an extended antiparallel triple helix. The existence of limited β -strand segments is also predicted with reasonable probability. Based on our secondary structure analysis, we propose a five-fold globular conformation for the 106-residue segment, with the tertiary structure model shown in Figure 2 being one possible model. Experimental approaches to evaluate and refine this model are under development.

Acknowledgements

This work was supported in part by USPHS Grants R01-HL38361 (LW-MF), R01-HL23697 (MEJ), by funds from Loyola University of Chicago (LW-MF and YX), by a USPHS BRSG Shared Instrumentation Grant (MEJ), and by an American Heart Association of Chicago Senior Fellowship Award (MP).

References and Footnotes

1. Stokke, B.T., Mikkelsen, A. and Elgsaeter, A., *Biophys. J.* 49, 319-327 (1986).
2. Bodine, D.M., Birkenmeier, C.S. and Barker, J.E., *Cell* 37, 721-729 (1984).
3. Knowles, W., Marchesi, S.L. and Marchesi, V.T., *Seminars Hematology* 20, 159-174 (1983).
4. Speicher, D.W., *J. Cell. Biochem.* 30, 245-258 (1986).
5. Shotton, D.M., Burke, B.E. and Brank, D., *J. Mol. Biol.* 131, 303-329 (1979).
6. Calvert, R., Ungewickell, E. and Gratzner, W., *Eur. J. Biochem.* 107, 363-367 (1980).
7. Speicher, D.V., Gary, D. and Marchesi, V.T., *J. Biol. Chem.* 258, 15938-15947 (1983).
8. Curtis, P.J., Palumbo, A., Ming, J., Fraser, P., Cioe, L., Meo, P., Shane, S. and Rovera, G., *Gene* 36, 357-362 (1985).
9. Winkelmann, J.C., Leto, T.L., Watkins, P.C., Eddy, R., Shows, T.B., Linnenbach, A.J., Sahr, K.E., Kathuria, N., Marchesi, V.T. and Forget, B.T., *Blood* 72, 328-334 (1988).
10. Wasenius, W., Saraste, M., Salven, P., Eramaa, M., Holm, L. and Lehto, V., *J. Cell Biol.* 108, 79-93 (1989).
11. Davison, M.D. and Critchley, D.R., *Cell* 52, 159-150 (1988).
12. Koenig, M., Monaco, A.P. and Kunkel, L.M., *Cell* 53, 219-228 (1988).
13. Davison, M.D., Baron, M.D., Critchley, D.R. and Wootton, J.C., *Int. J. Biol. Macromol.* 11, 81-90 (1989).
14. Speicher, D.W. and Marchesi V.T., *Nature* 311, 177-180 (1984).
15. Cohen, F.E., Abarbanel, R.A., Kuntz, I.D. and Fletterich, R., *Biochemistry* 22, 4894-4904 (1983).
16. Cohen, F.E., Abarbanel, R.A., Kuntz, I.D. and Fletterich, R., *Biochemistry* 25, 266-275 (1986).
17. Nelson, D.R. and Strobel, H.W., *Biochemistry* 28, 656-660 (1989).
18. Chou, P.Y. and Fasman, G.D., *Biochemistry* 13, 211-222 and 222-245 (1974).
19. Rose, G.D. and Roy, S., *Proc. Natl. Acad. Sci. USA* 77, 4643-4647 (1980).
20. Fasman, G.D., *Prediction of Protein Structure and the Principles of Protein Conformation*, Plenum Press, New York/London (1989).
21. Richardson, J.S., *Adv. Protein. Chem.* 34, 168-339 (1981).
22. Cohen, F.E. and Kuntz, I.D., *Proteins* 3, 162-166 (1987).
23. Bernstein, F.C., Koetzle, T.F., Williams, G.J.B., Meyer, E.F., Jr., Brice, M.D., Rodgers, J.R., Kennard, O., Shimanouchi, T. and Tasumi, M., *J. Mol. Biol.* 112, 535-542 (1977).
24. Cornette, J.L., Cease, K.B., Margalit, H., Spouge, J.L., Berzofsky, J.A. and DeLisi, C., *J. Mol. Biol.* 195, 659-685 (1987).
25. Kyte, J. and Doolittle, R.F., *J. Mol. Biol.* 157, 105-132 (1982).
26. Garnier, J., Osguthorpe, D.J. and Robson, B., *J. Mol. Biol.* 120, 97-120 (1978).
27. Nagano, K., *J. Mol. Biol.* 75, 401-420 (1973).
28. Smith, W.W., Burnett, R.M., Darling, G.D. and Ludwig, M.L., *J. Mol. Biol.* 117, 195-225 (1977).
29. Fermi, G., Perutz, M.F., Shaanan, B. and Fourme, R., *J. Mol. Biol.* 175, 159-174 (1984).
30. Drenth, J., Hol, W.G.J., Jansonius, J.N. and Koekoek, R., *Cold Spring Harbor Symp. Quant. Biol.* 36, 107-116 (1971).
31. Wlodawer, A., Bott, R. and Sjolín, L., *J. Biol. Chem.* 257, 1325-1332 (1982).

Date Received: May 7, 1990

Communicated by the Editor R.H. Sarma

REFERENCES

- Ackers, G. K. (1964) *Biochem.* **3**, 723-730.
- Adams, D., Markes, M. E., Lewis, W. J. and Carraway, K. L. (1976) *Biochim. Biophys. Acta* **426**, 38-45.
- Arnheim, N. (1983) *Evolution of Genes and Proteins* (Nei, M. and Koehn, R. K. eds., Sinauer Associates, MA), pp38-61.
- Ausubel F. M., Brent R., Kingston R. E., Moore D. D., Seidman J. R., Smith J. A. and Struhl K. (1990) *Current Protocols in Molecular Biology* (John Wiley & Sun, NY), pp1.6.1-1.6.2.
- Baum, J., Dobsin, C. M., Evans, P. A. and Hanley, C. (1989) *Biochem.* **28**, 7-13.
- Becker, P. S., Cohen, C. M. and Lux, S. E. (1986) *J. Biol. Chem.* **261**, 4620-4628.
- Bennett, V. (1982) *J. Cell Biochem.* **18**, 49-65.
- Bennett, V. (1989) *Biochim. Biophys. Acta* **988**, 107-121.
- Bennett, B. (1990) *Am. Physiol. Soc.* **70**, 1029-1065.
- Berger, K. W., Barratt, M. D. and Kamat, V. B. (1971) *Chem. Phys. Lipids* **6**, 351-363.
- Boe, A., Elgsaeter, A., Oftedal, G. and Strand, K. A. (1979) *Acta Chem. Scand.* **33**, 245-249.
- Bradford, M. (1976) *Anal. Biochem.* **72**, 248.
- Brandts, J. F., Erickson, L., Lysko, K., Schwarts, A. T. and Taverna, R. D. (1977) *Biochem.* **16**, 3450-3454.
- Branton, D., Cohen, C. M. and Tyler, J. (1981) *Cell* **24**, 24-32.
- Budzynski, D. M., Benight, A. S., LaBrake, C. C. and Fung, L. W.-M. (1992) *Biochem.* **31**, 3653-3660.
- Butterfield, D. A. (1977) *Acc. Chem. Res.* **10**, 111-116.
- Byers, T. J. and Branton, D. (1985) *Proc. Natl. Acad. Sci. USA* **82**, 6153-6157.
- Calvert, R., Bennett, P. and Gratzner, W. (1980) *Eur. J. Biochem.* **107**, 363-367.

- Cantor, C. R. and Schimmel, P. R. (1980) *Biophysical Chemistry* (W. H. Freeman and Company, NY) pp675-676.
- Cassoly, R., Daveloose, D. and Leterrier, F. (1980) *Biochim. Biophys. Acta* **601**, 478-489.
- Catsimpoilas, N. and Wood, J. L. (1966) *J. Biol. Chem.* **241**, 1790-1796.
- Chapman, D., Barratt, M. D. and Kamat, V. B. (1969) *Biochim. Biophys. Acta* **173**, 154-157.
- Cheah, K., Sankar, S. and Porter, G. (1988) *Gene* **69**, 265-274.
- Chung, C. T., Niemela, S. L. and Miller, R. H. (1989) *Proc. Natl. Acad. Sci. USA* **86**, 2172-2175.
- Coetzer, T., Palek, J., Lawler, J., Liu, S. C., Jarolim, P., Lahav, M., Prchal, J. T., Wang, W., Alter, B. P., Schewitz, G., Mankad, V., Gallanello, R. and Cao, A. (1990) *Blood* **75**, 2235-2244.
- Christensen, H. and Pain, R. H. (1991) *Eur. Biophys. J.* **19**, 221-229.
- Curtis, P. J., Palumo, A., Jeffrey, M., Fraser, P., Cioe, L., Meo, P., Shane, S. and Rovera, G. (1985) *Gene* **36**, 357-362.
- Davison, M. D., Baron, M. D. and Critchley, D. R. (1989) *Int. J. Biol. Macromol.* **11**, 81-90.
- Degani, Y., Neumann, H. and Patchornik, A. (1970) *J. Amer. Chem. Soc.* **92**, 6969-6971.
- Deuticke, B. P., Poster, B., Lutkemeier, P. and Haest, C. W. M. (1983) *Biochim. Biophys. Acta* **731**, 196-210.
- Delaunay, J. and Dhermy, D. (1993) *Semin. Hematol.* **30**, 21-33.
- DeSilva T. M., Peng, K.-C., Speicher K. D. and Speicher, D. W. (1992) *Biochem.* **31**, 10872-10878.
- Doolittle, R. F. (1981) *Science* **214**, 149.
- Dubreuil, Y. L. and Cassoly, R. (1983) *Arch. Biochem. Biophys.* **223**, 495-502.
- Dubreuil, R. R., Byers, T. J., Sillman, A. L., Bar-Zvi, L. S., Goldstein, B. and Branton, D. (1989) *J. Cell Biol.* **109**, 2197-2205.
- Dubreuil, R. R., Brandin, E., Reisberg, J. H. S., Goldstein, L. S. B. and Branton, D. (1991) *J. Biol. Chem.* **266**, 7189-7193.
- Elgsaeter, A. (1978) *Biochim. Biophys. Acta* **526**, 235-244.
- Elgsaeter, A., Stokke, B. T., Mikkelsen, A. and Branton, D. (1986) *Science* **234**, 1217-1223.
- Elgsaeter, A. and Mikkelsen, A. (1991) *Biochim. Biophys. Acta* **1071**, 273-290.

- Ellman, G. L. (1959) *Arch. Biochem. Biophys.* **82**, 70-77.
- Ewbank, J. J. and Creighton, T. (1991) *Nature* **350**, 518-520.
- Fischer, T. M., Haest, C. W. M., Stohr, M., Kamp, O. and Deuticke, B. (1978) *Biochim. Biophys. Acta* **510**, 270-282.
- Fung, L. W.-M. and Simpson, M. J. (1979) *FEBS Lett.* **108**, 269-273.
- Fung, L. W.-M., SooHoo, M. J. and Meena, W. A. (1979) *FEBS Lett.* **105**, 379-383.
- Fung, L. W.-M. (1981) *Biophys. J.* **33**, 253-262.
- Fung, L. W.-M. (1983) *Ann. N. Y. Acad. Sci.* 253-262.
- Fung, L. W.-M. and Johnson, M. E. (1983) *J. Magn. Reson.* **51**, 233-244.
- Fung, L. W.-M. and Johnson, M. E. (1984) *Current Topics in Bioenergetics* **13**, 107-157.
- Fung, L. W.-M., Lu., H.-Z., Hjelm, R. P., Jr. and Johnson, M. E. (1986) *FEBS Lett.* **197**, 234-238.
- Fung, L. W.-M., Lu., H.-Z., Hjelm, R. P., Jr. and Johnson, M. E. (1989) *Life Sci.* **44**, 735-740.
- Furste, P., Pansegrau, W., Frank, R., Blocker, H., Scholz, P., Bagdasarian, M. and Lanka, E. (1986) *Gene* **48**, 119-131.
- Garbarz, M., Lecomte, M. C., Feo, V., Devaux, I., Picat, C., Lefebvre, C., Galibert, F., Gautero, P., Bournier, O., Galand, C., Forget, B. G., Boivin, P. and Dhermy, D. (1990) *Blood* **75**, 1691-1698.
- Goldman, S. A., Bruno, G. V. and Freed, H. J. (1975) *J. Phys. Chem.* **76**, 1858-1860.
- Goodman, S. R. and Branton, D. (1978) *J. Supramol. Struct.* **8**, 455-463.
- Goodman, S. R. and Shiffer, K. (1983) *Am. J. Physiol.* **244**, c121-c141.
- Gratzer, W. B. (1983) *Muscle and Nonmuscle Mobility* (Stracher, A. ed., Academic Press, NY).
- Gratzer, W. B. (1984) *Nature* **310**, 368-369.
- Grip, W. J. D. and Daemen, F. J. M. (1982) *Methods Enzymol.* **81**, 223-237.
- Haest, C. W. M., Kamp, D., Plasa, G. and Deuticke, B. (1979) *Biochim. Biophys. Acta* **469**, 226-230.
- Hensley, K., Postlewaite, J., Dobbs, P. and Butterfield, D. A. (1993) *Biochim. Biophys. Acta* **1145**, 205-211.

- Huebner, K., Palumbo, A., Isobe, M., Kozak, C., Monaco, S., Rovera, G., Croce, C. and Curtis, P. (1985) *Proc. Natl. Acad. Sci. USA* **82**, 3790-3793.
- Hughson, F. M., Wright, P. E. and Baldwin, R. L. (1990) *Science* **249**, 1544-1548.
- Jacobson, G. R., Schaffer, M. H., Stark, G. R. and Vanaman, T. C. (1973) *J. Biol. Chem.* **248**, 6583-6591.
- Jozwiak, Z., Schon, W., Kraft, G. and Gartner, H. (1993) *Biochem. Int.* **28**, 265-272.
- Kam, Z., Josephs, R., Eisenberg, H. and Gratzer, W. B. (1977) *Biochem.* **16**, 5568-5572.
- Keim, P., Heinrichson, R. L., Fitch, W. M. (1981) *J. Mol. Biol.* **151**, 179-197.
- Kemple, M. D., Ray, B. D., Jarori, G. K., Rao, B. D. N. and Prendergast, F. G. (1984) *Biochem.* **23**, 4383-4390.
- Kennedy, S.P., Warren, S.L., Forget, B.G., and Morrow, J. S. (1991). *J Cell Biol.* **115**, 267-277.
- Keonig, M., Monaco, A. P. and Kunkel, L. M. (1988) *Cell* **53**, 219-228.
- Kim, P. S. and Baldwin, R. L. (1982) *Annu. Rev. Biochem.* **51**, 459-489.
- Kim, P. S. and Baldwin, R. L. (1990) *Annu. Rev. Biochem.* **59**, 631-660.
- LaBrake, C. C. (1993) *Ph.D. Thesis* (Loyola University of Chicago).
- LaBrake, C. C., Wang, L., Keiderling, T. A. and Fung, L. W.-M. (1993) *Biochem.* **32**, 10296-10302.
- Laemmli, U. K. (1970) *Nature* **227**, 680-685.
- Lai, C.-S., Tooney, N. M. and Ankel, E. G. (1984) *FEBS Lett.* **173**, 283-286.
- Laurent, T. C. and Killander, J. (1964) *J. Chromatog.* **14**, 317-330.
- Learmonth, R., Woodhouse, A. G. and Sawyer, W. H. (1989) *Biochim. Biophys. Acta* **987**, 124-128.
- Lemaigre-Dubreuil, Y., Henry, Y. and Cassoly, R. (1980) *FEBS Lett.* **113**, 231-234.
- Li, W. H. (1983) *Evolution of Gene and Proteins* (Nei, M., Koehn, R. K. eds., Sinauer Associates, MA), pp14-37.
- Liu, S.-C., Derick, L. H. and Palek, J. (1987) *J. Cell Biol.* **104**, 527-536.
- Lux, S. E. (1979) *Semin. Hematol.* **16**, 21-51.
- Lux, S. E. and Glader, B. E. (1981) *Hematology of Infancy and Childhood*, 456-565.

- Marchesi, S. L., Letsinger, J. T., Speicher, D. W., Marchesi, V. T., Agre, P., Hyun, B. and Gulati, G. (1987) *J. Clin. Invest.* **80**, 191-198.
- Marchesi, S. L. (1989) *Red Blood Cell Membranes: Structure, Function, and Clinical Implications* (Agre, P., and Parker, J. C., eds., Marcel Dekker, Inc., NY), pp77-110.
- Marchesi V. T. and Steer, E. J. (1968) *Science* **159**, 203-204.
- Marchesi, V. T. (1985) *Hospital Practice.* **15**, 113-131.
- McGough, A. M. and Josephs, R. (1990) *Proc. Natl. Acad. Sci. USA* **87**, 5208-5212.
- McGuire, M. and Agre, P. (1988) *Hematologic Pathol.* **2**, 1-14.
- Mikkelson, A. and Elgsaeter, A. (1978) *Biochim. Biophys. Acta* **536**, 245-251.
- Mikkelson, A. and Elgsaeter, A. (1981) *Biochim. Biophys. Acta* **668**, 74-80.
- Minetti, M., Ceccarini, M., Stasi, A. M. M., Petrucci, T. C. and Marchesi, V. T. (1986) *J. Cell. Biochem.* **30**, 361-370.
- Morris, M. and Ralston, G. B. (1989) *Biochem.* **28**, 8561-8567.
- Morrow, J. S., Speicher, D. W., Knowles, W. J., Hsu, C. J. and Marchesi, V. T. (1980) *Proc. Natl. Acad. Sci. USA* **77**, 6592-6596.
- Morrow, J. S. and Marchesi, V. T. (1981) *J. Cell Biol.* **88**, 463-468.
- Musacchio, A., Noble, M., Panptit, R., Wierenga, R. and Saraste, M. (1992) *Nature* **359**, 851-855.
- Ohgushi, M. and Wada, A. (1983) *FEBS Lett.* **164**, 21-24.
- Pace, C. N. (1975) *Crit. Rev. Biochem.* **3**, 1-43.
- Pace, C. N. (1986) *Methods Enzymol.* **131**, 266-280.
- Pace, C. N. (1990) *Trends Biochem. Sci.* **15**, 14-17.
- Palek, J. and Lambert, S. (1990) *Semin. Hematol.* **27**, 290-332.
- Parry, D. A. D. and Cohen, C. (1991) *AIP. Conf. Proc.* **226**, 367-377.
- Parry, D. A. D., Dixon, T. W. and Cohen, C. (1992) *Biophys. J.* **61**, 858-867.
- Persico, M. G., Ciccodicola, A., Martini, G. and Rosner, J. L. (1989) *Gene* **78**, 365-370.
- Pink, J. R. L. (1981) *Biochemical Evolution* (Gutfreund, H. ed., Cambridge University Press, Cambridge, England).

- Prchal, J., Morley, B., Yoon, S., Coetzer, T., Palek, J., Conboy, J. and Kan, Y. (1987) *Proc. Natl. Acad. Sci.* **84**, 7468-7472.
- Ptitsyn, O. B. (1987) *J. Protein Chem.* **6**, 272-293.
- Ralston, G. B. (1976) *Biochim. Biophys. Acta* **455**, 163-172.
- Ralston, G. B. and Dunbar, J. C. (1979) *Biochim. Biophys. Acta* **579**, 20-30.
- Reich, M. H., Kam, Z., Eisenberg, H., Worcester, D., Ungewickell, E. and Gratzer, W. B. (1982) *Biophys. Chem.* **16**, 307-316.
- Rosenberg, A. H., Lade, B. N., Chui, D., Lin, S., Dunn, J. J., and Studier, F. W. (1987) *Gene* **56**, 125 - 135.
- Sahr, K. E., Laurila, P., Kotula, L., Scarpa, A. L., Coupal, E., Leta, T. L., Linnenbach, A. J., Winkelmann, J. C., Speicher, D. W., Marchesi, V. T., Curtis, P. J. and Forget, B. G. (1990) *J. Biol. Chem.* **265**, 4434-4443.
- Sambrook, J., Fritsch, E. F. and Maniatis, T. (1989) *Molecular Cloning* (Cold Spring Harbor Laboratory Press, NY), pp1.74-1.84.
- Sandberg, H. E., Bryant, R. G. and Piette, L. H. (1969) *Arch. Biochem. Biophys.* **133**, 144-152.
- Schneider, H. and Smith I. C. P. (1970) *Biochim. Biophys. Acta* **219**, 73-80.
- Schulz, G. E. and Schirmer, R. H. (1979) *Principles of Protein Structure* (Cantor, C. R. ed., Springer-Verlag, NY), pp674-678.
- Shen, B. W., Josephs, R. and Steck, T. L. (1986) *J. Cell Biol.* **102**, 997-1006.
- Shohet, S. B. and Marchesi, V. T. (1983) *J. Clin. Invest.* **71**, 1867-1877.
- Shotton, D. M., Burke, B. E. and Branton D. (1979) *J. Mol. Biol.* **131**, 303-329.
- Smith, D. B. and Johnson, K. S. (1988) *Gene* **67**, 31-43.
- Speicher, D. W., Morrow, J. S., Knowles, W. and Marchesi, V. T. (1980) *Proc. Natl. Acad. Sci. USA* **77**, 5673-5677.
- Speicher, D. W., Morrow, J. S., Knowles, W. J. and Marchesi, V. T. (1982) *J. Biol. Chem.* **257**, 9093-9101.
- Speicher, D. W., Davis, G., Yurchenco, P. D. and Marchesi V. T. (1983a) *J. Biol. Chem.* **258**, 14931-14937.
- Speicher, D. W., Davis, G. and Marchesi V. T. (1983b) *J. Biol. Chem.* **258**, 14938-14947.
- Speicher, D. W. and Marchesi, V. T. (1984) *Nature* **311**, 177-180.

- Speicher, D. W., Weglarz, L. and DeSilva, T. (1992) *J. Biol. Chem.* **267**, 14775-14782.
- Speicher, D. W., DeSilva, T. M., Speicher, K. D., Ursitti, J. A., Hembach, P. and Weglarz, L. (1993) *J. Biol. Chem.* **268**, 4227-4235.
- Stark, M. (1987) *Gene* **51**, 255-267.
- Steck, T. L. (1974) *J. Cell Biol.* **62**, 1-19.
- Stokke, B. T. and Elgsaeter, A. (1981) *Biochim. Biophys. Acta* **640**, 640-645.
- Stokke, B. T., Mikkelsen, A. and Elgsaeter, A. (1985) *Biochim. Biophys. Acta* **816**, 102-110.
- Stokke, B. T., Mikkelsen, A. and Elgsaeter, A. (1986) *Biophys. J.* **49**, 319-327.
- Streichman, S., Hertz, E. and Tatarsky, I. (1988) *Biochim. Biophys. Acta* **942**, 333-340.
- Streichman, S., Kahana, E. and Silver, B. (1991) *Biochim. Biophys. Acta* **1066**, 9-13.
- Studier, F. W., Rosenberg, A. H., Dunn, J. J. and Dubendorff, J. W. (1990) *Methods Enzymol.* **185**, 60-89.
- Tanford, C. (1968) *Advan. Protein Chem.* **23**, 121-282.
- Tyler, J. M., Hargreaves, W. R. and Branton, D. (1979) *Proc. Natl. Acad. Sci. USA* **76**, 5192-5196.
- Ungewickell, E. and Gratzner, W. (1978) *Eur. J. Biochem.* **88**, 379-385.
- Vertessy, B. G. and Steck, T. L. (1989) *Biophys. J.* **55**, 255-262.
- Warburton, N., and Boseley, P. G. (1983) *Nucleic Acids Res.* **11**, 5837-5854.
- Winkelmann, J., Leto, T., Watson, P., Shows, T., Linneenbach, A., Sahr, K., Kathuria, N., Marchesi, V. and Forget, B. (1988) *Blood* **72**, 328-334.
- Winkelmann, J. C., Chang, J.-G., Tse, W. T., Scarpa, A. L., Marchesi, V. T. and Forget, B. G. (1990) *J. Biol. Chem.* **265**, 11827-11832.
- Winograd, E., Hume, D. and Branton, D. (1991) *Proc. Natl. Acad. Sci. USA* **88**, 10788-10791.
- Xu, Y., Prabhakaram, M., Johnson, M. E. and Fung, L. W.-M. (1990) *J. Biomolec. Struct. & Dynamics* **8**, 55-62.
- Yoshino, H. and Marchesi, V. T. (1984) *J. Biol. Chem.* **259**, 4496-4500.
- Yoshino, H. and Minari, O. (1987) *Biochim. Biophys. Acta* **905**, 100-108.
- Yu, B. P., Masoro, E. J., Downs, J. and Wharton, D. (1977) *J. Biol. Chem.* **252**, 5262-5266.

Yurchenco, P. D., Speicher, D. W., Morrow, J. S., Knowles, W. J. and Marchesi, V. T. (1982)
J. Biol. Chem. **257**, 9102-9107.

VITA

The author, Yirong Xu was born on December 27, 1964 in Shanghai, China. She graduated from Xiang Min high school in July, 1982. In the same year, she entered Pharmacy School of Shanghai Medical College. She received a Bachelor of Science degree in Pharmacy in July, 1987.

In August 1987, Xu came to the United States and was enrolled in the graduate program of Department of Chemistry at the Illinois Institute of Technology. Following one semester of study at Illinois Institute of Technology, she transferred to Loyola University of Chicago. In July, 1988, she joined the research laboratory of Dr. Leslie W.-M. Fung to pursue her graduate research in Biophysical Chemistry. She was awarded a teaching assistantship from January, 1988 to January, 1989, a research assistantship from January, 1989 to August, 1991, a University Fellowship from September, 1991 to May, 1992 and another research assistantship from June, 1992 to December, 1992. With this financial support throughout the years, Xu was able to complete the doctoral dissertation in June 1993 under the direction of her thesis advisor, Dr. Leslie W.-M. Fung.

Xu is a member of the American Chemical Society. She is also a member of Alpha Sigma Nu National Jesuit Honor Society. She has participated in several national scientific meetings as well as university-sponsored research forums, during her five-year graduate study, including poster presentations at the Biophysical Society Meeting in February, 1990, the Gordon Conference in August, 1991, the 19th Annual Sigma Xi Graduate Student Forum of Loyola University in May, 1989 and the 20th Annual Sigma Xi Graduate Student Forum of Loyola University in May, 1990.

Xu's Publications includes: (1) "A Prediction of the Three Dimensional Structure of Spectrin 106-Amino Acid Repeat Segment" (1990) *J. Biophys.*, **89a**; (2) "Secondary Structure Prediction for the Spectrin 106-Amino Acid Segment, and a Proposed Model for Tertiary Structure" (1990) *J.*

Biomol. Struct. Dynam. **8**, 55-62.

APPROVAL SHEET

The dissertation submitted by Yirong Xu has been read and approved by the following committee:

Dr. Leslie W.-M. Fung, Director
Professor, Department of Chemistry, Loyola University of Chicago

Dr. Alanah Fitch
Associate Professor, Department of Chemistry, Loyola University of Chicago

Dr. Howard M. Laten
Associate Professor, Department of Biology, Loyola University of Chicago

Dr. Michael E. Johnson
Professor, Department of Medicinal Chemistry, University of Illinois, Chicago

Dr. John Smarrelli
Associate Professor, Department of Biology, Loyola University of Chicago

The final copies have been examined by the director of the dissertation and the signature which appears below verifies the fact that any necessary changes have been incorporated and that the dissertation is now given the final approval by the Committee with reference to content and form.

This dissertation is therefore accepted in partial fulfillment of the requirements for the degree of Doctor of Philosophy.

April 29, 1994

Date

Leslie W.-M. Fung

Director's Signature